

## Electronic Supplementary Information

### Potent Pincer-Zinc Catalyzed Homogeneous $\alpha$ -Alkylation and Friedländer Quinoline Synthesis of Secondary alcohols/Ketones with Primary Alcohols

Debashis Jana<sup>a</sup>, Sima Roy<sup>a</sup>, Srijita Naskar<sup>a</sup>, Supriyo Halder<sup>a</sup>, Gopal Kanrar<sup>b</sup>, Kausikisankar  
Pramanik<sup>a\*</sup>

<sup>a</sup>Department of Chemistry, Jadavpur University, Kolkata – 700032, India

<sup>b</sup>Department of Chemistry, St. Xavier's College (Autonomous), Kolkata – 700016, India

\*To whom correspondence should be addressed.

kpramanik@hotmail.com Tel: +91 94333 66013

## INDEX

1	Crystallographic details of complexes	S3-S4
2	Physical measurements, computational study, synthetic procedure for the preparation of ligands, complexes.	S5-S7
3	NMR Spectrum of Complexes	S8-S9
4	MO Contributions and optimized geometry of complexes	S10-S11
5	Optical Transitions of Complexes and NTOs of Complexes	S11-S18
6	MO Diagram of Complexes	S19-S20
7	Theoretical and experimental absorption spectrum	S21
8	Coordinates of Optimized Geometry	S21-S23
9	IR spectrum of reaction mixture, electronic spectra for the detection of H <sub>2</sub> O <sub>2</sub> , electrochemical study of complex <b>1a</b>	S24
10	X-Ray crystallographic information of <b>10aj</b> and <b>5ag</b>	S25-S26
11	Optimization table for Friedländer Quinoline Synthesis	S27-S28
12	General procedure for Zn-catalyzed reactions	S29
13	Characterization data of alkylated ketones	S29-S32
14	Characterization data of quinolines	S32-S38
15	NMR spectra of alkylated ketones	S39-S53
16	NMR spectra of quinolines	S54-S85
16	Some NMR spectra and HRMS for mechanistic study	S86-S89
17	Appendix: supplementary data	S90
18	References	S90-S92

**Table S1.** Crystallographic Details of complexes **1a** and **1b**.

	<b>1a</b>	<b>1b</b>
Empirical formula	C <sub>17</sub> H <sub>12</sub> N <sub>5</sub> Cl <sub>3</sub> Zn	C <sub>17</sub> H <sub>13</sub> N <sub>5</sub> Cl <sub>2</sub> Zn
<i>T</i> /K	298K	298K
fw	458.04	847.19
Crystal system	Monoclinic	Orthorhombic
Space Group	C12/c1	Pbca
<i>a</i> /Å	14.0244(8)	13.2739(4)
<i>b</i> /Å	15.2683(9)	13.0215(4)
<i>c</i> /Å	19.1822(11)	41.0373(12)
<i>α</i> /deg	90	90
<i>β</i> /deg	105.697(2)	90
<i>γ</i> /deg	90	90
<i>V</i> /Å <sup>3</sup>	3954.3(4)	7093.1(4)
<i>Z</i>	8	8
<i>D<sub>c</sub></i> /Mgm <sup>-3</sup>	1.539	1.587
<i>μ</i> /mm <sup>-1</sup>	1.658	1.696
<i>F</i> (000)	1840	3424
cryst size/mm <sup>3</sup>	0.5 × 0.3 × 0.2	0.5 × 0.3 × 0.2
<i>θ</i> /deg	2.091 – 25.712	2.405 – 28.733
Measured reflns	9889	9139
Unique reflns	3912	10062
<sup>a</sup> GOF on <i>F</i> <sup>2</sup>	1.117	1.191
<i>R</i> 1 <sup>b</sup> , <i>wR</i> 2 <sup>c</sup> [ <i>I</i> > 2σ( <i>I</i> )]	0.0425, 0.0986	0.0368, 0.0827
<i>R</i> 1, <i>wR</i> 2	0.0521, 0.1045	0.0423, 0.0858
<sup>a</sup> GOF = {Σ[w( <i>F<sub>o</sub></i> <sup>2</sup> - <i>F<sub>c</sub></i> <sup>2</sup> )]/( <i>n</i> - <i>p</i> )} <sup>1/2</sup> . <sup>b</sup> <i>R</i> 1 = Σ [  <i>F<sub>o</sub></i>  - <i>F<sub>c</sub></i> ]/ Σ   <i>F<sub>o</sub></i>  .		
<sup>c</sup> <i>wR</i> 2 = [Σ [w( <i>F<sub>o</sub></i> <sup>2</sup> - <i>F<sub>c</sub></i> <sup>2</sup> )]/ Σ [w( <i>F<sub>o</sub></i> <sup>2</sup> )] <sup>1/2</sup> where <i>w</i> = 1/[σ <sup>2</sup> ( <i>F<sub>o</sub></i> <sup>2</sup> )+( <i>aP</i> ) <sup>2</sup> + <i>bP</i> ], <i>P</i> = ( <i>F<sub>o</sub></i> <sup>2</sup> +2 <i>F<sub>c</sub></i> <sup>2</sup> )/3.		

**Table S2.** Selected Experimental and Theoretical Bond Parameters of **1a** and **1b** complex.

<b>1a</b>			<b>1b</b>		
<b>Parameter</b>	<b>Expt.</b>	<b>Theo.</b>	<b>Parameter</b>	<b>Expt.(average)</b>	<b>Theo.</b>
Zn1–Cl1	2.2125(9)	2.349	Zn1–Cl1	2.221(7)	2.299
Zn1–Cl2	2.2272(9)	2.355	Zn1–Cl2	2.210(7)	2.283
Zn1–N1	2.167(3)	2.228	Zn1–N1	2.170(19)	2.279
Zn1–N3	2.127(2)	2.245	Zn1–N3	2.126(17)	2.246
Zn1–N4	2.466(3)	2.593	Zn1–N4	2.452(17)	2.451
N2–N3	1.260(3)	1.261	N2–N3	1.259(2)	1.261
N4–N5	1.263(4)	1.263	N4–N5	1.257(3)	1.265
Cl1Zn1Cl2	123.35(4)	129.99	Cl1Zn1Cl2	126.54(3)	132.27
Cl1Zn1N4	94.71(6)	97.82	Cl1Zn1N4	95.78(5)	100.58
Cl2Zn1N4	98.87(6)	96.67	Cl2Zn1N4	96.53(5)	96.89
N1Zn1Cl1	99.51(7)	99.76	N1Zn1Cl1	99.90(5)	97.66
N1Zn1Cl2	100.84(7)	99.57	N1Zn1Cl2	99.98(5)	96.39
N1Zn1N4	143.59(9)	139.22	N1Zn1N4	143.54(6)	140.26
N3Zn1Cl1	126.89(7)	127.45	N3Zn1Cl1	115.64(5)	107.27
N3Zn1Cl2	109.54(7)	102.35	N3Zn1Cl2	117.54(5)	120.41
N3Zn1N1	73.25(9)	71.54	N3Zn1N1	73.14(7)	70.10
N3Zn1N4	71.40(9)	68.88	N3Zn1N4	72.51(6)	70.86
C1N1Zn1	128.9(2)	127.08	C1N1Zn1	128.99(17)	126.89
C5N1Zn1	113.5(2)	114.02	C5N1Zn1	113.04(2)	114.16
N3N2C5	113.6(2)	114.92	N3N2C5	113.30(17)	114.25
C6N3Zn1	123.02(19)	123.35	C6N3Zn1	122.48(13)	120.81
N2N3C6	116.0(2)	117.11	N2N3C6	116.38(17)	117.51
N2N3Zn1	120.85(19)	119.38	N2N3Zn1	120.73(13)	121.50
C11N4Zn1	110.28(18)	110.20	C11N4Zn1	110.11(12)	112.27
N5N4C11	112.4(3)	113.42	N5N4C11	113.04(18)	113.33
N5N4Zn1	135.2(2)	133.11	N5N4Zn1	134.57(15)	132.25
N4N5C12	116.6(3)	118.24	N4N5C12	116.34(19)	118.41

## Physical measurements

NMR spectra ( $^1\text{H}$ ,  $^{13}\text{C}$ , and  $^{19}\text{F}$ ) of all complexes were obtained from Bruker FT 300 and 400 MHz spectrometer. Electron Paramagnetic Resonance (EPR) spectrum was taken for the sample in standard quartz EPR tubes using a JEOL JES-FA200 X-band spectrometer. Instrument settings: microwave frequency, 9.458 GHz; microwave power, 0.998 mW; modulation frequency, 100 kHz. According to residual protium in the NMR solvent ( $\text{CHCl}_3 = \delta 7.26$ ), chemical shifts for protons are reported in parts per million downfield from tetramethylsilane. The chemical shifts for carbon produced from tetramethylsilane are given in parts per million with references to the carbon resonances of the solvent ( $\text{CDCl}_3 = \delta 77.16$ ). The following data are shown: chemical shift, multiplicity (s = singlet, d = doublet, t = triplet, q = quartet, m = multiplet, dd = doublet of doublets, ddd = doublet of doublets of doublets, dt = doublet of triplets, dq = doublet of quartets, tt = triplet of triplets, td = triplet of doublets, coupling constants in Hertz (Hz), integration. Elemental analysis (C, H, N) was done on a Perkin Elmer 2400 series II Analyzer. Infrared spectra were acquired from PerkinElmer L-0010 spectrometer. The absorption spectra were recorded using PerkinElmer LAMDA 25 spectrometer with solute concentration about  $10^{-5}$  M.

## Computational Study

The singlet ground state ( $S_0$ ) and excited state molecular geometries of synthesised complex **1a** and **1b** were computed by DFT method by employing (R)B3LYP<sup>1,2</sup> in GAUSSIAN 09<sup>3</sup> programme package. The solution phase optimised geometries of the complexes were found without applying any geometry constraints. In order to verify all stationary points as the true minima in potential energy surface, frequency calculation was executed. The absence of any imaginary frequency (NImag = 0) indicates that all the obtained stationary points are indeed the true minima in potential energy surface. The X-Ray positional coordinates of complex **1a** and **1b** were directly used as the initial input for geometry optimisation calculation. By using these ground state optimised geometries as well as excited state geometries, we performed subsequent Single Point Energy and TD-DFT<sup>4-7</sup> calculation. In TD-DFT calculation we employ conductor like continuum model (CPCM)<sup>8-10</sup> and dichloromethane ( $\text{CH}_2\text{Cl}_2$ ) as solvent to simulate absorption spectra in dichloromethane solvent. The lowest 100 singlet-singlet transitions in absorption and emission processes for the complex **1a** and **1b** were evaluated gradually. The experimental results and the results obtained from TD calculations were qualitatively comparable. Presently the approach of

TD-DFT is documented as a rigorous formalism for the electronic excitation energies among the DFT framework for calculating spectral properties of many transition metal complexes<sup>11-14</sup>. In order to acquire the information and nature of absorption and emission processes natural transition orbital (NTO) analysis was executed. This method delivers the most accurate representation of the transition density between the ground and excited states in terms of an expansion into single-particle transitions (hole and electron states for each given excitation). We refer to the unoccupied and occupied NTOs as “electron” and “hole” transition orbitals. The computed vertical transitions were calculated at the equilibrium geometry of the  $S_0$  state and described in terms of one-electron excitations of molecular orbitals of the corresponding  $S_0$  geometry. The calculated transitions with moderate intensities ( $f \geq 0.02$ ) can be envisaged going from the lower to the higher energy region of the spectrum. The zinc atom was described by a double- $\zeta$  basis set with the effective core potential of Hay and Wadt (LANL2DZ)<sup>15,16</sup>, and the 6-311++G(d,p)<sup>17,18</sup> basis set was used for the other elements except hydrogen atom (6-31G) present in the complexes to optimize the ground state geometries. The calculated electronic density plots for frontier molecular orbitals were prepared by using the GaussView 6.0 software. GaussSum program, version 3.2<sup>19</sup>, was used to calculate the molecular orbital contributions from groups or atoms.

### Synthesis of ligands:

The organic ligands  $L^{Cl}$  and  $L^H$  comprising two electron-deficient azo moieties along with an aromatic heterocyclic group have been prepared by condensation of (*E*)-2-((4-chlorophenyl)azo)aniline or (*E*)-2-(phenylazo)aniline with 2-nitrosopyridine using the previously reported procedure.<sup>20</sup>

### Synthesis of complexes:

**[Zn( $L^{Cl}$ )Cl<sub>2</sub>] 1a** Anhydrous ZnCl<sub>2</sub> (136 mg, 1.00 mmol) was added to a solution of ( $L^{Cl}$ ) (354 mg, 1.10 mmol) in ethanol (25 mL) under open air. The reaction mixture was stirred at room temperature for 6 hrs. The solvent was removed under reduced pressure. Slow diffusion of the dichloromethane solution of the complex into n-hexane led to the crystallisation of **1a** as rod-shaped crystals. Yield and characterization data: Blood-red crystal, Yield 90% (412 mg). Anal. Calcd. for C<sub>17</sub>H<sub>12</sub>N<sub>5</sub>Cl<sub>3</sub>Zn: C 44.58, H 2.64, N 15.29; Found C 44.98, H 2.69, N 15.16%. <sup>1</sup>H-NMR (400 MHz, DMSO-*d*<sub>6</sub>):  $\delta$  (ppm) 8.76 (d,  $J = 5.4$  Hz, 1H), 8.07 (t,  $J = 7.8$  Hz, 1H), 7.93-7.90 (m, 2H), 7.79-7.75 (m, 4H), 7.70-7.64 (m, 3H), 7.62-7.59 (m, 1H). <sup>13</sup>C-NMR (100 MHz, DMSO-*d*<sub>6</sub>):

$\delta$  (ppm) 163.3, 151.3, 150.0, 149.9, 147.8, 147.4, 137.0, 132.9, 132.3, 130.2, 126.6, 125.0, 124.9, 119.4, 119.0, 113.5. FT-IR ( $\text{cm}^{-1}$ ): 1459, 1390 ( $\nu_{\text{N}=\text{N}}$ ).

**[Zn(L<sup>H</sup>)Cl<sub>2</sub>] 1b** The former procedure has been applied with same stoichiometrically amount to synthesised complex **1b**. Yield and characterization data: Blood-red crystal, Yield 85% (360 mg). Anal. Calcd. for C<sub>17</sub>H<sub>13</sub>N<sub>5</sub>Cl<sub>2</sub>Zn: C 48.20, H 3.09, N 16.53; Found C 48.61, H 3.13, N 16.41%. <sup>1</sup>H-NMR (400 MHz, DMSO-*d*<sub>6</sub>):  $\delta$  (ppm) 8.75 (d,  $J = 5.4$  Hz, 1H), 8.06 (t,  $J = 7.8$  Hz, 1H), 7.90 (d,  $J = 7.7$  Hz, 2H), 7.79-7.74 (m, 4H), 7.68 (d,  $J = 8.1$  Hz, 1H), 7.62-7.59 (m, 4H). <sup>13</sup>C-NMR (100 MHz, DMSO-*d*<sub>6</sub>):  $\delta$  (ppm) 163.4, 152.8, 149.9, 148.0, 147.4, 139.5, 132.8, 132.5, 131.9, 130.0, 129.1, 128.7, 126.6, 123.3, 119.5, 118.8, 113.4. FT-IR ( $\text{cm}^{-1}$ ): 1456, 1397 ( $\nu_{\text{N}=\text{N}}$ ).

## NMR Spectrum of Complexes

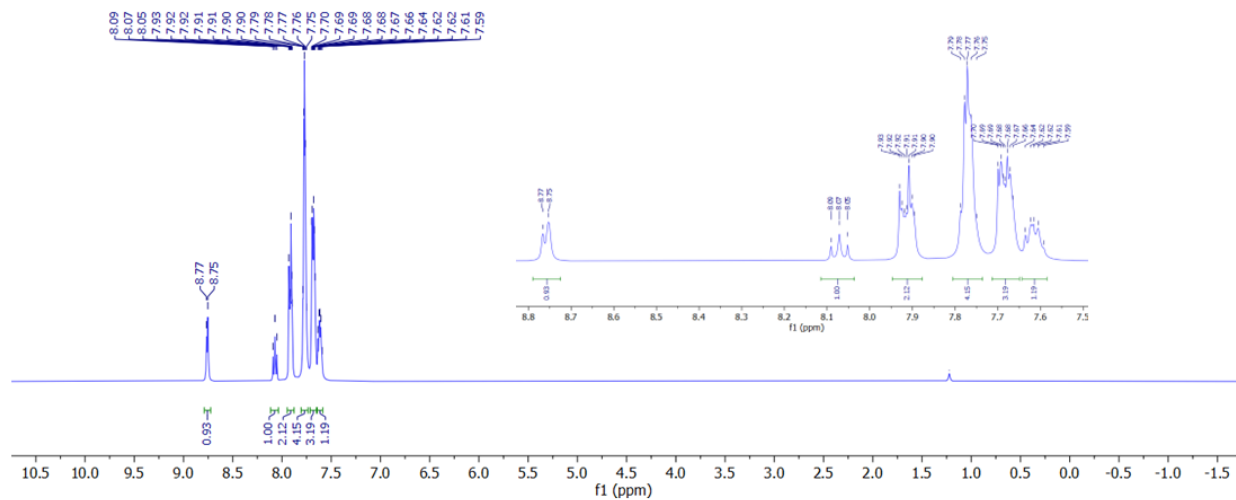


**Fig. S1** <sup>1</sup>H NMR spectrum of complex **1a** (400 MHz, DMSO-*d*<sub>6</sub>).

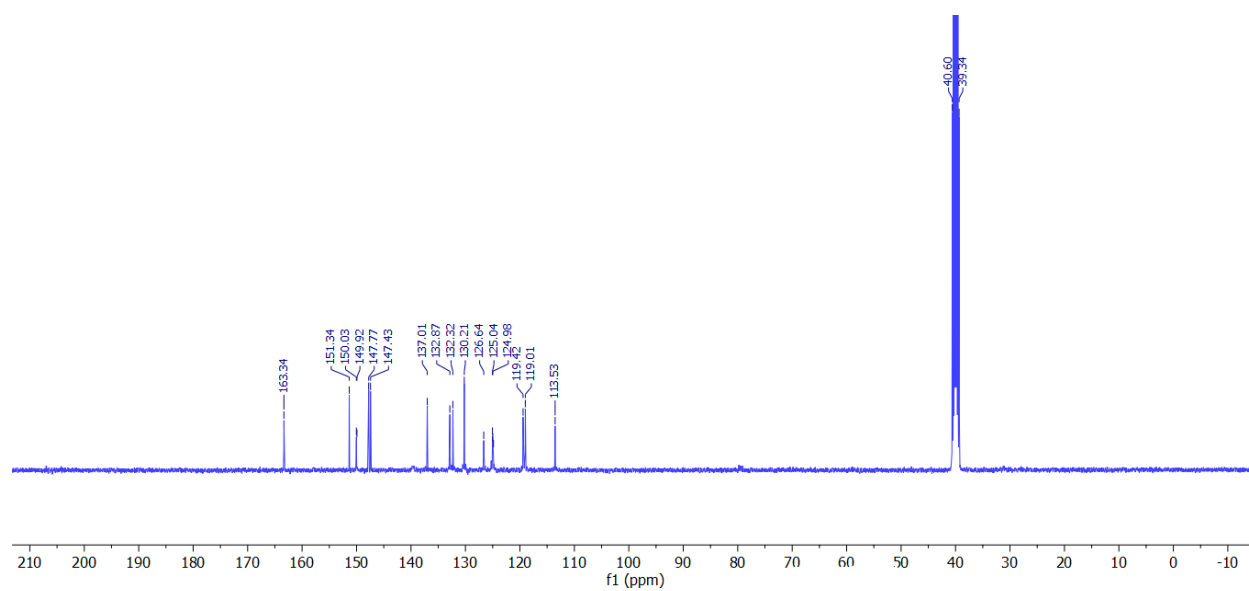


**Fig. S2** <sup>13</sup>C NMR spectrum of complex **1a** (101 MHz, DMSO-*d*<sub>6</sub>).



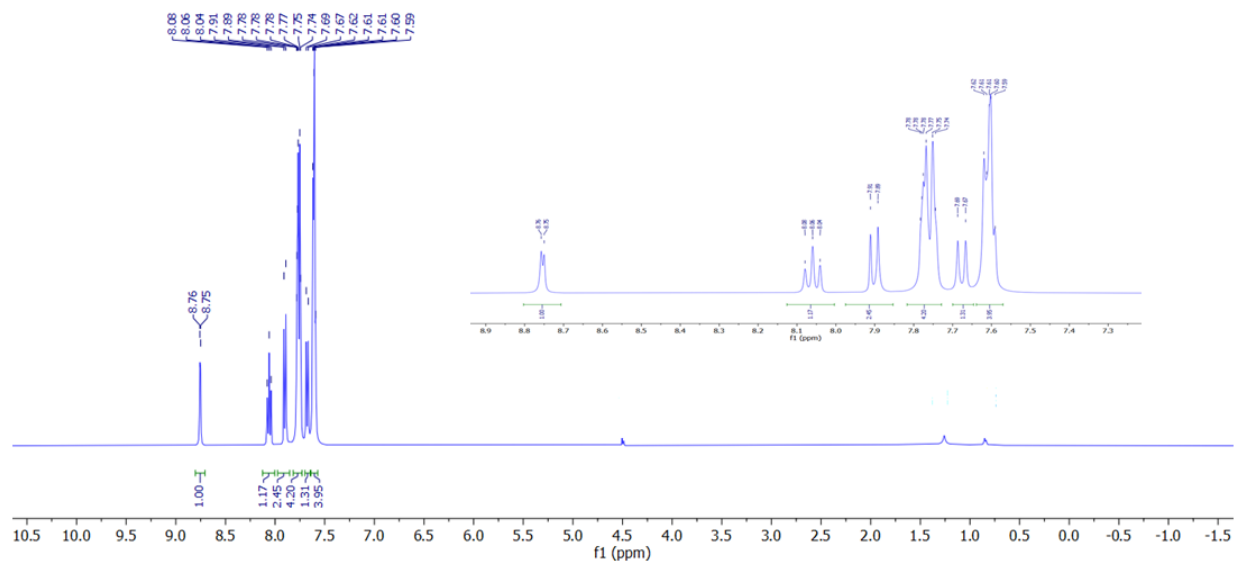


**Fig. S3**  $^1\text{H}$  NMR spectrum of complex **1b** (400 MHz,  $\text{DMSO-}d_6$ ).

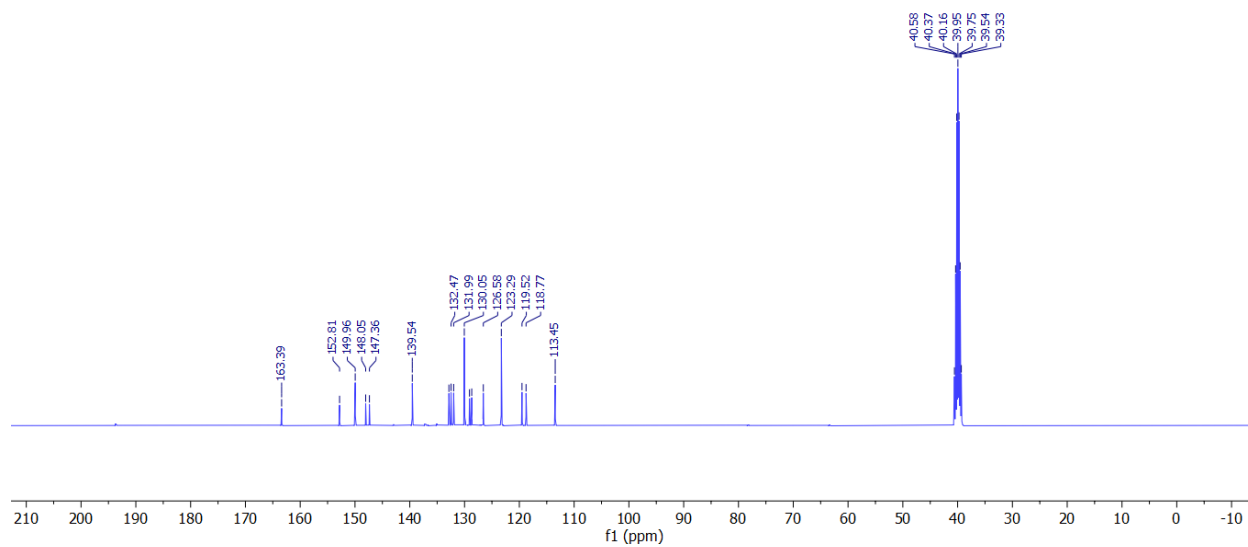


**Fig. S4**  $^{13}\text{C}$  NMR spectrum of complex **1b** (101 MHz,  $\text{DMSO-}d_6$ ).

**Table S3.** Frontier Molecular Orbital Composition (%) in the Ground State for **1a** complex.

Orbital	MO	Energy (eV)	Composition						Contribution
			Zn	Azo 1	Azo 2	Cl	Py	Ph	
112	L+5	-0.80	0	0	4	0	3	93	$\pi^*$ (Ph)
111	L+4	-0.82	0	0	5	0	2	93	$\pi^*$ (Ph)
110	L+3	-1.27	0	5	1	0	55	39	$\pi^*$ (Py + Ph)
109	L+2	-2.01	0	2	0	0	94	4	$\pi^*$ (Py)
108	L+1	-3.05	1	4	46	1	3	45	$\pi^*$ (Azo + Ph)
107	LUMO	-3.99	0	44	5	1	25	24	$\pi^*$ (Azo +Py +Ph)
106	HOMO	-6.54	1	1	22	31	1	43	lp (Azo) + $\pi$ (Cl + Ph)
105	H-1	-6.67	1	0	1	95	0	3	$\pi$ (Cl + Ph)
104	H-2	-6.73	1	0	1	93	1	4	$\pi$ (Cl)
103	H-3	-6.78	5	1	0	90	2	3	$\pi$ (Cl)
102	H-4	-6.90	9	0	4	63	0	24	$\pi$ (Cl + Ph + Py + Azo)
101	H-5	-7.39	3	8	38	20	3	28	$\pi$ (Azo + Ph + Cl)

**Table S4.** Frontier Molecular Orbital Composition (%) in the Ground State for **1b** complex.

Orbital	MO	Energy (eV)	Composition						Contribution
			Zn	Azo 1	Azo 2	Cl	Py	Ph	
104	L+5	-0.54	0	0	3	0	0	97	$\pi^*$ (Ph)
103	L+4	-0.67	0	1	7	0	5	87	$\pi^*$ (Ph)
102	L+3	-1.14	0	4	1	0	55	39	$\pi^*$ (Py + Ph + Azo)
101	L+2	-1.82	0	1	0	0	94	4	$\pi^*$ (Py)
100	L+1	-2.97	1	5	45	1	3	45	$\pi^*$ (Azo + Ph)
99	LUMO	-3.85	0	44	6	1	24	25	$\pi^*$ (Azo +Py +Ph)
98	HOMO	-6.53	2	1	19	44	1	32	lp (Azo) + $\pi$ (Cl + Ph)
97	H-1	-6.67	2	0	4	88	1	5	$\pi$ (Cl)
96	H-2	-6.73	1	0	4	85	1	10	$\pi$ (Cl)

95	H-3	-6.79	3	1	0	90	2	4	$\pi$ (Cl)
94	H-4	-6.91	9	1	6	58	1	26	$\pi$ (Cl + Ph + Azo)
93	H-5	-7.24	1	2	1	8	0	88	$\pi$ (Ph + Cl)

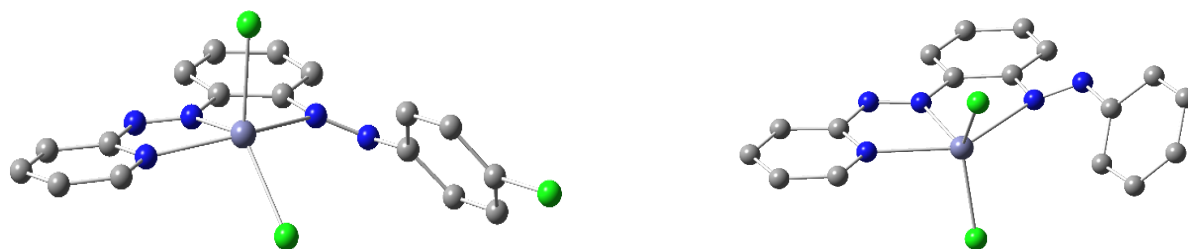


**Fig. S5** Solvent phase optimised geometry of **1a** (left) and **1b** (right) complex (H's are omitted for clarity) calculated at B3LYP/6-311+G(d,p) level of theory.

**Table S5.** Main Optical Transition at the TD-DFT/B3LYP/6-31+G(d,p) Level for the complex **1a** with composition in terms of Molecular Orbital Contribution of the Transition, Computed Vertical Excitation Energies, and Oscillator Strength in Dichloromethane.

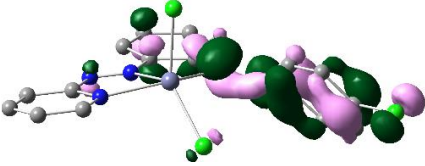
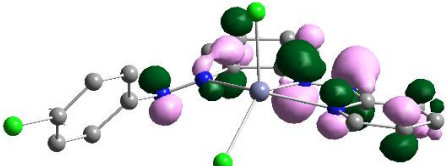
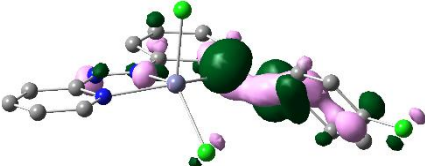
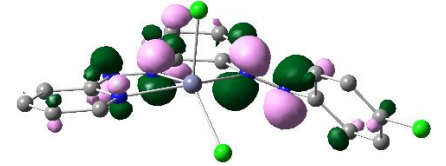
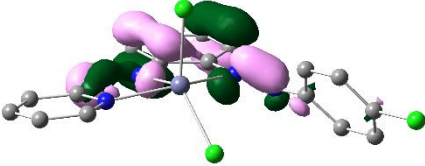
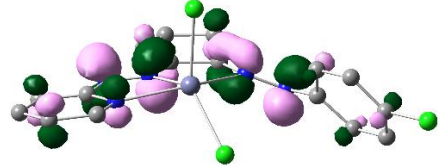
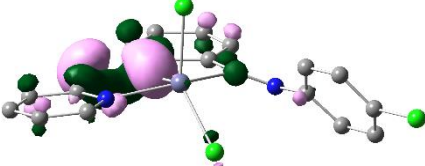
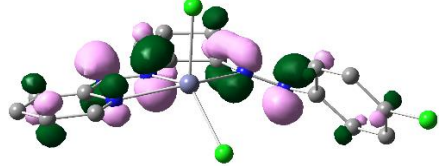
Transition	CI	Composition	E (eV)	Oscillator Strength ( <i>f</i> )	$\lambda_{\text{theo}}$ (nm)
$S_0 \rightarrow S_1$	0.63460	HOMO $\rightarrow$ LUMO (81%)	2.23654	0.1586	554.39
$S_0 \rightarrow S_3$	0.51482	HOMO $\rightarrow$ L+1 (53%)	2.7684	0.0243	447.86
$S_0 \rightarrow S_7$	0.55532 0.32956	H-5 $\rightarrow$ LUMO (62%) H-4 $\rightarrow$ LUMO (22%)	3.0766	0.1091	402.99
$S_0 \rightarrow S_8$	0.42948 0.40887	H-2 $\rightarrow$ LUMO (37%) H-3 $\rightarrow$ LUMO (33%)	3.1584	0.4438	392.56
$S_0 \rightarrow S_{12}$	0.42254 0.35229	H-1 $\rightarrow$ L+1 (36%) H-2 $\rightarrow$ L+1 (25%)	3.6283	0.3418	341.71

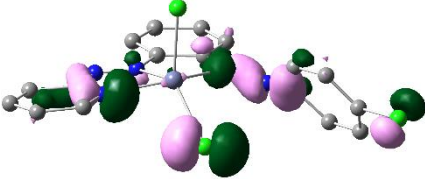
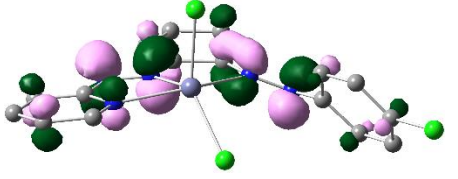
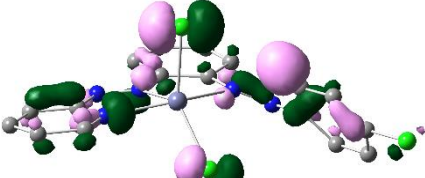
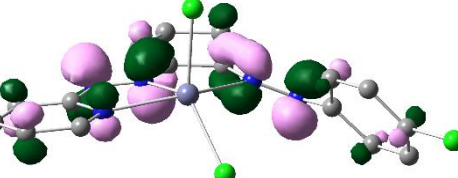
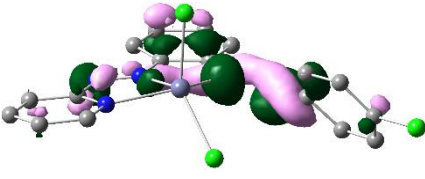
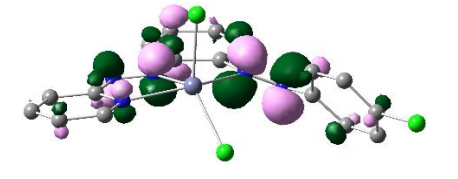
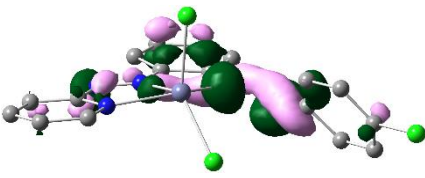
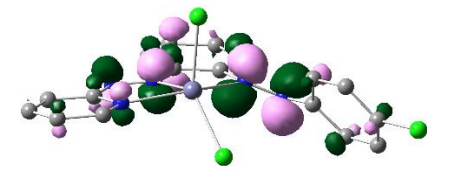
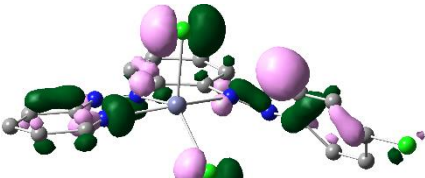
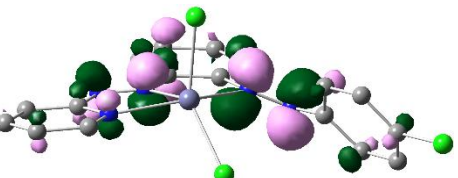
$S_0 \rightarrow S_{14}$	0.48405 0.38441	H-1 $\rightarrow$ L+1 (47%) H-3 $\rightarrow$ L+1 (30%)	3.7226	0.1571	333.05
$S_0 \rightarrow S_{15}$	0.67201	H-4 $\rightarrow$ L+1 (90%)	3.7960	0.0121	326.62
$S_0 \rightarrow S_{17}$	0.66652	H-5 $\rightarrow$ L+1 (89%)	3.8345	0.0315	323.34
$S_0 \rightarrow S_{30}$	0.52252 0.27871	HOMO $\rightarrow$ L+4 (55%) HOMO $\rightarrow$ L+3 (16%)	5.0444	0.0282	245.79
$S_0 \rightarrow S_{38}$	0.50026 -0.43140	H-5 $\rightarrow$ L+2 (50%) H-2 $\rightarrow$ L+2 (37%)	5.2230	0.0294	237.38
$S_0 \rightarrow S_{41}$	0.61394	HOMO $\rightarrow$ L+5 (75%)	5.3973	0.0176	229.72

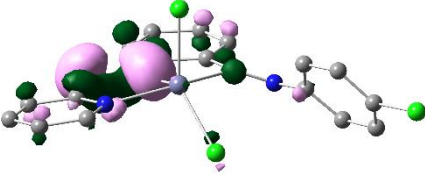
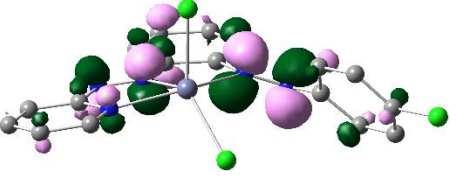
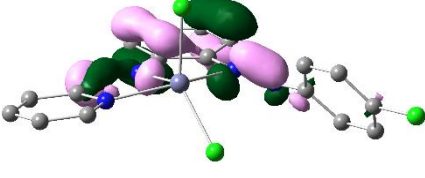
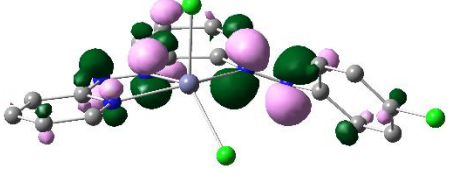
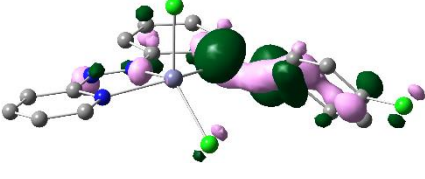
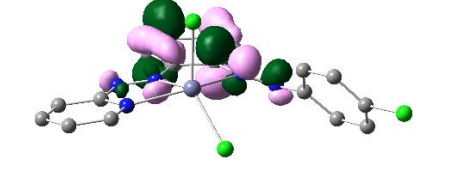
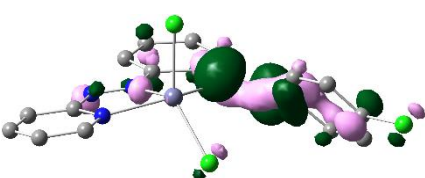
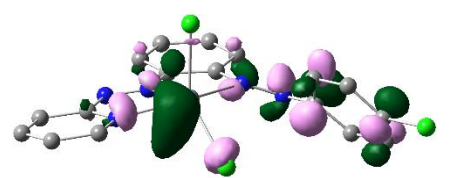
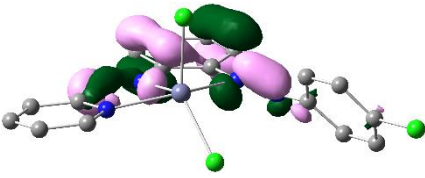
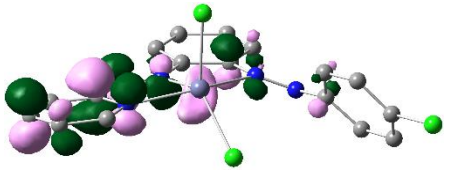
**Table S6.** Main Optical Transition at the TD-DFT/B3LYP/6-31+G(d,p) Level for the complex **1b** with composition in terms of Molecular Orbital Contribution of the Transition, Computed Vertical Excitation Energies, and Oscillator Strength in Dichloromethane.

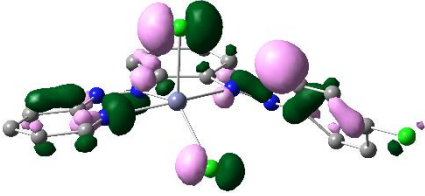
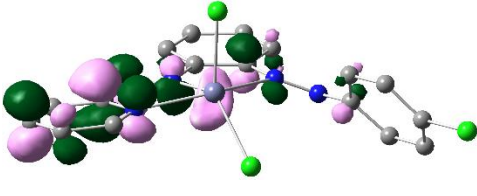
<b>Transition</b>	<b>CI</b>	<b>Composition</b>	<b>E (eV)</b>	<b>Oscillator Strength (<i>f</i>)</b>	<b><math>\lambda_{\text{theo}}</math> (nm)</b>
$S_0 \rightarrow S_1$	0.61198	HOMO $\rightarrow$ LUMO (75%)	2.3093	0.1272	536.90
$S_0 \rightarrow S_3$	0.48488	HOMO $\rightarrow$ L+1 (47%)	2.8147	0.0180	440.49
$S_0 \rightarrow S_6$	0.64522	H-4 $\rightarrow$ LUMO (83%)	3.1318	0.0125	395.88
$S_0 \rightarrow S_{11}$	0.56551	H-1 $\rightarrow$ L+1 (64%)	3.6127	0.1311	343.19
$S_0 \rightarrow S_{12}$	0.49452 -0.31640	H-2 $\rightarrow$ L+1 (49%) H-1 $\rightarrow$ L+1 (20%)	3.6914	0.3604	335.87
$S_0 \rightarrow S_{26}$	0.65379	HOMO $\rightarrow$ L+2 (85%)	4.7083	0.0162	263.33
$S_0 \rightarrow S_{35}$	0.49423 0.39368	HOMO $\rightarrow$ L+4 (49%) H-4 $\rightarrow$ L+2 (31%)	5.3128	0.0216	233.37

**Table S7.** Natural transition orbitals (NTOs) for complex **1a** illustrating the nature of singlet excited states in the absorption bands in the range 200–700 nm. For each state, the respective number of the state, transition energy (eV), and the oscillator strength (in parentheses) are listed. Shown are only occupied (holes) and unoccupied (electrons) NTO pairs that contribute more than 15% to each excited state.

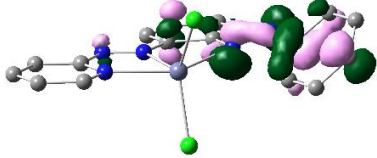
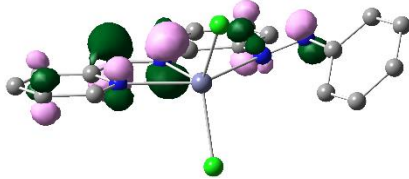
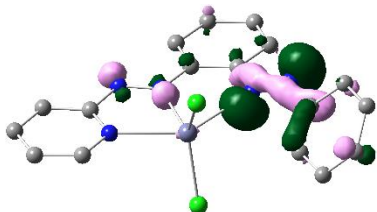
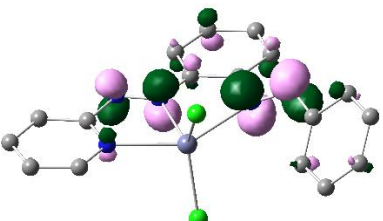
Wavelength	Transition	Hole	electron
500 nm	S1 w = 0.8055 f = 0.1586 554.39 nm		
	S3 w = 0.5300 f = 0.0243 447.86 nm		
360 nm	S7 w = 0.6167 f = 0.1091 402.99 nm		
	S7 w = 0.2172 f = 0.1091 402.99 nm		

	<p>S8</p> <p><math>w = 0.3689</math></p> <p><math>f = 0.4438</math></p> <p>392.56 nm</p>		
	<p>S8</p> <p><math>w = 0.3343</math></p> <p><math>f = 0.4438</math></p> <p>392.56 nm</p>		
333 nm	<p>S12</p> <p><math>w = 0.3570</math></p> <p><math>f = 0.1571</math></p> <p>341.71 nm</p>		
	<p>S14</p> <p><math>w = 0.4686</math></p> <p><math>f = 0.1571</math></p> <p>333.05 nm</p>		
	<p>S14</p> <p><math>w = 0.2955</math></p> <p><math>f = 0.1571</math></p> <p>333.05 nm</p>		

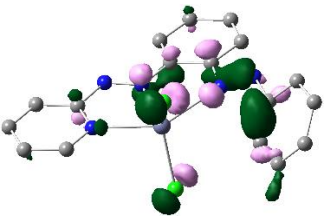
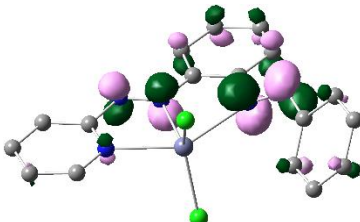
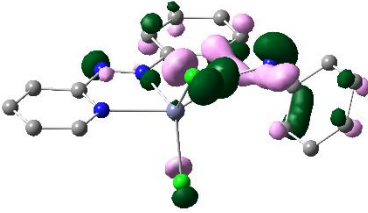
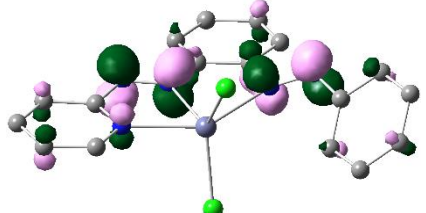
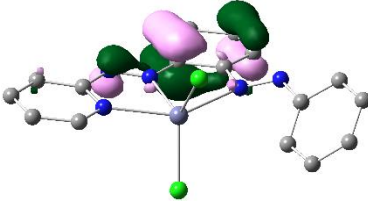
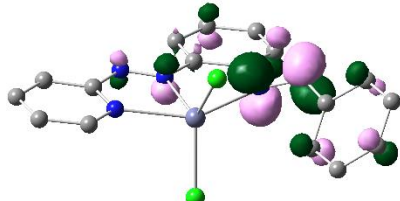
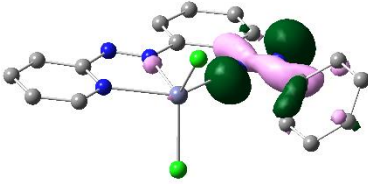
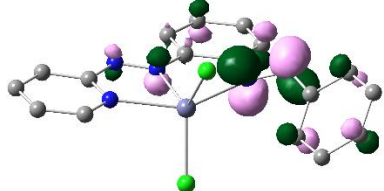
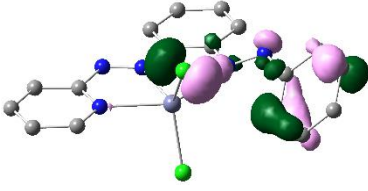
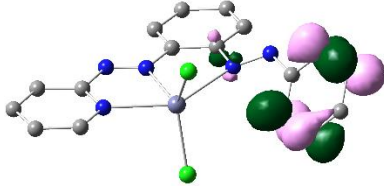
	<p>S15</p> <p><math>w = 0.9031</math></p> <p><math>f = 0.0121</math></p> <p>326.62 nm</p>		
	<p>S17</p> <p><math>w = 0.8885</math></p> <p><math>f = 0.0315</math></p> <p>323.34 nm</p>		
236 nm	<p>S30</p> <p><math>w = 0.5460</math></p> <p><math>f = 0.0282</math></p> <p>245.79 nm</p>		
	<p>S30</p> <p><math>w = 0.1553</math></p> <p><math>f = 0.0282</math></p> <p>245.79 nm</p>		
	<p>S38</p> <p><math>w = 0.5005</math></p> <p><math>f = 0.0294</math></p> <p>237.38 nm</p>		

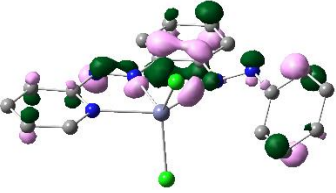
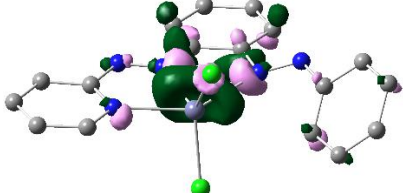
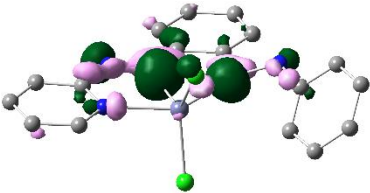
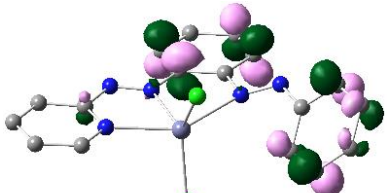
	<p>S38</p> <p>w = 0.3722</p> <p>f = 0.0294</p> <p>237.38 nm</p>		
--	---	--	---

**Table S8.** Natural transition orbitals (NTOs) for complex **1b** illustrating the nature of singlet excited states in the absorption bands in the range 200–700 nm. For each state, the respective number of the state, transition energy (eV), and the oscillator strength (in parentheses) are listed. Shown are only occupied (holes) and unoccupied (electrons) NTO pairs that contribute more than 15% to each excited state.

Wavelength	Transition	Hole	Electron
499 nm	<p>S1</p> <p>w = 0.7490</p> <p>f = 0.1272</p> <p>536.90 nm</p>		
	<p>S3</p> <p>w = 0.4702</p> <p>f = 0.0180</p> <p>440.49 nm</p>		



365 nm	<p>S6</p> <p><math>w = 0.8326</math></p> <p><math>f = 0.0125</math></p> <p>395.88 nm</p>		
	<p>S11</p> <p><math>w = 0.6396</math></p> <p><math>f = 0.1311</math></p> <p>343.19 nm</p>		
335 nm	<p>S12</p> <p><math>w = 0.4891</math></p> <p><math>f = 0.3604</math></p> <p>335.87 nm</p>		
	<p>S12</p> <p><math>w = 0.2002</math></p> <p><math>f = 0.3604</math></p> <p>335.87 nm</p>		
235 nm	<p>S26</p> <p><math>w = 0.8548</math></p> <p><math>f = 0.0162</math></p> <p>263.33 nm</p>		

	<p>S35</p> <p><math>w = 0.4885</math></p> <p><math>f = 0.0216</math></p> <p>233.37 nm</p>		
	<p>S35</p> <p><math>w = 0.3099</math></p> <p><math>f = 0.0216</math></p> <p>233.37 nm</p>		

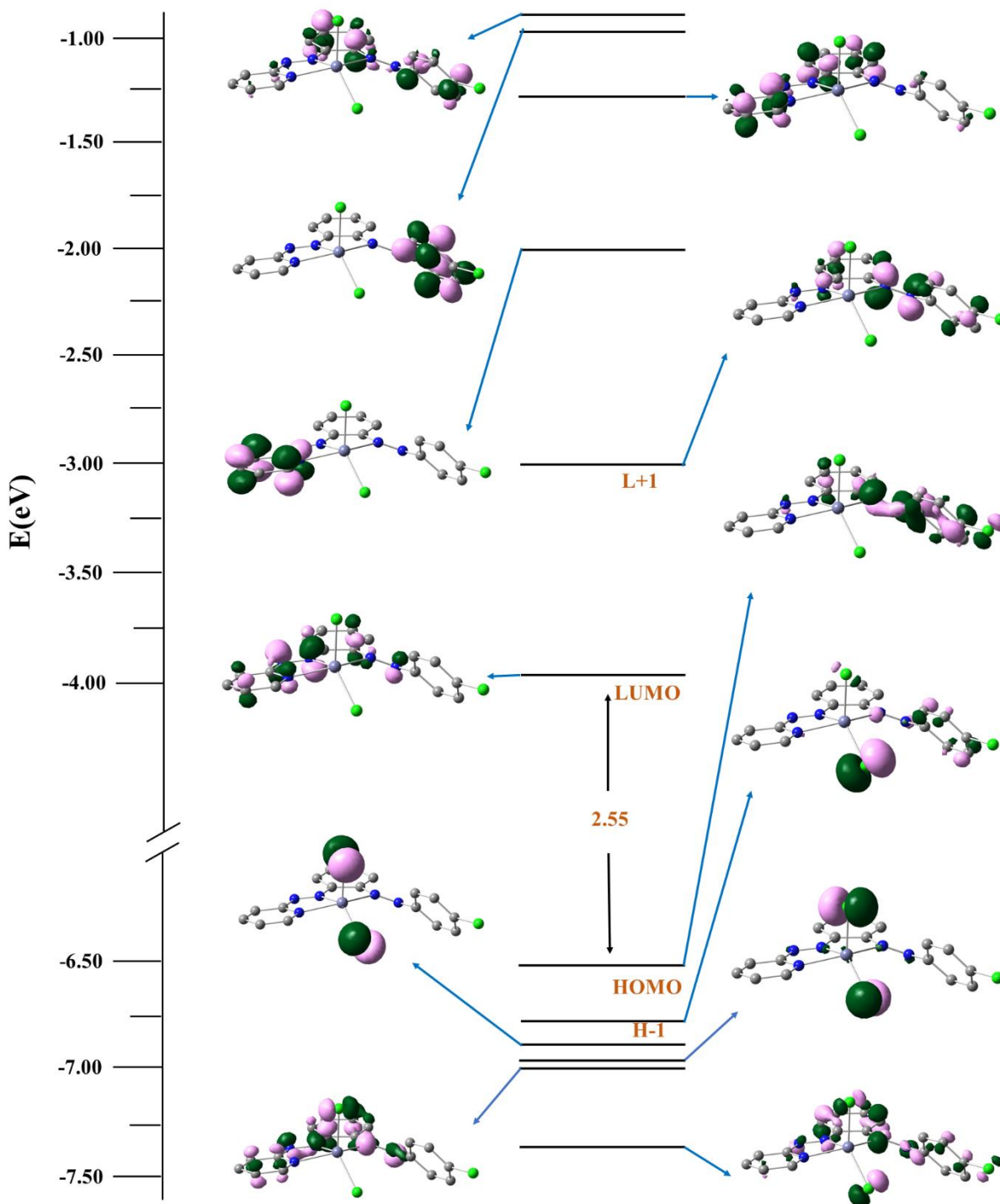


**Fig. S6** Partial MO diagram and isodensity surface plots (isovalued = 0.06) for selected FMOs of the **1a** complex. The arrows are used to highlight the HOMO–LUMO energy gaps. All the DFT energy values are given in eV.

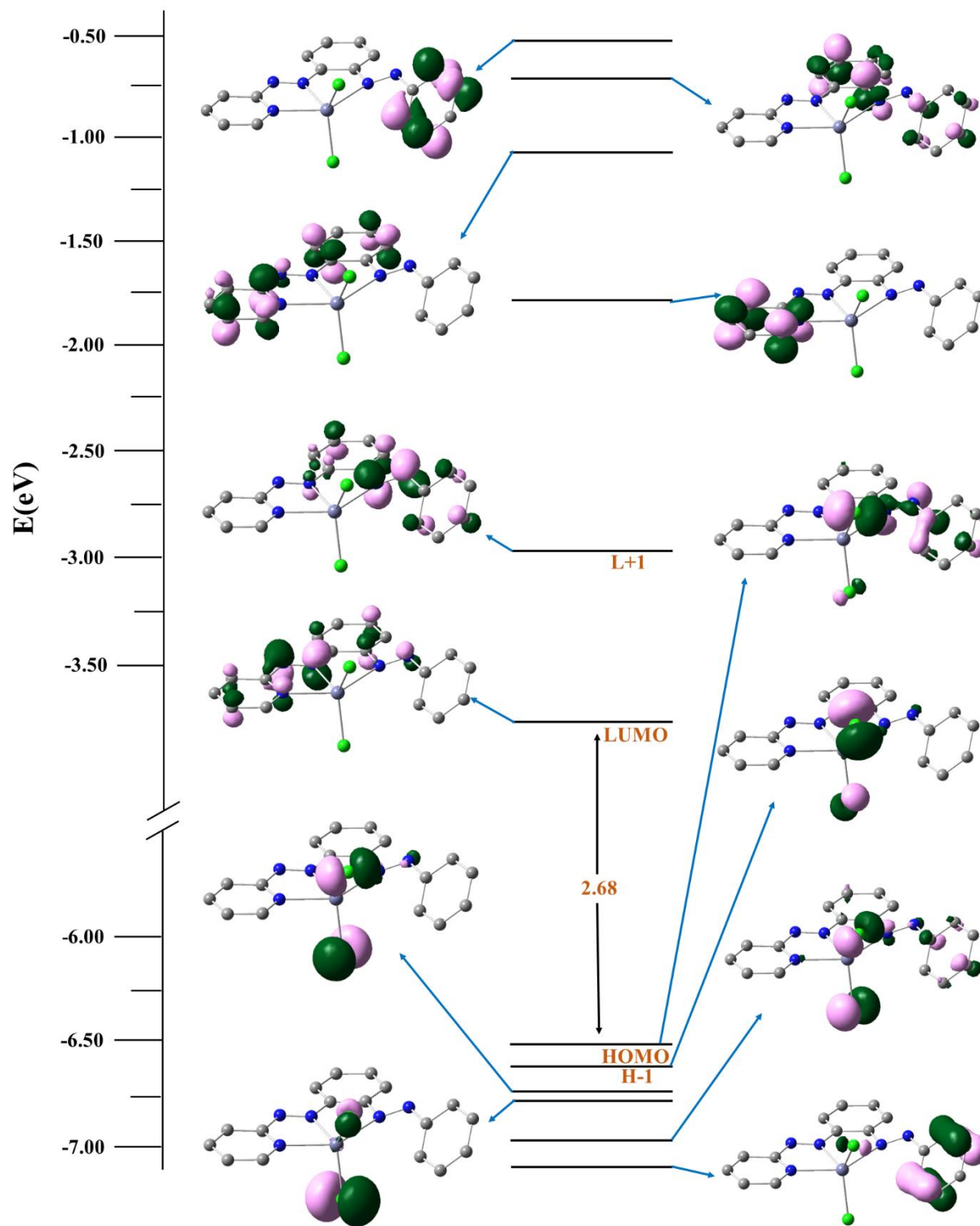


**Fig. S7** Partial MO diagram and isodensity surface plots (isovalue = 0.06) for selected FMOs of the **1b** complex. The arrows are used to highlight the HOMO-LUMO energy gaps. All the DFT energy values are given in eV.

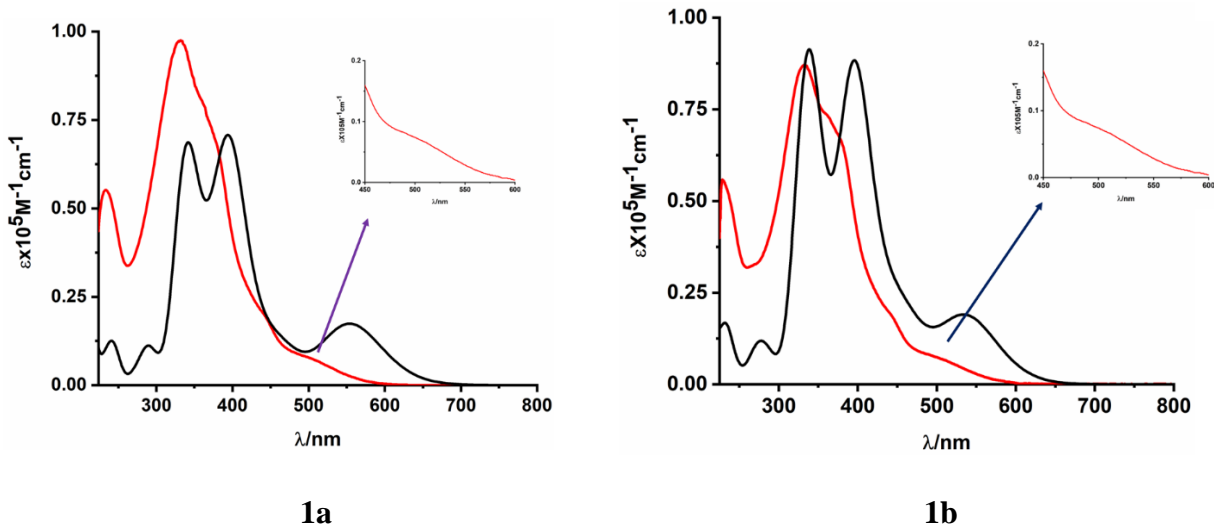


**Fig. S8** Experimental (red) and theoretical (black) absorption spectrum of **1a**(left) & **1b**(right) complex in CH<sub>2</sub>Cl<sub>2</sub> solution at 298 K.

**Table S9.** Coordinates of Optimised structure of complex **1a**.

Tag	Symbol	X	Y	Z
1	Zn	8.195225	9.3534933	6.8816697
2	Cl	10.5395086	9.3140769	6.7379555
3	Cl	6.7964702	9.4627584	8.7729097
4	Cl	8.5346613	5.3713459	12.8137888
5	N	7.5781739	9.0897911	4.7398266
6	N	7.3755557	10.1081465	4.0244872
7	N	7.7969172	11.3645132	6.0095758
8	N	7.7661971	6.8559533	6.3337638
9	N	7.3599379	5.878426	7.0228991
10	C	7.4901647	7.8375653	4.1101687
11	C	6.8133036	5.0961576	9.1974576
12	H	5.940998	4.6334343	8.7459912
13	C	7.501684	11.3436185	4.6981732
14	C	7.5572423	6.6888177	4.9389039
15	C	7.330742	7.6948734	2.7190553
16	H	7.2814801	8.5848944	2.103042
17	C	7.6851666	5.8475035	8.3883322

18	C	7.0535772	4.9687139	10.5620618
19	H	6.3714212	4.4110513	11.1946516
20	C	7.2441754	6.4294949	2.1549169
21	H	7.1281834	6.3237752	1.0805968
22	C	7.4789157	5.4165197	4.3482557
23	H	7.5609815	4.5408497	4.9813916
24	C	9.1085302	6.2623082	10.3027310
25	H	10.0084059	6.6830454	10.7388405
26	C	8.2036428	5.5535223	11.1011149
27	C	7.9042476	12.5445906	6.6251061
28	H	8.1378767	12.5168765	7.6851964
29	C	8.8467769	6.4155244	8.9451071
30	H	9.5559003	6.9397604	8.3137055
31	C	7.3047263	12.5031092	3.9450312
32	H	7.0676651	12.4223881	2.8899530
33	C	7.7294793	13.7600077	5.9508887
34	H	7.8311258	14.6949441	6.4913524
35	C	7.3188712	5.2886223	2.9723370
36	H	7.2645836	4.2989972	2.5283440
37	C	7.4259900	13.7363608	4.5898590
38	H	7.2846168	14.6598917	4.0373759

**Table S10.** Coordinates of Optimised structure of complex **1b**.

Tag	Symbol	X	Y	Z
1	Zn	5.8497188	10.6952617	8.0950091
2	N	5.4630069	12.9379152	8.2243246
3	C	5.6604181	13.8404438	7.2637583
4	H	5.9919415	13.4531045	6.3044442
5	C	5.4518569	15.210381	7.4702044
6	H	5.6275327	15.9118275	6.6609138
7	C	5.0173749	15.6425416	8.7238049

8	H	4.8460902	16.6975783	8.9172224
9	C	4.8020651	14.6974959	9.7282816
10	H	4.4599458	14.9700212	10.721001
11	C	5.0400722	13.353528	9.4270628
12	N	4.8060736	12.4087187	10.4547683
13	N	5.0260824	11.2134739	10.1191645
14	C	4.8302288	10.2211965	11.0907359
15	C	4.4825731	10.5085388	12.4243122
16	H	4.3654642	11.5446357	12.720157
17	C	4.299952	9.4750911	13.3310387
18	H	4.0379638	9.6977853	14.3614287
19	C	4.4640754	8.1411123	12.9172608
20	H	4.33138	7.3329533	13.6314688
21	C	4.8088633	7.8452624	11.6038152
22	H	4.952326	6.8213612	11.2791681
23	C	4.9893165	8.8776197	10.6676221
24	N	5.3818142	8.6282055	9.3253945
25	N	5.1368713	7.4477	8.9428968
26	C	5.6214787	7.037783	7.6952693
27	C	4.945617	5.9401727	7.1271904
28	H	4.0987793	5.5177564	7.6598718
29	C	5.3505882	5.439488	5.893779
30	H	4.8145361	4.6098317	5.4414059
31	C	6.4589912	5.9999601	5.2464033
32	H	6.7855757	5.6006153	4.2896422
33	C	7.1589088	7.0616543	5.833783
34	H	8.0301914	7.4811185	5.3389451
35	C	6.7472981	7.5899617	7.0534580
36	H	7.3126904	8.3912510	7.5187598
37	Cl	8.1421580	10.7701299	8.2514943
38	Cl	4.4420951	10.2952533	6.3421649

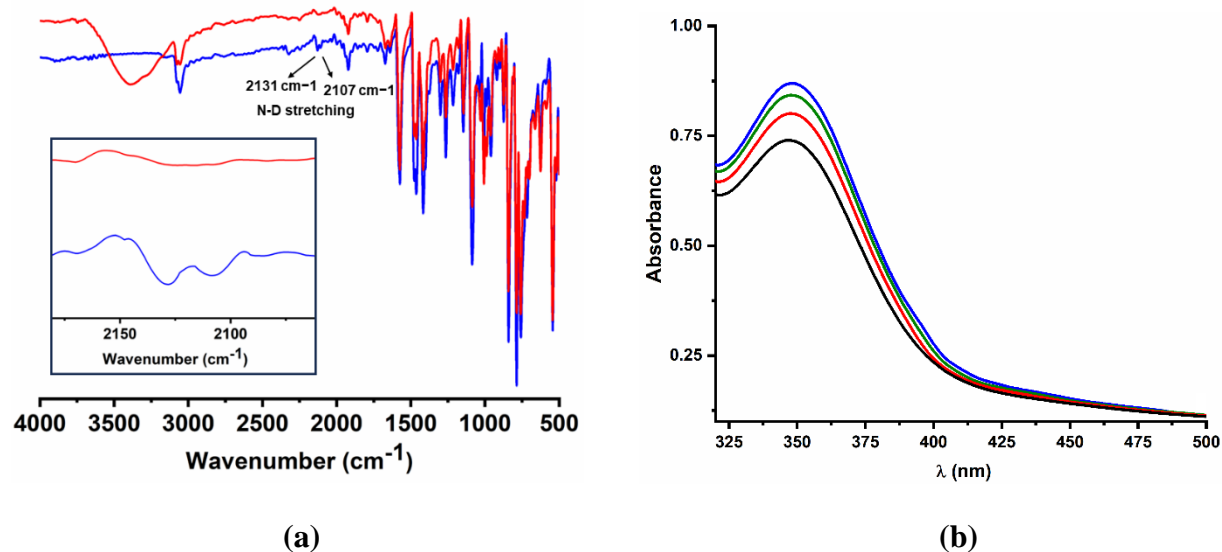


**Fig. S9** (a) IR spectrum of reaction mixture showing N-D stretching during dehydrogenation of non-deuterated 1-phenylethanol (red) and deuterated 1-phenylethanol (blue). (b) Electronic spectra of the formation of  $I_3^-$  ion in presence of  $H_2O_2$  (detection of  $H_2O_2$  was achieved as described in the text).

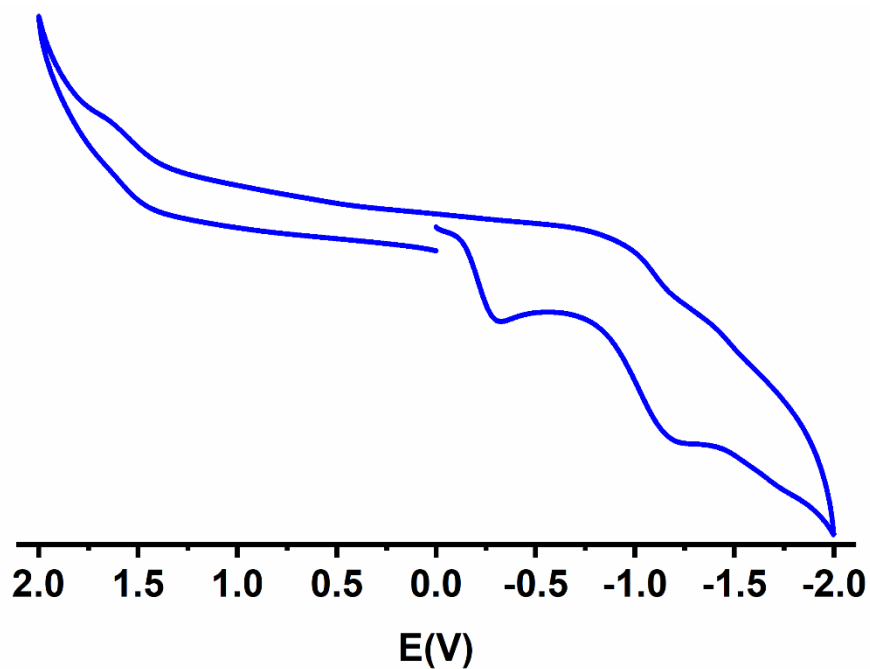


**Fig. S10** Cyclic voltammogram of **1a** in  $CH_3CN$  using 0.1 M  $Bu_4NPF_6$  using a Pt working electrode at  $50\text{ mV s}^{-1}$  with respect to Ag/AgCl reference electrode.



## X-Ray crystallographic information of 10aj and 5ag

The suitable crystals of all complexes were placed on Bruker D8 QUEST SC-XRD Diffractometer equipped with graphite monochromator (Mo K $\alpha$ ,  $\lambda = 0.71073 \text{ \AA}$ ) the crystals were kept at steady T= 273K during data collection. SAINT<sup>21</sup> crystallographic programme was utilized to integrate and scale the intensity data. SADABS<sup>22</sup> program was employed to process and rectify the integrated data. Data collection, reduction, absorption corrections were performed. The structure solution was carried out with SHELXT 2014/5<sup>23</sup> solution programme using iterative method and Olex2 1.5-dev<sup>24</sup> as the graphical user interface. The SHELXL 2018/3<sup>23</sup> programme was utilised to refine the model structure using full matrix least square minimisation on F<sup>2</sup>. Lastly, the consistency regarding thermal parameters, bond distances and estimated standard deviation (ESD) within respective atoms were accomplished using suitable commands in SHELXL programme. All non-hydrogen atoms were refined anisotropically. Riding model was applied to determine the position of H atoms geometrically and refined. ORTEP plot was used to draw the molecular structure using Olex2 1.5-dev as GUI. Crystallographic and refinement data of both complexes are given in Table S13. Additional refinement data can be found in CIF files.

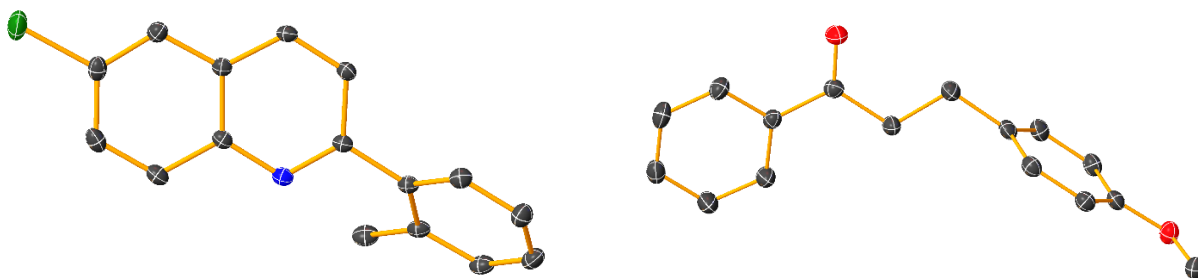
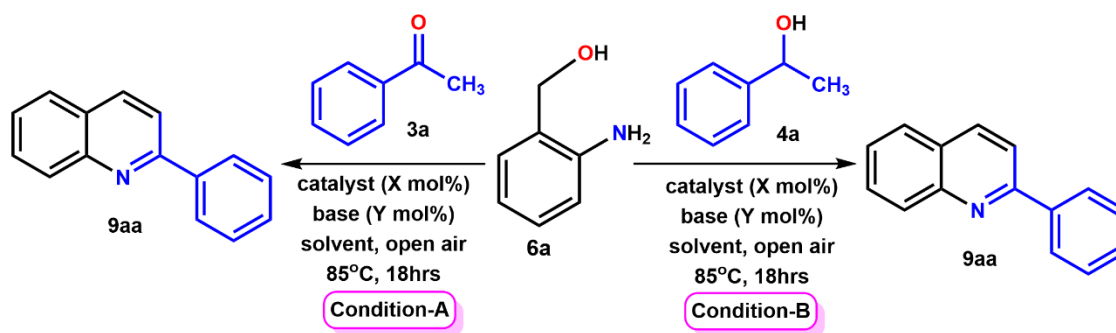


**Fig. S11** ORTEP view of **10aj** and **5ag** (hydrogen atoms are omitted for clarity, and thermal ellipsoids are set at 30% probability).

**Table S11.** Crystallographic Details of compound **10aj** and **5ag**.

	<b>10aj</b>	<b>5ag</b>
Empirical formula	C <sub>16</sub> H <sub>12</sub> N <sub>1</sub> Cl <sub>1</sub>	C <sub>16</sub> H <sub>16</sub> O <sub>2</sub>
<i>T</i> /K	298K	298K
fw	253.72	240.30
Crystal system	orthorhombic	monoclinic
Space Group	P 2c -2n	P 1 21/n 1
<i>a</i> /Å	7.6371(5)	9.1890(14)
<i>b</i> /Å	12.4931(8)	5.6168(9)
<i>c</i> /Å	13.4370(8)	24.833(4)
<i>α</i> /deg	90	90
<i>β</i> /deg	90	90.297(6)
<i>γ</i> /deg	90	90
<i>V</i> /Å <sup>3</sup>	1282.04(14)	1281.7(3)
<i>Z</i>	4	26
D <sub>c</sub> /Mgm <sup>-3</sup>	1.314	1.245
μ/mm <sup>-1</sup>	0.277	0.081
<i>F</i> (000)	528	512
cryst size/mm <sup>3</sup>	0.38 × 0.24 × 0.16	0.4 × 0.3 × 0.2
<i>θ</i> /deg	2.226 – 25.719	2.359 – 28.481
Measured reflns	9897	6764
<sup>a</sup> GOF on <i>F</i> <sup>2</sup>	1.210	1.034
R1 <sup>b</sup> , wR2 <sup>c</sup> [ <i>I</i> > 2σ( <i>I</i> )]	0.0496, 0.0976	0.0543, 0.1323
R1, wR2	0.0578, 0.1013	0.0710, 0.1479
<sup>a</sup> GOF = {Σ[w( <i>F</i> <sub>o</sub> <sup>2</sup> - <i>F</i> <sub>c</sub> <sup>2</sup> )]/( <i>n</i> - <i>p</i> )} <sup>1/2</sup> . <sup>b</sup> R1 = Σ [  <i>F</i> <sub>o</sub>  - <i>F</i> <sub>c</sub> ] / Σ   <i>F</i> <sub>o</sub>  . <sup>c</sup> wR2 = [Σ [w( <i>F</i> <sub>o</sub> <sup>2</sup> - <i>F</i> <sub>c</sub> <sup>2</sup> ) <sup>2</sup> ]/ Σ [w( <i>F</i> <sub>o</sub> <sup>2</sup> ) <sup>2</sup> ] <sup>1/2</sup> where w = 1/[σ <sup>2</sup> ( <i>F</i> <sub>o</sub> <sup>2</sup> )+(a <i>P</i> ) <sup>2</sup> +b <i>P</i> ], <i>P</i> = ( <i>F</i> <sub>o</sub> <sup>2</sup> +2 <i>F</i> <sub>c</sub> <sup>2</sup> )/3.		

**Table S12.** Optimization of the reaction conditions for the zinc catalyzed acceptorless mono- and double-dehydrogenative coupling of 2-aminobenzylalcohol (**6a**) with acetophenone (**3a**) and 1-phenylethanol (**4a**)<sup>a</sup>



Entry	Catalyst (X mol%)	Solvent	Base (Y mol%)	Temp (°C)	Yield <sup>b,f</sup> (%)	Yield <sup>b,g</sup> (%)
1	<b>1a</b> (1.00 mol%)	Toluene	KO <sup>t</sup> Bu (100)	85	92	90
2	<b>1a</b> (0.1 mol%)	Toluene	KO <sup>t</sup> Bu (100)	85	91	90
3	<b>1a</b> (0.01 mol%)	Toluene	KO <sup>t</sup> Bu (100)	85	92	91
4	<b>1a</b> (0.005 mol%)	Toluene	KO <sup>t</sup> Bu (100)	85	92	87
5	<b>1a</b> (0.001 mol%)	Toluene	KO <sup>t</sup> Bu (100)	85	53	47
6	<b>1a</b> (0.005 mol%)	Toluene	KO <sup>t</sup> Bu (50)	85	92	87
7	<b>1a</b> (0.005 mol%)	<b>Toluene</b>	<b>KO<sup>t</sup>Bu (20)</b>	<b>85</b>	<b>92</b>	<b>60</b>
8	<b>1a</b> (0.005 mol%)	<b>Toluene</b>	<b>KO<sup>t</sup>Bu (40)</b>	<b>85</b>	<b>92</b>	<b>90</b>
9	<b>1a</b> (0.005 mol%)	Toluene	NaBH <sub>4</sub> (20)	85	74	42
10	<b>1a</b> (0.005 mol%)	Toluene	NaO <sup>t</sup> Bu (20)	85	85	57
11	<b>1a</b> (0.005 mol%)	Toluene	NaOH (20)	85	90	59
12	<b>1a</b> (0.005 mol%)	Toluene	KOH (20)	85	90	57

13	<b>1a</b> (0.005 mol%)	Toluene	K <sub>2</sub> CO <sub>3</sub> (20)	85	52	19
14	<b>1a</b> (0.005 mol%)	Xylene	KO <sup>t</sup> Bu (20)	85	82	55
15	<b>1a</b> (0.005 mol%)	THF	KO <sup>t</sup> Bu (20)	85	45	23
16	<b>1a</b> (0.005 mol%)	EtOH	KO <sup>t</sup> Bu (20)	85	NR	NR
17 <sup>c</sup>	<b>1a</b> (0.005 mol%)	Toluene	KO <sup>t</sup> Bu (20)	RT	NR	NR
18	<b>1a</b> (0.005 mol%)	Toluene	KO <sup>t</sup> Bu (20)	100	90	58
19	ZnCl <sub>2</sub> + Ligand (1:1)	Toluene	KO <sup>t</sup> Bu (20)	85	Trace	NR
20	ZnCl <sub>2</sub> (0.005 & 1 mol%)	Toluene	KO <sup>t</sup> Bu (20)	85	NR	NR
21	Ligand (1 mol%)	Toluene	KO <sup>t</sup> Bu (20)	85	NR	NR
22		Toluene	KO <sup>t</sup> Bu (20)	85	NR	NR
23 <sup>d</sup>	<b>1a</b> (0.005 mol%)	Toluene	KO <sup>t</sup> Bu (20)	85	trace	trace
24 <sup>e</sup>	<b>1a</b> (0.005 mol%)	Toluene	KO <sup>t</sup> Bu (20)	85	68	37
25	<b>1a</b> (0.005 mol%)	Neat	KO <sup>t</sup> Bu (20)	85	45	trace
26	<b>1b</b> (0.005 mol%)	Toluene	KO <sup>t</sup> Bu (20)	85	87	59

<sup>a</sup>Reaction Conditions: mono-dehydrogenation: condition **A**: 2-Amino benzyl alcohol **6a** (1.00 mmol), acetophenone **3a** (1.00 mmol). Double-dehydrogenation: condition **B**: 2-Amino benzyl alcohol **6a** (1.00 mmol), 1-phenylethanol **4a** (1.00 mmol), Base, 5.0 ml toluene, Reaction time 18 hrs, open air.

<sup>b</sup>Isolated yield after column chromatography.

<sup>c</sup>RT = Room Temperature.

<sup>d</sup>Under an argon atmosphere.

<sup>e</sup>Reaction time 6 hrs, NR = No Reaction.

<sup>f</sup>represents the yield of the mono-dehydrogenative coupling reaction.

<sup>g</sup>represents the yield of the double-dehydrogenative coupling reaction.

### General procedure for synthesis of $\alpha$ -alkylated ketone derivatives:

In aerial condition, a mixture of catalyst **1a** (0.008 mol%), KO<sup>t</sup>Bu (30 mol%), secondary alcohols/ketones (1.0 mmol), and primary alcohols (1.0 mmol) had been placed into a 50.0 ml round-bottom flask. The reaction mixture was then placed in a preheated oil bath at 110 °C prior 5.0 ml of toluene was added to it. The reaction was continuing for 21 hrs. Following the reaction, the resulting mixture was vacuum-concentrated and purified using column chromatography on silica gel 60-120 mesh (hexane/ethyl acetate) to afford the desired product.

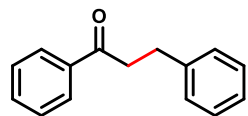
### General procedure for Friedländer quinoline synthesis:

Catalyst **1a** (0.005 mol%), KO<sup>t</sup>Bu (20 mol%), secondary alcohols/ketones (1.0 mmol), and 2-aminobenzyl alcohol derivatives (1.0 mmol) were added to a 50.0 ml round-bottom flask under aerial condition. The reaction mixture was then placed in an oil bath that had been heated to 85 °C before 5.0 ml of toluene was added to it. The reaction continued for 18 hrs. The resulting mixture was subsequently concentrated under vacuum and purified using column chromatography on silica gel 60-120 mesh (hexane/ethyl acetate) to afford the desired product.

### Characterization data of Zn catalyzed compounds:

All the reactions were carried out in 1.0 mmol scale of reactant and according to the general procedure for synthesis of  $\alpha$ -alkylated ketone derivatives.

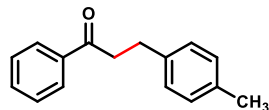
**1,3-diphenylpropan-1-one<sup>25</sup> (5aa):** Eluent: Hexane/Ethyl acetate (20:1). White solid (yield =



88%, 185mg). <sup>1</sup>H NMR (300 MHz, CDCl<sub>3</sub>):  $\delta$  (ppm) 8.00 (d,  $J = 7.4$  Hz, 2H) 7.59 (t,  $J = 7.3$  Hz, 1H), 7.49 (t,  $J = 7.5$  Hz, 2H), 7.37 – 7.22 (m, 5H), 3.34 (t,  $J = 7.7$  Hz, 2H), 3.11 (t,  $J = 7.7$  Hz, 2H). <sup>13</sup>C NMR (75 MHz, CDCl<sub>3</sub>):  $\delta$  (ppm)

199.3, 141.3, 136.9, 133.0, 128.6, 128.5, 128.4, 128.0, 126.2, 40.5, 30.1.

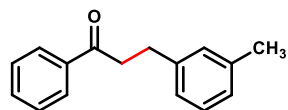
**1-phenyl-3-(p-tolyl)propan-1-one<sup>25</sup> (5ab):** Eluent: Hexane/Ethyl acetate (20:1). White solid



(yield = 76%, 170 mg). <sup>1</sup>H NMR (300 MHz, CDCl<sub>3</sub>):  $\delta$  (ppm) 8.09 – 8.05 (m, 2H), 7.64 – 7.60 (m, 1H), 7.56 – 7.52 (m, 2H), 7.29 – 7.25 (m, 4H), 3.37 – 3.31 (m, 2H), 3.19 – 3.14 (m, 2H), 2.45 (s, 3H). <sup>13</sup>C NMR (75 MHz, CDCl<sub>3</sub>):  $\delta$  (ppm) 198.9,

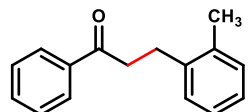
143.9, 141.4, 134.4, 129.3, 128.5, 128.4, 128.2, 126.1, 40.4, 30.2, 21.7.

**1-phenyl-3-(m-tolyl)propan-1-one<sup>25</sup> (5ac):** Eluent: Hexane/Ethyl acetate (20:1). White solid



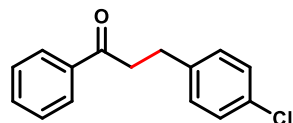
(yield = 72%, 161 mg). <sup>1</sup>H NMR (300 MHz, CDCl<sub>3</sub>): δ (ppm) 7.99 (d, *J* = 8.6 Hz, 2H), 7.61- 7.56 (m, 1H), 7.51-7.45 (m, 2H), 7.22 (t, *J* = 7.1 Hz, 1H), 7.11-7.04 (m, 3H), 3.32 (dd, *J* = 8.5, 6.4 Hz, 2H), 3.09-3.03 (m, 2H), 2.36 (s, 3H). <sup>13</sup>C NMR (75 MHz, CDCl<sub>3</sub>): δ (ppm) 199.4, 141.2, 138.1, 136.9, 133.0, 129.2, 128.6, 128.1, 126.9, 125.4, 40.6, 30.1, 21.4.

**1-phenyl-3-(o-tolyl)propan-1-one<sup>25</sup> (5ad):** Eluent: Hexane/Ethyl acetate (20:1). White solid



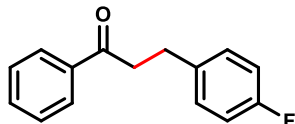
(yield = 69%, 155 mg). <sup>1</sup>H NMR (300 MHz, CDCl<sub>3</sub>): δ (ppm) 8.01- 7.98 (m, 2H), 7.62-7.57 (m, 1H), 7.51-7.45 (m, 2H), 7.21-7.16 (m, 4H), 3.31-3.26 (m, 2H), 3.11-3.06 (m, 2H), 2.38 (s, 3H). <sup>13</sup>C NMR (75 MHz, CDCl<sub>3</sub>): δ (ppm) 199.4, 139.5, 136.9, 136.0, 133.2, 130.5, 129.4, 128.9, 128.7, 128.2, 126.4 (d, *J* = 10.4 Hz), 39.2, 27.6, 19.5.

**3-(4-chlorophenyl)-1-phenylpropan-1-one<sup>25</sup> (5ae):** Eluent: Hexane/Ethyl acetate (20:1). White



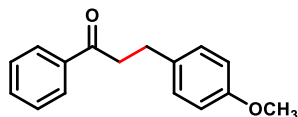
solid (yield = 78%, 191 mg). <sup>1</sup>H NMR (300 MHz, CDCl<sub>3</sub>): δ (ppm) 7.99- 7.96 (m, 2H), 7.60-7.56 (m, 1H), 7.51-7.48 (m, 2H), 7.28-7.20 (m, 4H), 3.33-3.28 (m, 2H), 3.09-3.04 (m, 2H). <sup>13</sup>C NMR (75 MHz, CDCl<sub>3</sub>): δ (ppm) 198.9, 139.8, 136.8, 133.2, 131.9, 129.8, 128.7, 128.6, 128.0, 40.1, 29.4.

**3-(4-fluorophenyl)-1-phenylpropan-1-one<sup>25</sup> (5af):** Eluent: Hexane/Ethyl acetate (20:1). White



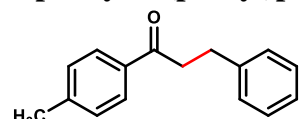
solid (yield = 85%, 194 mg). <sup>1</sup>H NMR (300 MHz, CDCl<sub>3</sub>): δ (ppm) 7.99- 7.96 (m, 2H), 7.61-7.56 (m, 1H), 7.50-7.45 (m, 2H), 7.25-7.21 (m, 2H), 7.03-6.97 (m, 2H), 3.31 (t, *J* = 7.5 Hz, 2H), 3.07 (t, *J* = 7.5 Hz, 2H). <sup>13</sup>C NMR (75 MHz, CDCl<sub>3</sub>): δ (ppm) 199.0, 163.0, 159.8, 136.8, 133.1, 129.9, 129.8, 128.6, 128.0, 115.4, 115.1, 40.4, 29.3. <sup>19</sup>F NMR (282 MHz, CDCl<sub>3</sub>): δ = -117.3 (s, 1F).

**3-(4-methoxyphenyl)-1-phenylpropan-1-one<sup>25</sup> (5ag):** Eluent: Hexane/Ethyl acetate (20:1).

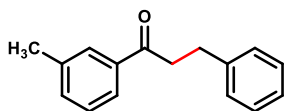


White solid (yield = 82%, 197mg). <sup>1</sup>H NMR (300 MHz, CDCl<sub>3</sub>): δ (ppm) 8.00-7.97 (m, 2H), 7.61-7.56 (m, 1H), 7.50-7.46 (m, 2H), 7.22- 7.19 (m, 2H), 6.89-6.85 (m, 2H), 3.81 (s, 3H), 3.30 (t, *J* = 7.6 Hz, 2H), 3.04 (t, *J* = 7.6 Hz, 2H). <sup>13</sup>C NMR (75 MHz, CDCl<sub>3</sub>): δ (ppm) 199.4, 158.0, 136.9, 133.3, 133.0, 129.4, 128.6, 128.0, 113.9, 55.3, 40.7, 29.3.

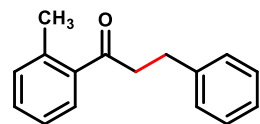
**3-phenyl-1-(p-tolyl)propan-1-one<sup>25</sup> (5ah):** Eluent: Hexane/Ethyl acetate (20:1). Colourless liquid (yield = 92%, 206mg). <sup>1</sup>H NMR (300 MHz, CDCl<sub>3</sub>):  $\delta$  (ppm) 7.92 (d,  $J$  = 8.0 Hz, 2H), 7.39-7.26 (m, 7H), 3.33 (t,  $J$  = 7.7 Hz, 2H), 3.12 (t,  $J$  = 7.7 Hz, 2H). <sup>13</sup>C NMR (75 MHz, CDCl<sub>3</sub>):  $\delta$  (ppm) 198.9, 143.9, 141.5, 134.5, 129.4, 128.6, 128.5, 128.3, 126.2, 40.4, 30.3, 21.7.



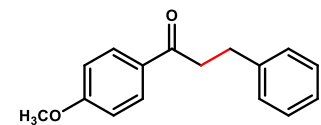
**3-phenyl-1-(m-tolyl)propan-1-one<sup>25</sup> (5ai):** Eluent: Hexane/Ethyl acetate (20:1). White solid (yield = 85%, 190 mg). <sup>1</sup>H NMR (300 MHz, CDCl<sub>3</sub>):  $\delta$  (ppm) 7.80-7.76 (m, 2H), 7.39-7.29 (m, 7H), 3.32 (t,  $J$  = 8.1 Hz, 2H), 3.12-3.07 (m, 2H), 2.43 (s, 3H). <sup>13</sup>C NMR (75 MHz, CDCl<sub>3</sub>):  $\delta$  (ppm) 199.5, 141.4, 138.4, 136.9, 133.8, 128.6, 128.4, 128.5, 128.4, 126.1, 125.3, 40.5, 30.2, 21.3.



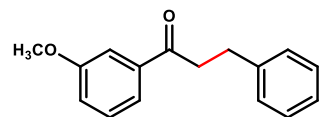
**3-phenyl-1-(o-tolyl)propan-1-one<sup>25</sup> (5aj):** Eluent: Hexane/Ethyl acetate (20:1). Colorless liquid (yield = 75%, 168mg). <sup>1</sup>H NMR (300 MHz, CDCl<sub>3</sub>):  $\delta$  (ppm) 7.62 (d,  $J$  = 7.0 Hz, 1H), 7.27-7.21 (m, 8H), 3.25 (t,  $J$  = 7.6 Hz, 2H), 3.07 (t,  $J$  = 7.6 Hz, 2H), 2.49 (s, 3H). <sup>13</sup>C NMR (75 MHz, CDCl<sub>3</sub>):  $\delta$  (ppm) 203.41, 141.2, 138.1, 136.4, 136.2, 131.9, 129.4, 128.5, 128.4, 126.1, 125.7, 125.2, 43.2, 30.4, 21.3.



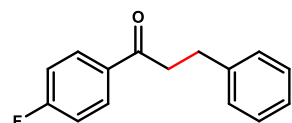
**1-(4-methoxyphenyl)-3-phenylpropan-1-one<sup>25</sup> (5ak):** Eluent: Hexane/Ethyl acetate (20:1). White solid (yield = 93%, 223mg). <sup>1</sup>H NMR (300 MHz, CDCl<sub>3</sub>):  $\delta$  (ppm) 7.97 (d,  $J$  = 8.8 Hz, 2H), 7.23 (d,  $J$  = 6.9 Hz, 1H), 7.17 (d,  $J$  = 7.0 Hz, 1H), 6.95 (d,  $J$  = 8.8 Hz, 2H), 3.89 (s, 3H), 3.28 (t,  $J$  = 7.6 Hz, 2H), 3.09 (t,  $J$  = 7.6 Hz, 2H). <sup>13</sup>C NMR (75 MHz, CDCl<sub>3</sub>):  $\delta$  (ppm) 197.9, 163.3, 141.5, 130.5, 129.0, 128.5, 128.4, 126.2, 113.6, 55.4, 40.1, 30.4.



**1-(3-methoxyphenyl)-3-phenylpropan-1-one<sup>26</sup> (5al):** Eluent: Hexane/Ethyl acetate (20:1). White solid (yield = 88%, 211mg). <sup>1</sup>H NMR (300 MHz, CDCl<sub>3</sub>):  $\delta$  (ppm) 7.58-7.52 (m, 2H), 7.41-7.30 (m, 5H), 7.19-7.15 (m, 2H), 3.88 (s, 3H), 3.33 (t,  $J$  = 7.7 Hz, 2H), 3.10 (t,  $J$  = 7.7 Hz, 2H). <sup>13</sup>C NMR (75 MHz, CDCl<sub>3</sub>):  $\delta$  (ppm) 199.1, 159.9, 141.3, 138.3, 129.6, 128.6, 128.5, 126.2, 120.7, 119.6, 112.3, 55.5, 40.6, 30.2.

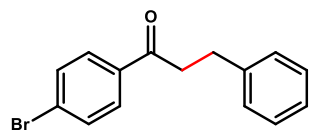


**1-(4-fluorophenyl)-3-phenylpropan-1-one<sup>26</sup> (5am):** Eluent: Hexane/Ethyl acetate (20:1). White solid (yield = 68%, 155mg). <sup>1</sup>H NMR (300 MHz, CDCl<sub>3</sub>):  $\delta$  (ppm) 8.05-8.00 (m, 2H), 7.38-7.24 (m, 5H), 7.19-7.12 (m, 2H), 3.31 (t,  $J$  = 7.6 Hz, 2H), 3.12 (t,  $J$  = 7.6 Hz, 2H). <sup>13</sup>C NMR (75 MHz, CDCl<sub>3</sub>):  $\delta$  (ppm) 197.6,



167.0, 164.5, 141.2, 133.47, 133.3, 130.71 (d,  $J = 9.3$  Hz), 128.55 (d,  $J = 13.0$  Hz), 115.71 (d,  $J = 21.8$  Hz), 40.4, 30.1.  $^{19}\text{F}$  NMR (282 MHz,  $\text{CDCl}_3$ ):  $\delta = -105.2$  (s, 1F).

**1-(4-Bromophenyl)-3-phenylpropan-1-one<sup>26</sup> (5an)**: Eluent: Hexane/Ethyl acetate (20:1). White

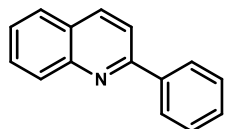


solid (yield = 57%, 165mg).  $^1\text{H}$  NMR (300 MHz,  $\text{CDCl}_3$ ):  $\delta$  (ppm) 7.84 (d,  $J = 8.6$  Hz, 2H), 7.61 (d,  $J = 8.6$  Hz, 2H), 7.33-7.30 (m, 2H), 7.25-7.21 (m, 3H), 3.32-3.26 (m, 2H), 3.11-3.06 (m, 2H).  $^{13}\text{C}$  NMR (75 MHz,  $\text{CDCl}_3$ ):  $\delta$  (ppm) 198.2, 141.0, 135.6, 131.9, 129.6, 128.9, 128.6, 128.5, 128.5, 128.4, 128.2, 126.4,

126.2, 40.4, 30.0.

All the reactions were carried out in 1.0 mmol scale of reactant and according to the general procedure for Friedländer quinoline synthesis.

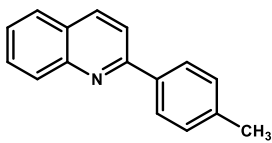
**2-phenyl quinoline<sup>27</sup> (9aa)**: Eluent: Hexane/Ethyl acetate (20:1). Fawn solid (yield = 92%,



189mg).  $^1\text{H}$  NMR (300 MHz,  $\text{CDCl}_3$ ):  $\delta$  (ppm) 8.26-8.18 (m, 4H), 7.92-7.84 (m, 2H), 7.78-7.73 (m, 1H), 7.59-7.47 (m, 4H).  $^{13}\text{C}$  NMR (75 MHz,  $\text{CDCl}_3$ ):  $\delta$  (ppm) 157.4, 148.3, 139.7, 136.8, 129.8, 129.7, 129.4, 128.9, 127.6, 127.5,

127.2, 126.3, 119.1.

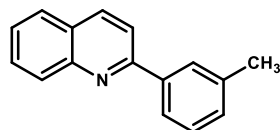
**2-(p-tolyl)quinoline<sup>27</sup> (9ab)**: Eluent: Hexane/Ethyl acetate (20:1). Fawn solid (yield = 94%,



207mg).  $^1\text{H}$  NMR (300 MHz,  $\text{CDCl}_3$ ):  $\delta$  (ppm) 8.21 (d,  $J = 8.5$  Hz, 2H), 8.11 (d,  $J = 8.2$  Hz, 2H), 7.89-7.82 (m, 2H), 7.78-7.72 (m, 1H), 7.57-7.51 (m, 1H), 7.37 (d,  $J = 7.8$  Hz, 2H), 2.47 (s, 3H).  $^{13}\text{C}$  NMR (75 MHz,  $\text{CDCl}_3$ ):  $\delta$  (ppm) 157.4, 148.3, 139.4, 136.8 (d,  $J = 16.6$  Hz), 129.6 (d,  $J = 5.7$  Hz), 129.3, 128.5, 127.5, 127.1,

126.1, 118.9, 21.4.

**2-(m-tolyl)quinoline<sup>28</sup> (9ac)**: Eluent: Hexane/Ethyl acetate (20:1). Yellowish Liquid (yield =

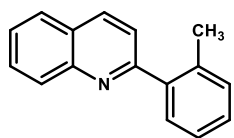


90%, 197mg).  $^1\text{H}$  NMR (300 MHz,  $\text{CDCl}_3$ ):  $\delta$  (ppm) 8.25-8.20 (m, 2H), 7.95 (d,  $J = 7.7$  Hz, 1H), 7.85 (d,  $J = 6.6$  Hz, 1H), 7.80-7.73 (m, 2H), 7.55 (t,  $J = 6.9$  Hz, 1H), 7.47-7.37 (m, 2H), 7.31 (d,  $J = 6.7$  Hz, 1H), 2.51 (s,

3H).  $^{13}\text{C}$  NMR (75 MHz,  $\text{CDCl}_3$ ):  $\delta$  (ppm) 157.6, 148.3, 138.5, 136.7, 133.8, 130.1, 129.7, 129.6, 128.7, 128.4, 128.3, 127.4, 126.2, 124.7, 119.1, 21.6.



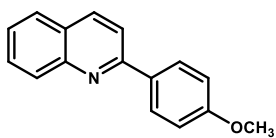
**2-(o-tolyl)quinoline<sup>28</sup> (9ad)**: Eluent: Hexane/Ethyl acetate (20:1). Fawn solid (yield = 84%,



185mg). <sup>1</sup>H NMR (300 MHz, CDCl<sub>3</sub>): δ (ppm) 8.22 (dd, *J* = 15.9, 8.5 Hz, 2H), 7.89 (dd, *J* = 8.2, 1.5 Hz, 1H), 7.77 (m, 1H), 7.62-7.51 (m, 3H), 7.40-7.31 (m, 3H), 2.44 (s, 3H). <sup>13</sup>C NMR (75 MHz, CDCl<sub>3</sub>): δ (ppm) 160.3, 147.9,

140.8, 136.1, 136.0, 130.9, 129.7, 129.6, 128.5, 127.5, 126.8, 126.4, 126.0, 122.4, 20.4.

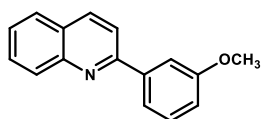
**2-(4-methoxyphenyl)quinoline<sup>27</sup> (9ae)**: Eluent: Hexane/Ethyl acetate (20:1). White solid (yield



= 89%, 209mg). <sup>1</sup>H NMR (300 MHz, CDCl<sub>3</sub>): δ (ppm) 8.22-8.15 (m, 4H), 7.88-7.82 (m, 2H), 7.73 (t, *J* = 6.9 Hz, 1H), 7.52 (t, *J* = 7.5 Hz, 1H), 7.08 (d, *J* = 8.9 Hz, 2H), 3.92 (s, 3H). <sup>13</sup>C NMR (75 MHz, CDCl<sub>3</sub>): δ (ppm)

160.8, 157.0, 148.3, 136.7, 132.3, 129.6, 129.5, 128.9, 127.4, 126.9, 125.9, 118.6, 114.2, 55.4.

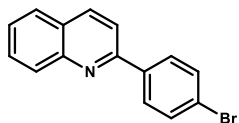
**2-(3-methoxyphenyl)quinoline<sup>28</sup> (9af)**: Eluent: Hexane/Ethyl acetate (20:1). White solid (yield =



87%, 205mg). <sup>1</sup>H NMR (300 MHz, CDCl<sub>3</sub>): δ (ppm) 8.24-8.20 (m, 2H), 7.89-7.81 (m, 3H), 7.78-7.72 (m, 2H), 7.57-7.51 (m, 2H), 7.07-7.03 (m, 1H), 3.95 (s, 3H). <sup>13</sup>C NMR (75 MHz, CDCl<sub>3</sub>): δ (ppm) 160.2, 159.8, 148.2,

141.2, 136.8, 129.8, 129.8, 129.7, 127.5, 126.4, 120.0, 119.1, 115.4, 112.8, 55.4.

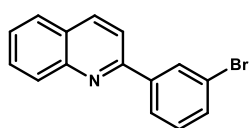
**2-(4-bromophenyl)quinoline<sup>28</sup> (9ag)**: Eluent: Hexane/Ethyl acetate (20:1). Beige solid (yield =



86%, 245mg). <sup>1</sup>H NMR (300 MHz, CDCl<sub>3</sub>): δ (ppm) 8.26 (d, *J* = 7.8 Hz, 1H), 8.18 (dd, *J* = 8.5, 1.0 Hz, 1H), 8.08 (d, *J* = 8.6 Hz, 2H), 7.87 (d, *J* = 8.6 Hz, 2H), 7.79-7.74 (m, 1H), 7.68 (d, *J* = 8.6 Hz, 2H), 7.57 (t, *J* = 6.9 Hz, 1H). <sup>13</sup>C NMR

(75 MHz, CDCl<sub>3</sub>): δ (ppm) 156.1, 148.3, 138.5, 137.0, 132.0, 131.4, 129.9, 129.7, 129.1, 127.5, 127.3, 126.6, 123.9, 118.5.

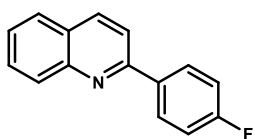
**2-(3-bromophenyl)quinoline<sup>29</sup> (9ah)**: Eluent: Hexane/Ethyl acetate (20:1). Beige solid (yield =



72%, 204mg). <sup>1</sup>H NMR (300 MHz, CDCl<sub>3</sub>): δ (ppm) 8.38 (s, 1H), 8.26-8.18 (m, 2H), 8.10 (s, 1H), 7.85 (d, *J* = 8.0 Hz, 2H), 7.76 (t, *J* = 7.8 Hz, 1H), 7.59 (t, *J* = 8.4 Hz, 2H), 7.43-7.33 (m, 1H). <sup>13</sup>C NMR (75 MHz, CDCl<sub>3</sub>): δ (ppm)

155.6, 148.2, 141.7, 137.0, 132.2, 131.4, 130.6, 130.3, 129.9, 129.8, 127.5, 126.7, 126.0, 123.2, 118.7

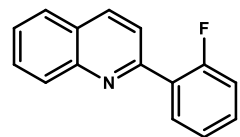
**2-(4-fluorophenyl)quinoline<sup>28</sup> (9ai)**: Eluent: Hexane/Ethyl acetate (20:1). Beige solid (yield =



84%, 188mg). <sup>1</sup>H NMR (300 MHz, CDCl<sub>3</sub>): δ (ppm) 8.26-8.16 (m, 4H), 7.86 (d, *J* = 8.6 Hz, 2H), 7.76 (t, *J* = 6.9 Hz, 1H), 7.56 (t, *J* = 7.5 Hz, 1H), 7.27-7.21 (m, 2H). <sup>13</sup>C-NMR (75 MHz, CDCl<sub>3</sub>): δ (ppm) 165.5, 162.2, 156.3,

148.2, 136.9, 135.9, 129.8, 129.5, 129.4, 127.5, 126.4, 118.7, 115.9, 115.7.  $^{19}\text{F}$  NMR (282 MHz,  $\text{CDCl}_3$ ):  $\delta = -117.3$  (s, 1F)

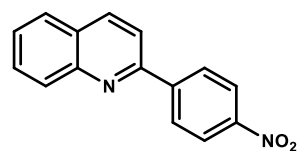
**2-(2-fluorophenyl)quinoline<sup>29</sup> (9aj)**: Eluent: Hexane/Ethyl acetate (20:1). Fawn Liquid (yield =



55%, 123mg).  $^1\text{H}$  NMR (300 MHz,  $\text{CDCl}_3$ ):  $\delta$  (ppm) 8.32-8.29 (m, 1H), 8.09-8.05 (m, 2H), 8.0-7.97 (m, 1H), 7.87-7.84 (m, 1H), 7.80-7.74 (m, 1H), 7.61-7.55 (m, 1H), 7.42-7.34 (m, 1H), 7.13-7.10 (m, 1H), 7.02-6.96 (m, 1H).  $^{13}\text{C}$

NMR (75 MHz,  $\text{CDCl}_3$ ):  $\delta$  (ppm) 161.0, 158.0, 144.8, 137.7, 132.1, 130.5, 127.6 (d,  $J = 4.3$  Hz), 127.0, 126.7, 118.7 (d,  $J = 6.3$  Hz), 117.3.  $^{19}\text{F}$  NMR (282 MHz,  $\text{CDCl}_3$ ):  $\delta = -117.3$  (s, F).

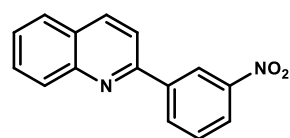
**2-(4-nitrophenyl)quinoline<sup>29</sup> (9ak)**: Eluent: Hexane/Ethyl acetate (20:1). Pastel orange solid



(yield = 81%, 203mg).  $^1\text{H}$  NMR (300 MHz,  $\text{CDCl}_3$ ):  $\delta$  (ppm) 8.43-8.36 (m, 4H), 8.35-8.32 (m, 1H), 8.24-8.20 (m, 1H), 7.96 (d,  $J = 8.6$  Hz, 1H), 7.92-7.89 (m, 1H), 7.84-7.78 (m, 1H), 7.65-7.60 (m, 1H).  $^{13}\text{C}$  NMR (75

MHz,  $\text{CDCl}_3$ ):  $\delta$  (ppm) 157.6, 148.4, 148.3, 145.5, 137.4, 130.3, 130.0, 128.4, 128.2, 127.6, 127.3, 124.1, 118.8.

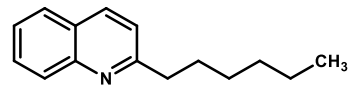
**2-(3-nitrophenyl)quinoline<sup>30</sup> (9al)**: Eluent: Hexane/Ethyl acetate (20:1). Pastel orange solid



(yield = 67%, 168mg).  $^1\text{H}$  NMR (300 MHz,  $\text{CDCl}_3$ ):  $\delta$  (ppm) 9.07 (s, 1H), 8.58 (d,  $J = 7.8$  Hz, 1H), 8.33 (d,  $J = 8.2$  Hz, 2H), 8.22 (d,  $J = 8.5$  Hz, 1H), 7.97 (d,  $J = 8.6$  Hz, 1H), 7.90 (d,  $J = 6.7$  Hz, 1H), 7.83-7.70 (m, 2H), 7.61

(t,  $J = 6.9$  Hz, 1H).  $^{13}\text{C}$  NMR (75 MHz,  $\text{CDCl}_3$ ):  $\delta$  (ppm) 154.5, 148.9, 148.3, 141.3, 137.5, 133.3, 130.2, 129.9, 129.8, 129.0, 127.6, 127.1, 123.9, 122.5, 118.4.

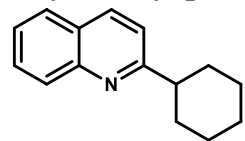
**2-hexylquinoline<sup>32</sup> (9am)**: Eluent: Hexane/Ethyl acetate (20:1). Colorless Liquid (yield = 85%,



182mg).  $^1\text{H}$  NMR (300 MHz,  $\text{CDCl}_3$ ):  $\delta$  (ppm) 8.06 (t,  $J = 8.1$  Hz, 2H), 7.76 (dd,  $J = 8.1, 1.5$  Hz, 1H), 7.68 (ddd,  $J = 8.5, 6.8, 1.5$  Hz,

1H), 7.47 (ddd,  $J = 8.1, 6.8, 1.2$  Hz, 1H), 7.29 (d,  $J = 8.5$  Hz, 1H), 3.00 – 2.95 (m, 2H), 1.87 – 1.77 (m, 2H), 1.37-1.27 (m, 6H), 0.93-0.87 (m, 3H).  $^{13}\text{C}$  NMR (75 MHz,  $\text{CDCl}_3$ ):  $\delta$  (ppm) 163.1, 147.9, 136.1, 129.3, 128.8, 127.5, 126.7, 125.6, 121.3, 39.3, 31.7, 30.0, 29.2, 22.6, 14.1.

**2-cyclohexylquinoline<sup>33</sup> (9an)**: Eluent: Hexane/Ethyl acetate (20:1). Yellowish Oil (yield = 89%,

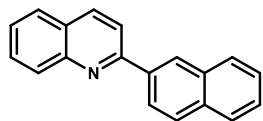


188mg).  $^1\text{H}$  NMR (300 MHz,  $\text{CDCl}_3$ ):  $\delta$  (ppm) 8.11 (d,  $J = 3.0$  Hz, 1H), 8.08 (d,  $J = 3.4$  Hz, 1H), 7.79 (dd,  $J = 8.1, 1.5$  Hz, 1H), 7.70 (ddd,  $J = 8.5, 6.9, 1.5$  Hz, 1H), 7.50 (ddd,  $J = 8.1, 6.9, 1.2$  Hz, 1H), 7.36 (d,  $J = 8.6$  Hz, 1H), 2.99-

2.93 (m, 1H), 2.09-2.03 (m, 3H), 1.95-1.90 (m, 2H), 1.69-1.48 (m, 5H).  $^{13}\text{C}$  NMR (75 MHz,

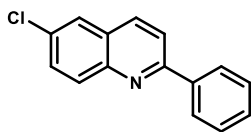
CDCl<sub>3</sub>):  $\delta$  (ppm) 166.8, 147.9, 136.2, 129.2, 129.0, 128.2, 127.4, 125.6, 119.6, 47.62, 32.8, 28.5, 26.6, 26.2, 25.7.

**2-(naphthalen-2-yl)quinoline<sup>28</sup> (9ao)**: Eluent: Hexane/Ethyl acetate (20:1). White solid (yield =



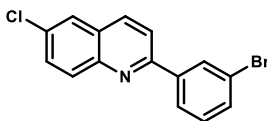
84%, 213mg). <sup>1</sup>H NMR (300 MHz, CDCl<sub>3</sub>):  $\delta$  (ppm) 8.65 (s, 1H), 8.41 (dd,  $J = 8.6, 1.8$  Hz, 1H), 8.27 (dd,  $J = 8.5, 4.6$  Hz, 2H), 8.07 – 8.02 (m, 3H), 7.94 – 7.92 (m, 1H), 7.87 (d,  $J = 6.7$ , Hz, 1H), 7.80 – 7.76 (m, 1H), 7.59 – 7.54 (m, 3H). <sup>13</sup>C NMR (75 MHz, CDCl<sub>3</sub>):  $\delta$  (ppm) 157.2, 148.4, 137.0, 136.8, 133.9, 133.5, 129.8, 129.7, 128.8, 128.6, 128.3, 127.7, 127.5, 127.3, 127.2, 126.7, 126.4, 125.1, 119.2.

**6-chloro-2-phenylquinoline<sup>30</sup> (10aa)**: Eluent: Hexane/Ethyl acetate (20:1). White solid (yield =



94%, 225mg). <sup>1</sup>H NMR (300 MHz, CDCl<sub>3</sub>):  $\delta$  (ppm) 8.19-8.12(m, 4H), 7.92 (d,  $J = 8.7$  Hz, 1H), 7.83 (d,  $J = 2.3$  Hz, 1H), 7.68 (dd,  $J = 9.0, 2.3$  Hz, 1H), 7.59-7.47 (m, 3H). <sup>13</sup>C NMR (75 MHz, CDCl<sub>3</sub>):  $\delta$  (ppm) 157.6, 146.7, 139.2, 135.9, 131.9, 131.3, 130.6, 129.6, 128.9, 127.7, 127.5, 126.2, 119.8.

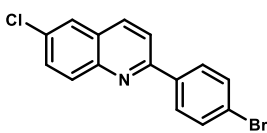
**6-chloro-2-(3-bromophenyl)quinoline (10ab)**: Eluent: Hexane/Ethyl acetate (20:1). White solid



(yield = 92%, 252mg). <sup>1</sup>H NMR (300 MHz, CDCl<sub>3</sub>):  $\delta$  (ppm) 8.17-8.09 (m, 4H), 7.89-7.83 (m, 2H), 7.69 (dd,  $J = 9.0, 2.3$  Hz, 1H), 7.54-7.50 (m, 2H). <sup>13</sup>C NMR (75 MHz, CDCl<sub>3</sub>):  $\delta$  (ppm) 156.2, 146.6, 137.6, 136.1,

135.8, 132.2, 131.3, 130.8, 129.1, 128.8, 127.8, 126.2, 119.4. MS (ESI+): C<sub>15</sub>H<sub>10</sub>BrClN ([M+H]<sup>+</sup>); calculated: 317.96, found: 317.98.

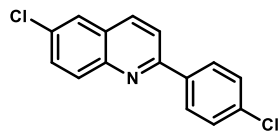
**6-chloro-2-(4-bromophenyl)quinoline (10ac)**: Eluent: Hexane/Ethyl acetate (20:1). White solid



(yield = 92%, 252mg). <sup>1</sup>H NMR (300 MHz, CDCl<sub>3</sub>):  $\delta$  (ppm) 8.17-8.09 (m, 4H), 7.89-7.83 (m, 2H), 7.69 (dd,  $J = 9.0, 2.3$  Hz, 1H), 7.54-7.50 (m, 2H). <sup>13</sup>C NMR (75 MHz, CDCl<sub>3</sub>):  $\delta$  (ppm) 156.2, 146.6, 137.6, 136.1,

135.8, 132.2, 131.3, 130.8, 129.1, 128.8, 127.8, 126.2, 119.4. MS (ESI+): C<sub>15</sub>H<sub>10</sub>BrClN ([M+H]<sup>+</sup>); calculated: 317.96, found: 317.98.

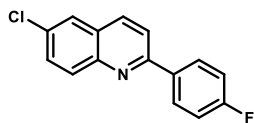
**6-chloro-2-(4-chlorophenyl)quinoline<sup>30</sup> (10ad)**: Eluent: Hexane/Ethyl acetate (20:1). White



solid (yield = 92%, 252mg). <sup>1</sup>H NMR (300 MHz, CDCl<sub>3</sub>):  $\delta$  (ppm) 8.17-8.09 (m, 4H), 7.89-7.83 (m, 2H), 7.69 (dd,  $J = 9.0, 2.3$  Hz, 1H), 7.54-7.50 (m, 2H). <sup>13</sup>C NMR (75 MHz, CDCl<sub>3</sub>):  $\delta$  (ppm) 156.2, 146.6, 137.6, 136.1,

135.8, 132.2, 131.3, 130.8, 129.1, 128.8, 127.8, 126.2, 119.4.

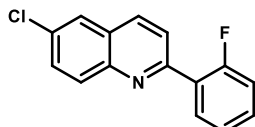
**6-chloro-2-(4-fluorophenyl)quinoline (10ae):** Eluent: Hexane/Ethyl acetate (20:1). White solid



(yield = 87%, 224mg).  $^1\text{H}$  NMR (300 MHz,  $\text{CDCl}_3$ ):  $\delta$  (ppm) 8.20-8.08 (m, 4H), 7.88-7.82 (m, 2H), 7.68 (dd,  $J = 9.0, 2.4$  Hz, 1H), 7.26-7.20 (m, 2H).

$^{13}\text{C}$  NMR (75 MHz,  $\text{CDCl}_3$ ):  $\delta$  (ppm) 165.6, 162.3, 156.4, 146.6, 135.9, 132.0, 131.2, 130.7, 129.5, 129.3, 127.6, 126.2, 119.4, 116.0, 115.7.  $^{19}\text{F}$  NMR (282 MHz,  $\text{CDCl}_3$ ):  $\delta = -111.9$  (s, 1F). MS (ESI+):  $\text{C}_{15}\text{H}_{10}\text{ClFN}$  ( $[\text{M}+\text{H}]^+$ ); calculated: 258.04, found: 258.06.

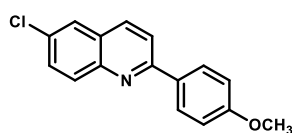
**6-chloro-2-(2-fluorophenyl)quinoline (10af):** Eluent: Hexane/Ethyl acetate (20:1). White solid



(yield = 60%, 154mg).  $^1\text{H}$  NMR (300 MHz,  $\text{CDCl}_3$ ):  $\delta$  (ppm) 8.16-8.10 (m, 3H), 7.94 (dd,  $J = 8.6, 2.6$  Hz, 1H), 7.85 (d,  $J = 2.3$  Hz, 1H), 7.69 (dd,  $J = 9.0, 2.3$  Hz, 1H), 7.49-7.44 (m, 1H), 7.34 (td,  $J = 7.5, 1.2$  Hz, 1H), 7.23 (ddd,

$J = 11.4, 8.2, 1.2$  Hz, 1H).  $^{13}\text{C}$  NMR (75 MHz,  $\text{CDCl}_3$ ):  $\delta$  (ppm) 162.1, 159.6, 154.3 (d,  $J = 2.0$  Hz), 146.7, 135.3, 132.4, 131.43 (d,  $J = 2.9$  Hz), 131.3, 131.1 (d,  $J = 8.6$  Hz), 130.6, 127.8, 126.2, 124.8 (d,  $J = 3.4$  Hz), 123.3 (d,  $J = 8.4$  Hz), 116.3 (d,  $J = 22.8$  Hz).  $^{19}\text{F}$  NMR (282 MHz,  $\text{CDCl}_3$ ):  $\delta = -117.0$  (s, 1F) MS (ESI+):  $\text{C}_{15}\text{H}_{10}\text{ClFN}$  ( $[\text{M}+\text{H}]^+$ ); calculated: 258.04, found: 258.06.

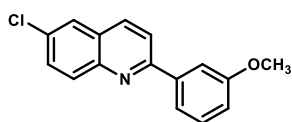
**6-chloro-2-(4-methoxyphenyl)quinoline (10ag):** Eluent: Hexane/Ethyl acetate (20:1). White



solid (yield = 92%, 245mg).  $^1\text{H}$  NMR (300 MHz,  $\text{CDCl}_3$ ):  $\delta$  (ppm) 8.17-8.07 (m, 4H), 7.87 (d,  $J = 8.7$  Hz, 1H), 7.80 (d,  $J = 2.3$  Hz, 1H), 7.66 (dd,  $J = 9.0, 2.4$  Hz, 1H), 7.07 (d,  $J = 8.9$  Hz, 2H), 3.91 (s, 1H).  $^{13}\text{C}$  NMR (75

MHz,  $\text{CDCl}_3$ ):  $\delta$  (ppm) 161.0, 157.1, 146.7, 135.7, 131.8, 131.5, 131.1, 130.5, 128.9, 127.5, 126.1, 119.4, 114.3, 55.4. MS (ESI+):  $\text{C}_{16}\text{H}_{13}\text{ClNO}$  ( $[\text{M}+\text{H}]^+$ ); calculated: 270.06, found: 270.07.

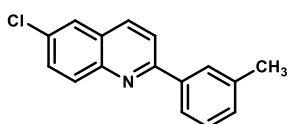
**6-chloro-2-(3-methoxyphenyl)quinoline (10ah):** Eluent: Hexane/Ethyl acetate (20:1). White



solid (yield = 90%, 240mg).  $^1\text{H}$  NMR (300 MHz,  $\text{CDCl}_3$ ):  $\delta$  (ppm) 8.13-8.07 (m, 2H), 7.86 (d,  $J = 9.6$  Hz, 1H), 7.79-7.76 (m, 2H), 7.71-7.67 (m, 2H), 7.44 (t,  $J = 7.9$  Hz, 1H), 7.04 (dd,  $J = 8.2, 2.5$  Hz, 1H), 3.94 (s,

3H).  $^{13}\text{C}$  NMR (75 MHz,  $\text{CDCl}_3$ ):  $\delta$  (ppm) 160.2, 157.3, 146.6, 140.6, 135.8, 131.9, 131.3, 130.6, 129.9, 127.8, 126.1, 119.9, 119.8, 115.6, 112.7, 55.4. MS (ESI+):  $\text{C}_{16}\text{H}_{13}\text{ClNO}$  ( $[\text{M}+\text{H}]^+$ ); calculated: 270.06, found: 270.07.

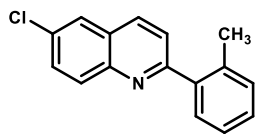
**6-chloro-2-(m-tolyl)quinoline (10ai):** Eluent: Hexane/Ethyl acetate (20:1). White solid (yield =



92%, 233mg).  $^1\text{H}$  NMR (300 MHz,  $\text{CDCl}_3$ ):  $\delta$  (ppm) 8.12-8.06 (m, 4H), 7.88 (d,  $J = 8.7$  Hz, 1H), 7.80 (d,  $J = 2.4$  Hz, 1H), 7.66 (dd,  $J = 9.0, 2.4$  Hz, 1H), 7.38-7.34 (m, 2H), 2.46 (s, 3H).  $^{13}\text{C}$  NMR (75 MHz,  $\text{CDCl}_3$ ):  $\delta$

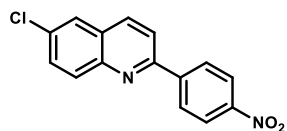
(ppm) 157.5, 146.7, 139.7, 136.4, 135.7, 131.7, 131.3, 130.5, 129.7, 129.3, 128.5, 127.6, 127.4, 126.1, 119.7, 21.4. MS (ESI+): C<sub>16</sub>H<sub>13</sub>ClN ([M+H]<sup>+</sup>); calculated: 254.07, found: 254.09.

**6-chloro-2-(o-tolyl)quinoline (10aj):** Eluent: Hexane/Ethyl acetate (20:1). White solid (yield =



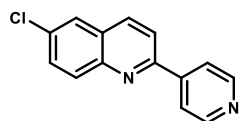
86%, 218mg). <sup>1</sup>H NMR (300 MHz, CDCl<sub>3</sub>): δ (ppm) 8.13 (t, *J* = 8.1 Hz, 2H), 7.87 (d, *J* = 2.4 Hz, 1H), 7.69 (dd, *J* = 9.0, 2.3 Hz, 1H), 7.59 (d, *J* = 8.5 Hz, 1H), 7.53-7.50 (m, 1H), 7.41-7.32 (m, 3H), 2.44 (s, 3H). <sup>13</sup>C NMR (75 MHz, CDCl<sub>3</sub>): δ (ppm) 160.5, 146.3, 140.3, 136.0, 132.1, 131.2, 130.9, 129.7, 128.7, 127.3, 126.2, 126.1, 123.3, 20.4. MS (ESI+): C<sub>16</sub>H<sub>13</sub>ClN ([M+H]<sup>+</sup>); calculated: 254.07, found: 254.09.

**6-chloro-2-(4-nitrophenyl)quinoline (10ak):** Eluent: Hexane/Ethyl acetate (20:1). White solid



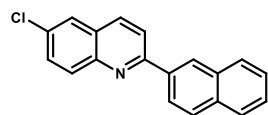
(yield = 70%, 198mg). <sup>1</sup>H NMR (300 MHz, CDCl<sub>3</sub>): δ (ppm) 8.23 (d, *J* = 8.7 Hz, 2H), 7.96 (d, *J* = 8.6 Hz, 2H), 7.86 (d, *J* = 2.3 Hz, 2H), 7.74 (d, *J* = 2.3 Hz, 1H), 7.45 (d, *J* = 2.5 Hz, 1H), 6.63 (d, *J* = 8.8 Hz, 1H). <sup>13</sup>C NMR (75 MHz, CDCl<sub>3</sub>): δ (ppm) 154.7, 148.5, 146.4, 144.7, 136.6, 133.2, 131.4, 129.3, 128.4, 128.1, 126.3, 124.1, 119.7. MS (ESI+): C<sub>15</sub>H<sub>9</sub>ClN<sub>2</sub>O<sub>2</sub> ([M]<sup>+</sup>); calculated: 284.03, found: 284.06.

**6-chloro-2-(pyridin-4-yl)quinoline (10al):** Eluent: Hexane/Ethyl acetate (20:1). White solid



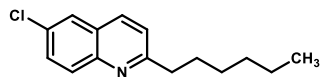
(yield = 76%, 182mg). <sup>1</sup>H NMR (300 MHz, CDCl<sub>3</sub>): δ (ppm) 8.73 (d, *J* = 5.1 Hz, 2H), 8.24 – 8.06 (m, 2H), 8.01 – 7.99 (m, 2H), 7.84 (dd, *J* = 8.7, 3.0 Hz, 1H), 7.78 – 7.72 (m, 1H), 7.67 – 7.63 (m, 1H). <sup>13</sup>C NMR (75 MHz, CDCl<sub>3</sub>): δ (ppm) 154.5, 150.4, 146.6, 137.3, 136.3, 132.9, 131.5, 131.0, 130.1, 129.9, 128.3, 127.6, 126.2, 121.5, 119.2. MS (ESI+): C<sub>14</sub>H<sub>9</sub>ClN<sub>2</sub> ([M]<sup>+</sup>); calculated: 240.04, found: 240.07.

**6-chloro-2-(naphthalen-2-yl)quinoline (10am):** Eluent: Hexane/Ethyl acetate (20:1). White



solid (yield = 88%, 253mg). <sup>1</sup>H NMR (300 MHz, CDCl<sub>3</sub>): δ (ppm) 8.61 (s, 1H), 8.37 (dd, *J* = 8.6, 1.8 Hz, 1H), 8.16 (dd, *J* = 8.8, 4.1 Hz, 2H), 8.06 – 7.98 (m, 3H), 7.95 – 7.89 (m, 1H), 7.83 (d, *J* = 2.4 Hz, 1H), 7.70 (dd, *J* = 9.0, 2.4 Hz, 1H), 7.59 – 7.54 (m, 2H). <sup>13</sup>C NMR (75 MHz, CDCl<sub>3</sub>): δ (ppm) 157.4, 149.8, 136.5, 135.9, 133.9, 133.5, 131.9, 131.3, 130.7, 128.9, 128.7, 127.8, 127.2, 126.9, 126.5, 126.2, 124.9, 119.9. MS (ESI+): C<sub>19</sub>H<sub>12</sub>ClN ([M]<sup>+</sup>); calculated: 289.06, found: 289.08.

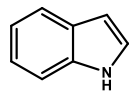
**6-chloro-2-hexylquinoline (10an):** Eluent: Hexane/Ethyl acetate (20:1). Colorless Oil (yield =



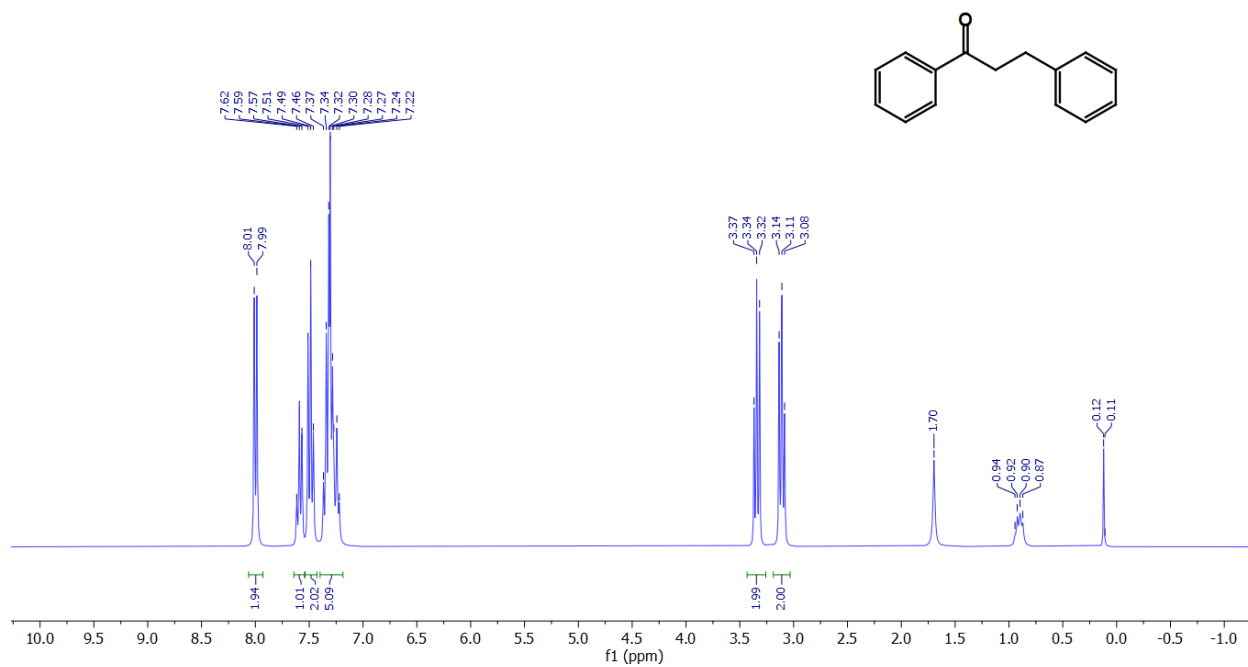
78%, 193mg). <sup>1</sup>H NMR (300 MHz, CDCl<sub>3</sub>): δ (ppm) 8.00-7.92 (m, 2H), 7.77-7.71 (m, 1H), 7.64-7.53 (m, 1H), 7.34-7.28 (m, 1H), 2.97 (dd,

$J = 8.6, 7.2$  Hz, 2H), 1.86-1.76 (m, 2H), 1.46-1.40 (m, 5H), 0.97-0.87 (m, 4H).  $^{13}\text{C}$  NMR (75 MHz,  $\text{CDCl}_3$ ):  $\delta$  (ppm) 163.5, 146.2, 135.3, 131.2, 130.4, 130.2, 127.3, 126.1, 122.3, 39.3, 31.7, 29.9, 29.2, 22.6, 14.1. MS (ESI+):  $\text{C}_{15}\text{H}_{19}\text{ClN}$  ( $[\text{M}+\text{H}]^+$ ); calculated: 248.120, found: 248.125.

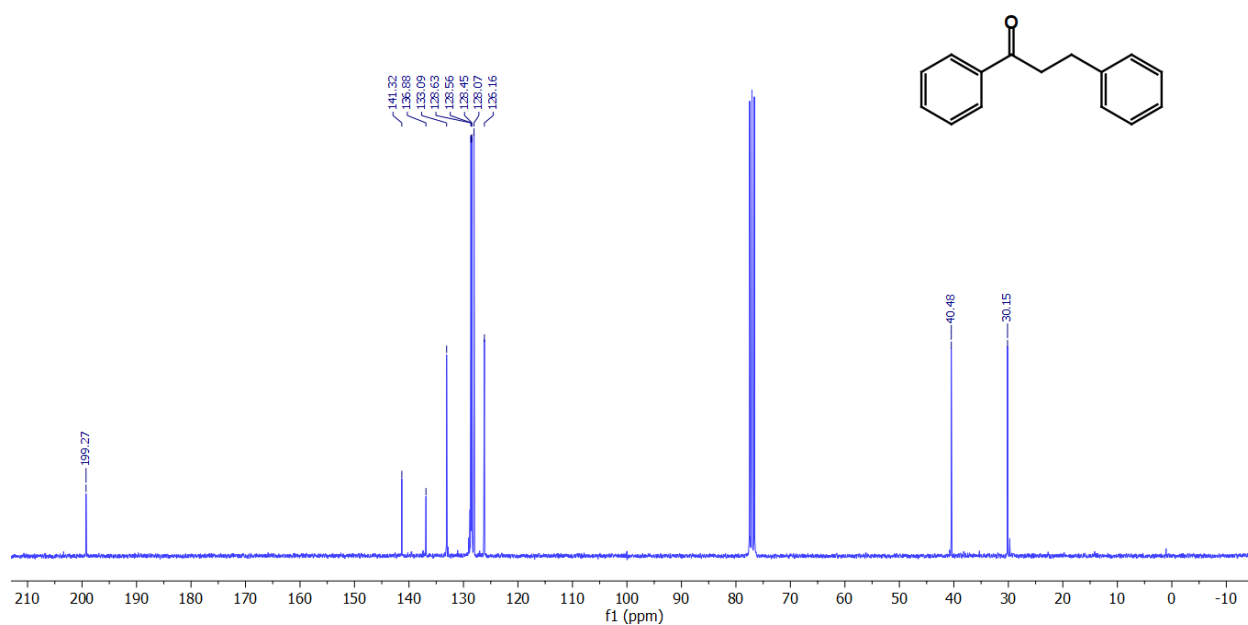
**1H-indole**<sup>31</sup> (**11a**): Eluent: Hexane/Ethyl acetate (20:1). Colorless Liquid (yield = 90%, 105mg).



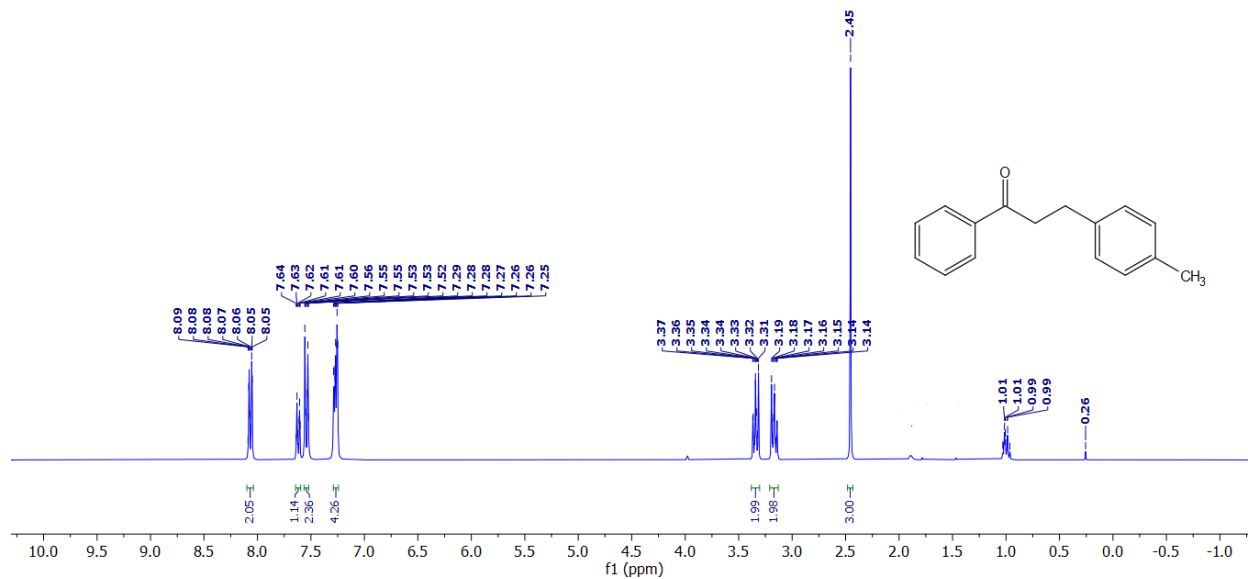
$^1\text{H}$  NMR (300 MHz,  $\text{CDCl}_3$ ):  $\delta$  (ppm) 8.17 (s, 1H), 7.70 (dd,  $J = 7.8, 1.2$  Hz, 1H), 7.45-7.41(m, 1H), 7.25-7.16(m, 3H), 6.61-6.59(m, 1H).  $^{13}\text{C}$  NMR (75 MHz,  $\text{CDCl}_3$ ):  $\delta$  (ppm) 135.8, 127.9, 124.1, 122.0, 120.7, 119.8, 111.0, 102.6.



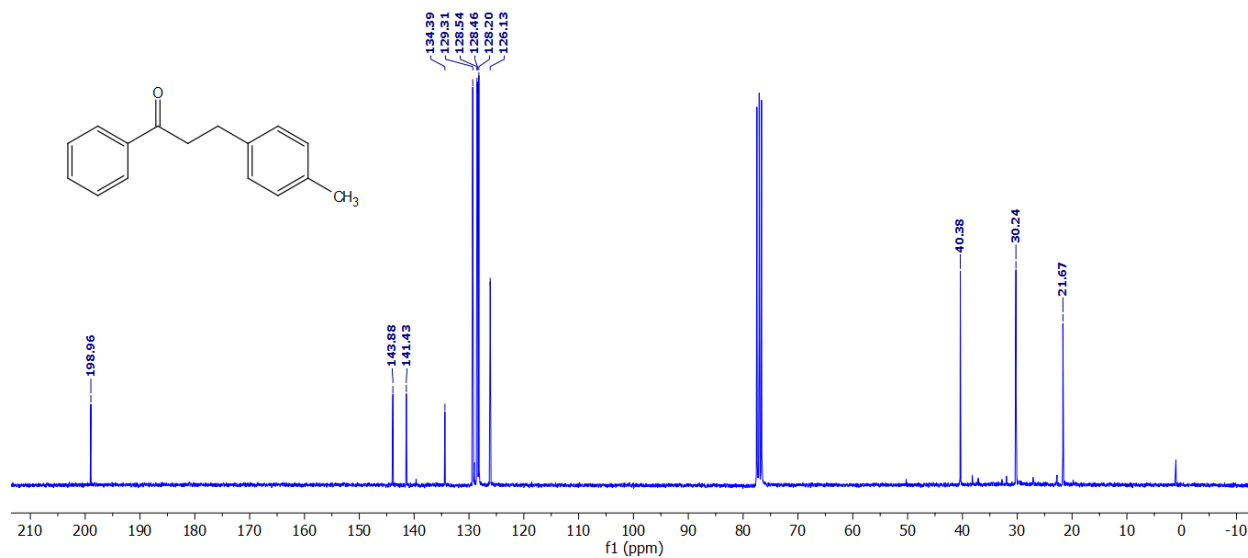
**Fig. S12**  $^1\text{H NMR}$  spectrum of compound **5aa** (300 MHz,  $\text{CDCl}_3$ ).



**Fig. S13**  $^{13}\text{C NMR}$  spectrum of compound **5aa** (75 MHz,  $\text{CDCl}_3$ ).

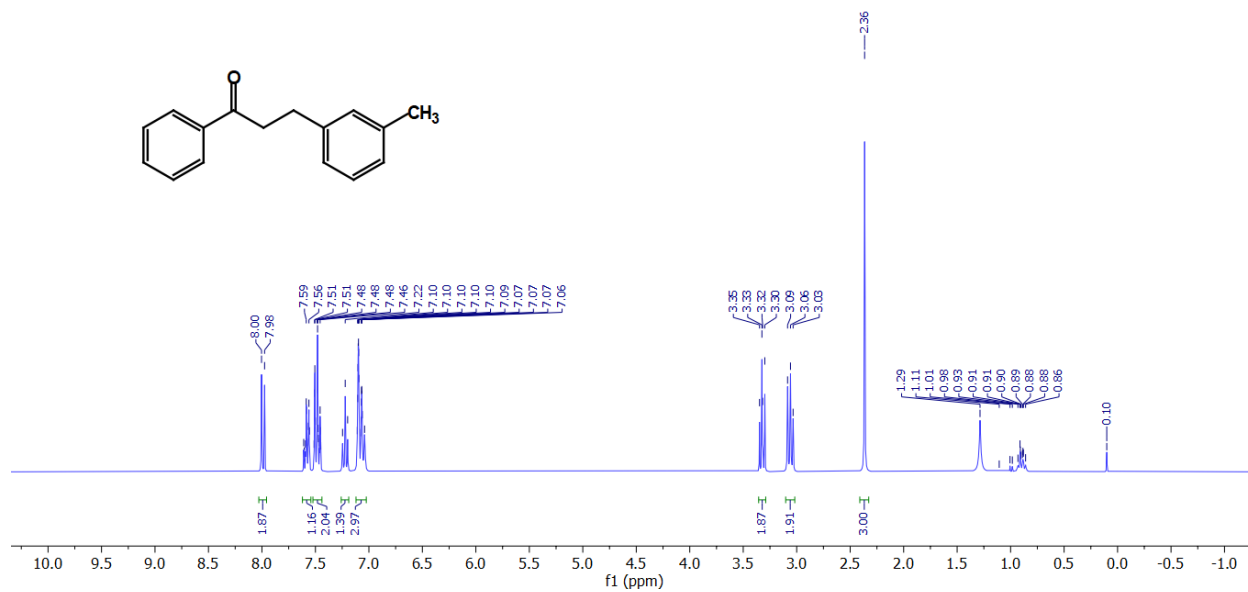


**Fig. S14**  $^1\text{H}$  NMR spectrum of compound **5ab** (300 MHz,  $\text{CDCl}_3$ ).

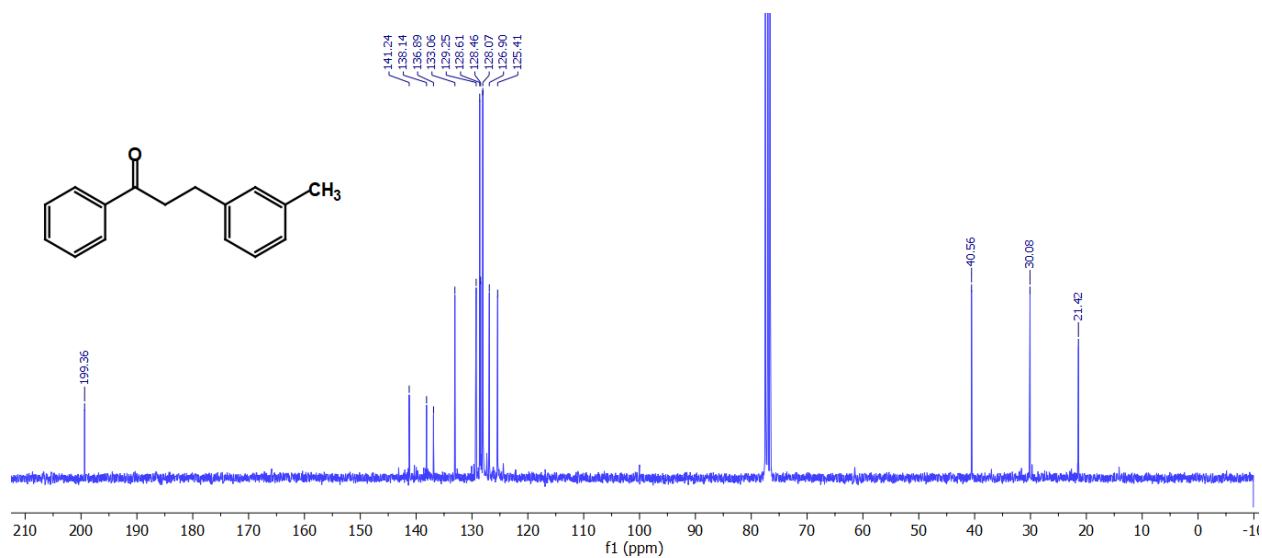


**Fig. S15**  $^{13}\text{C}$  NMR spectrum of compound **5ab** (75 MHz,  $\text{CDCl}_3$ ).

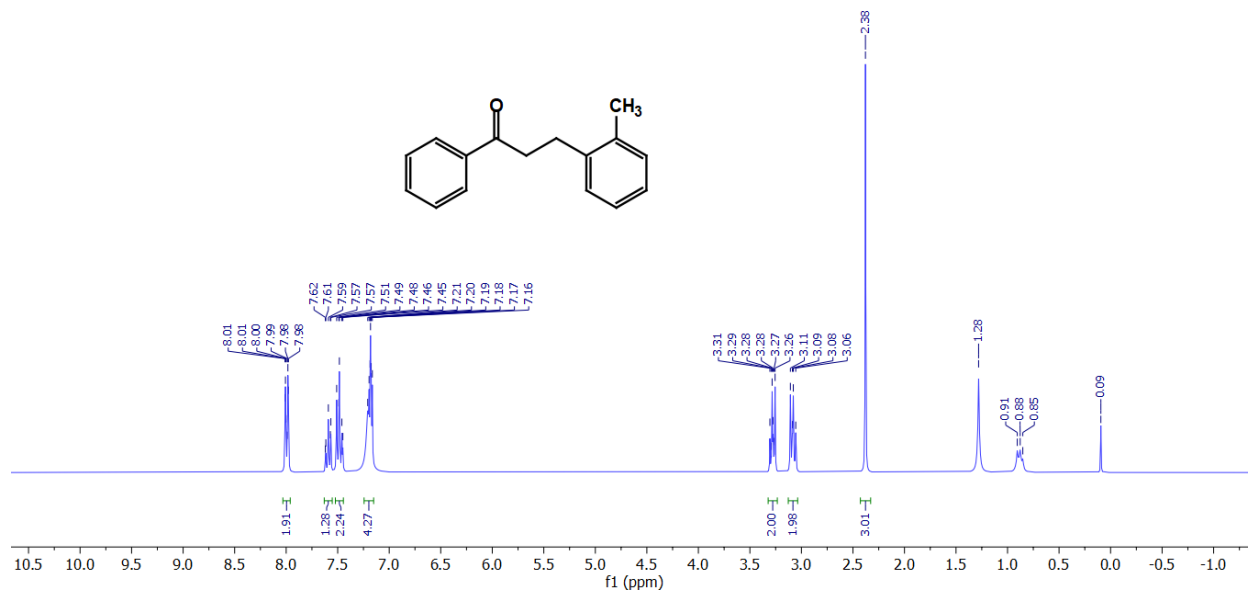




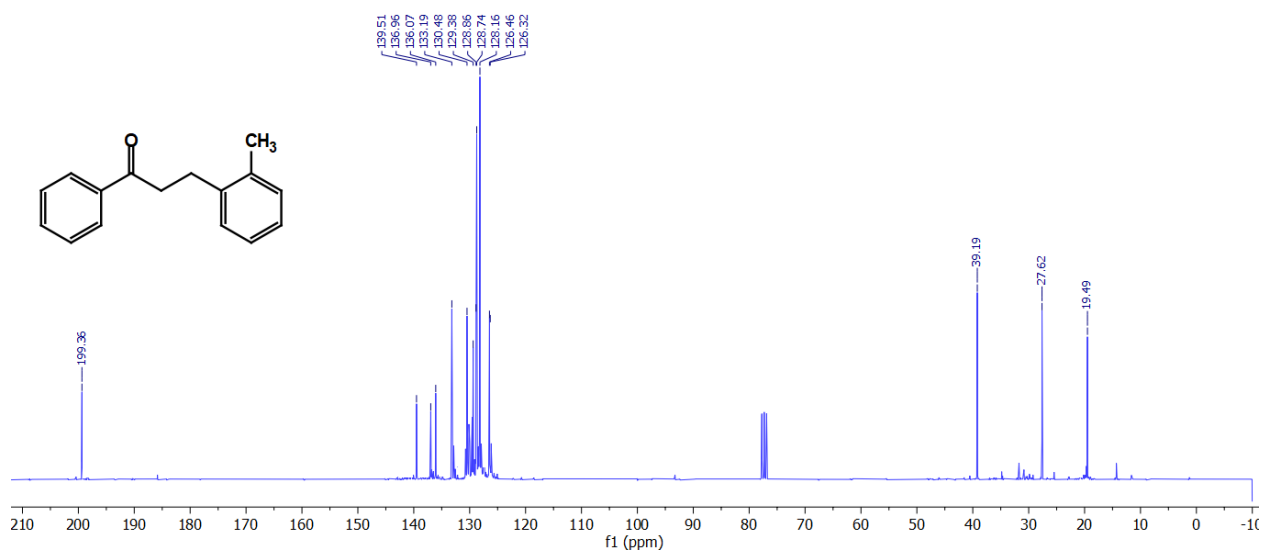
**Fig. S16** <sup>1</sup>H NMR spectrum of compound **5ac** (300 MHz, CDCl<sub>3</sub>).



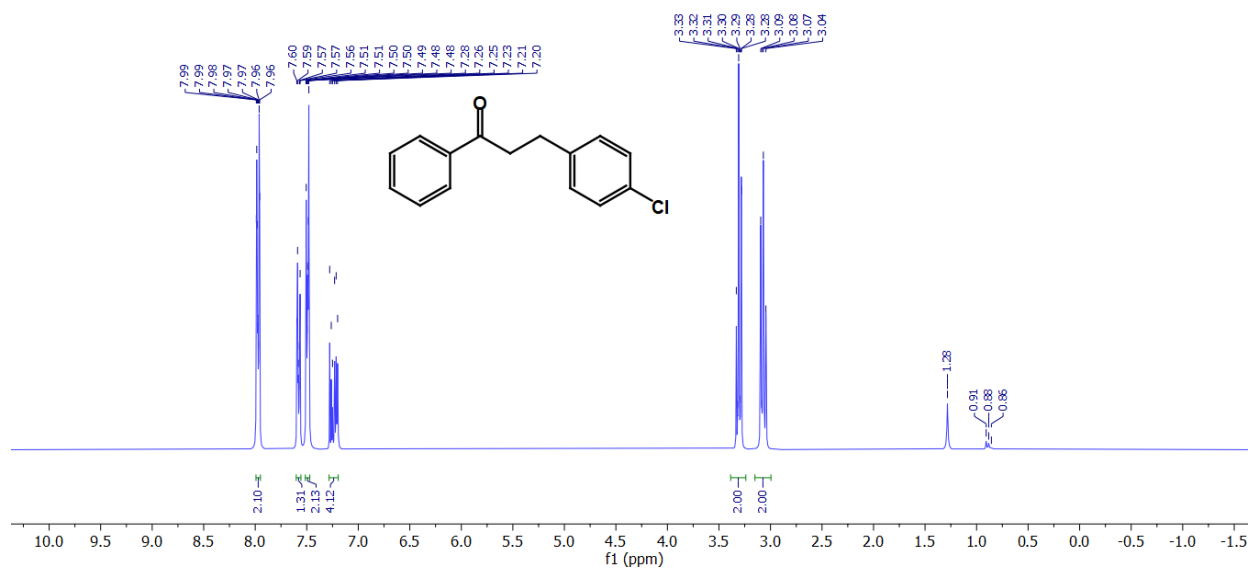
**Fig. S17** <sup>13</sup>C NMR spectrum of compound **5ac** (75 MHz, CDCl<sub>3</sub>).



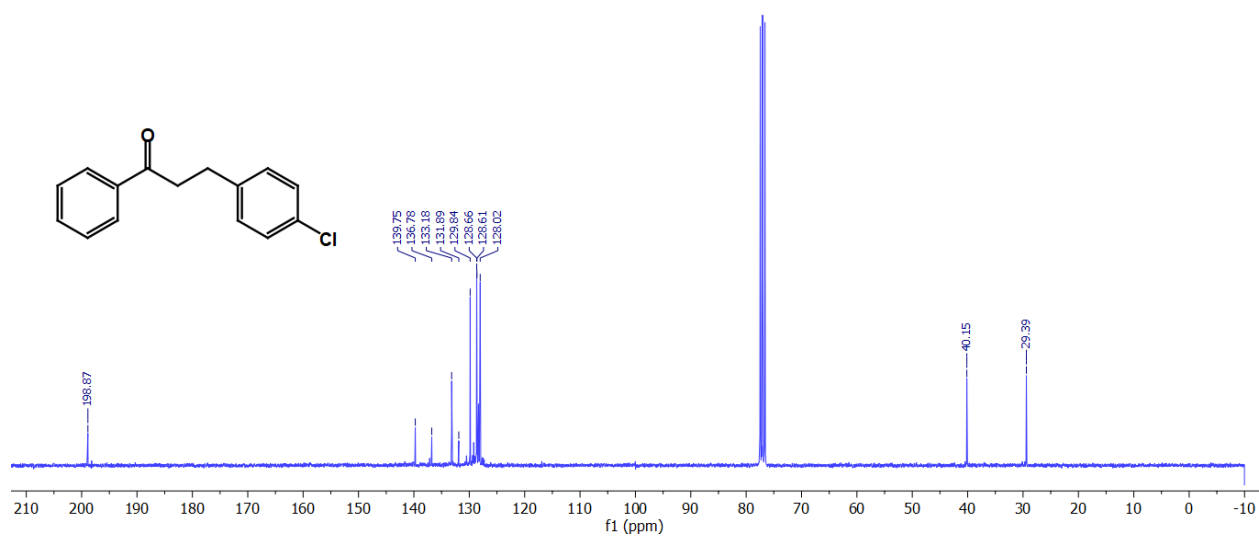
**Fig. S18** <sup>1</sup>H NMR spectrum of compound **5ad** (300 MHz, CDCl<sub>3</sub>).



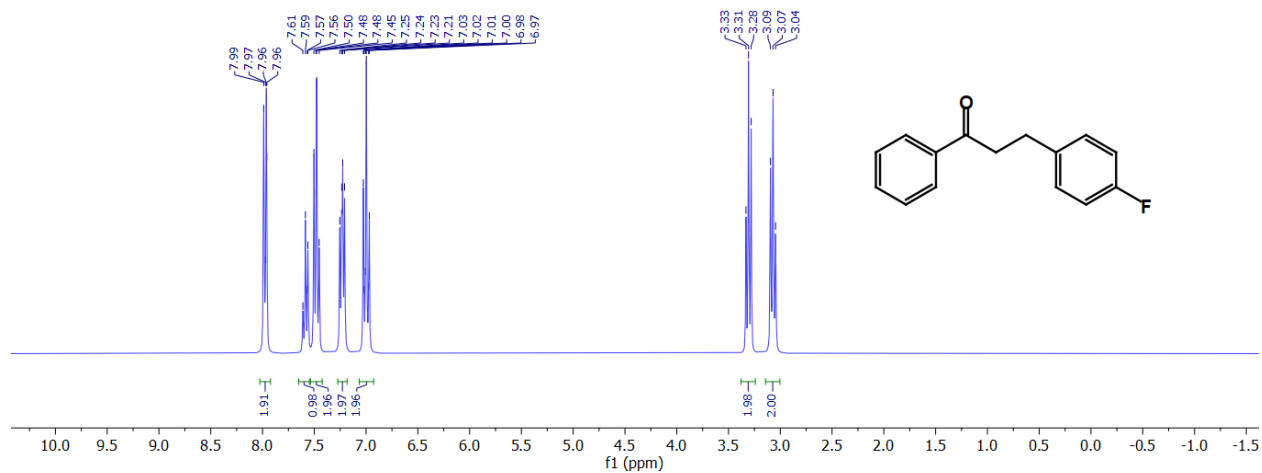
**Fig. S19** <sup>13</sup>C NMR spectrum of compound **5ad** (75 MHz, CDCl<sub>3</sub>).



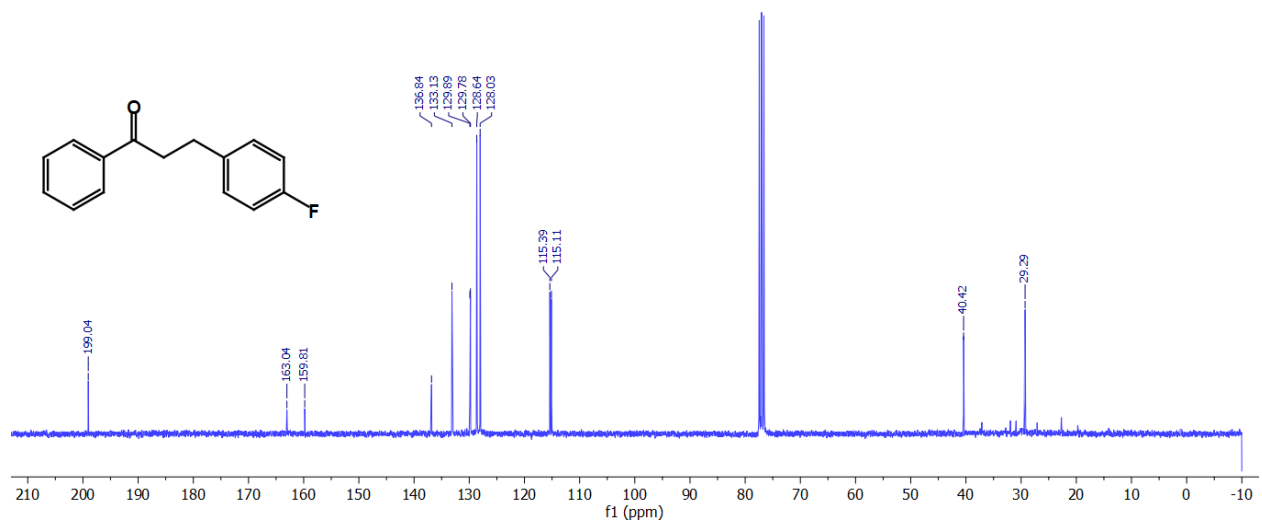
**Fig. S20** <sup>1</sup>H NMR spectrum of compound **5ae** (300 MHz, CDCl<sub>3</sub>).



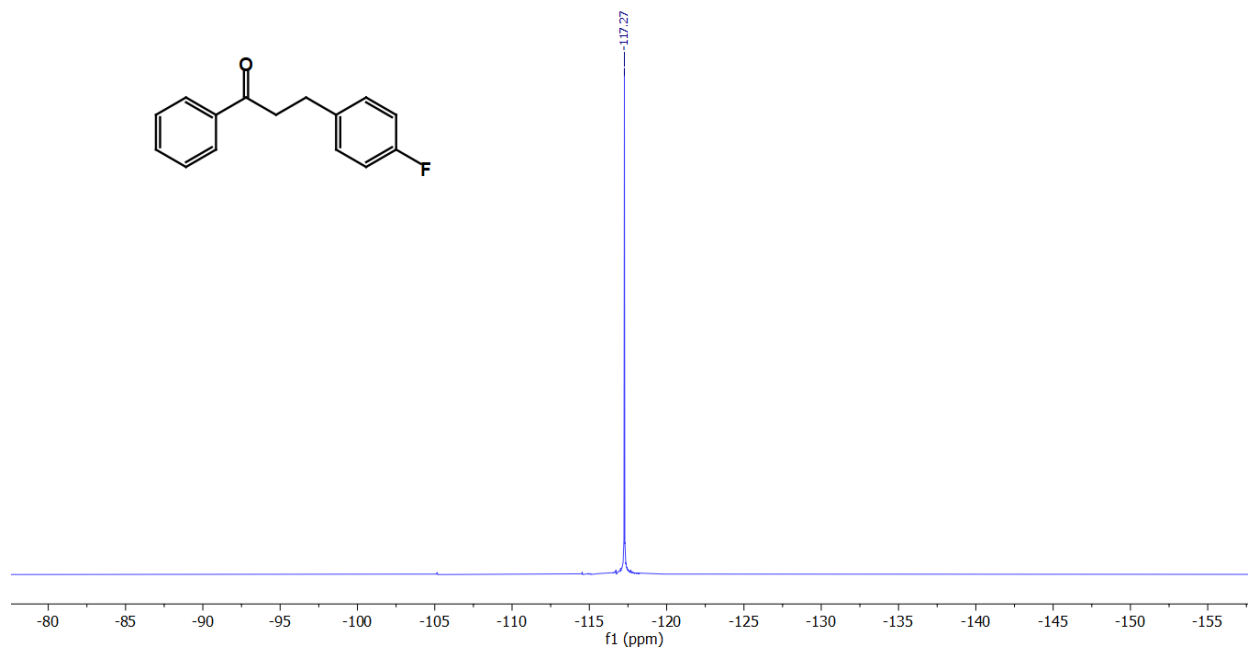
**Fig. S21** <sup>13</sup>C NMR spectrum of compound **5ae** (75 MHz, CDCl<sub>3</sub>).



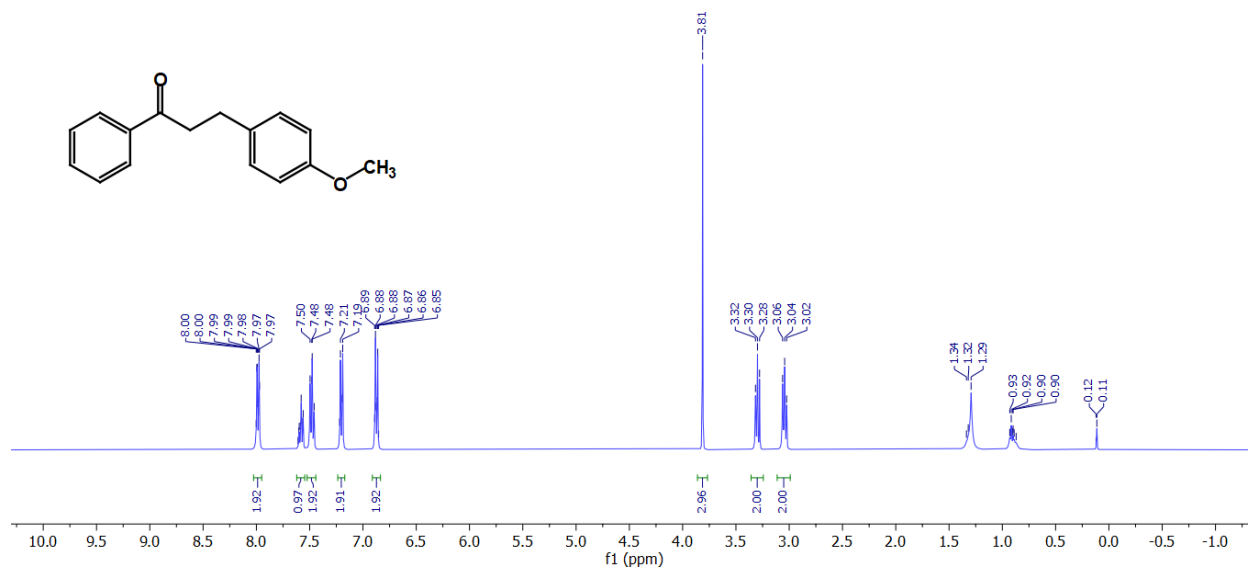
**Fig. S22**  $^1\text{H}$  NMR spectrum of compound **5af** (300 MHz,  $\text{CDCl}_3$ ).



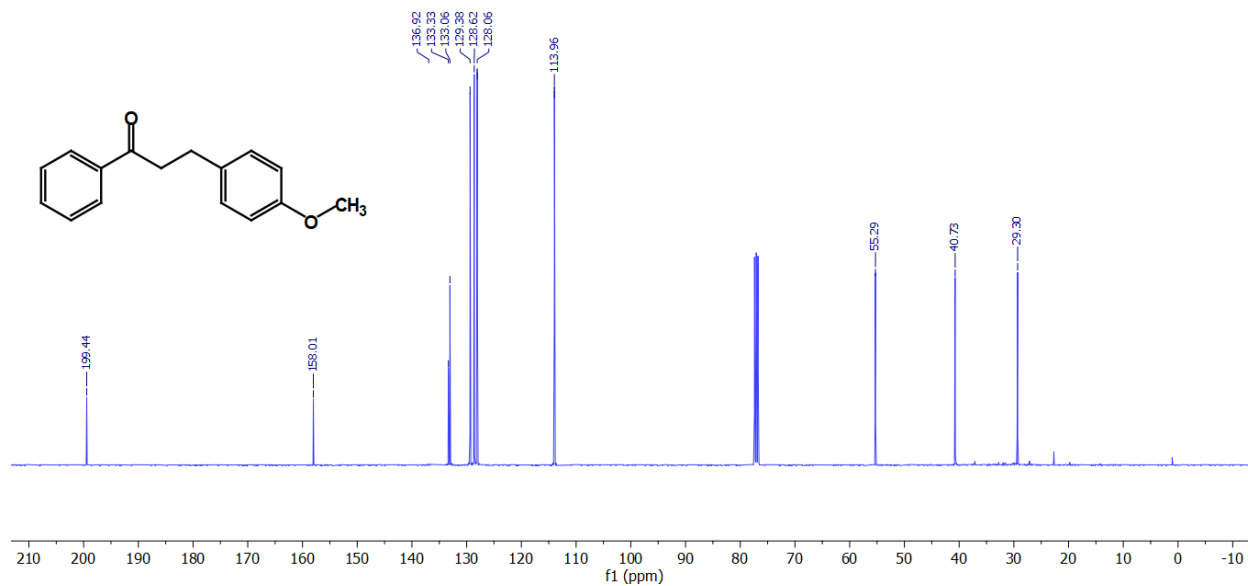
**Fig. S23**  $^{13}\text{C}$  NMR spectrum of compound **5af** (75 MHz,  $\text{CDCl}_3$ ).



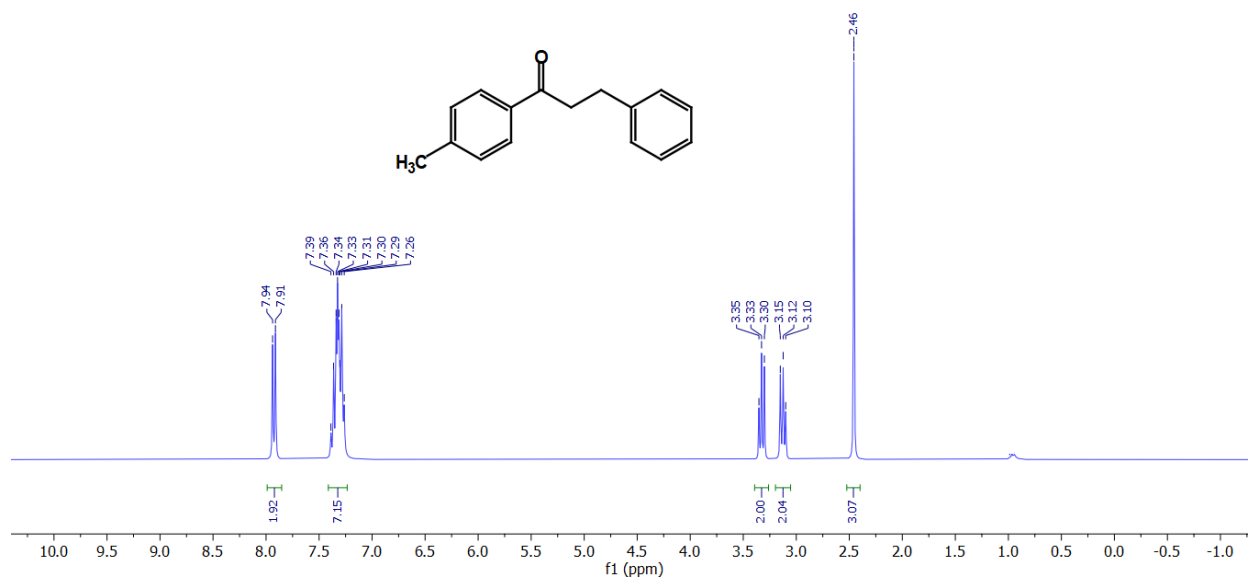
**Fig. S24**  $^{19}\text{F}$  NMR spectrum of compound **5af** (282 MHz,  $\text{CDCl}_3$ ).



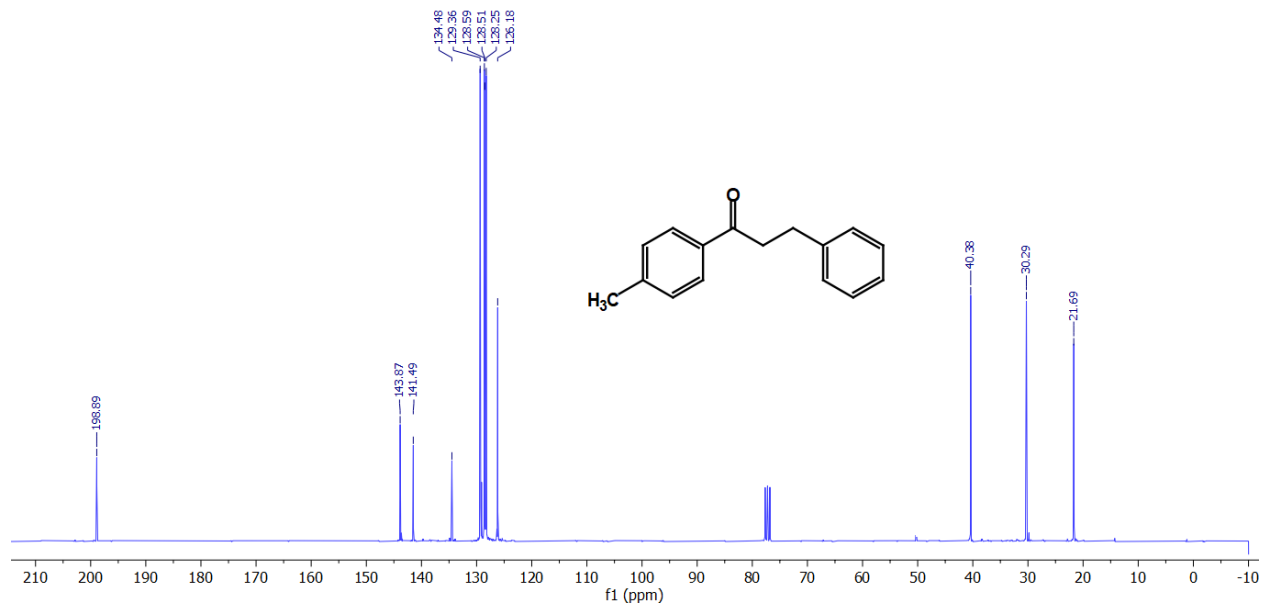
**Fig. S25**  $^1\text{H}$  NMR spectrum of compound **5ag** (300 MHz,  $\text{CDCl}_3$ ).



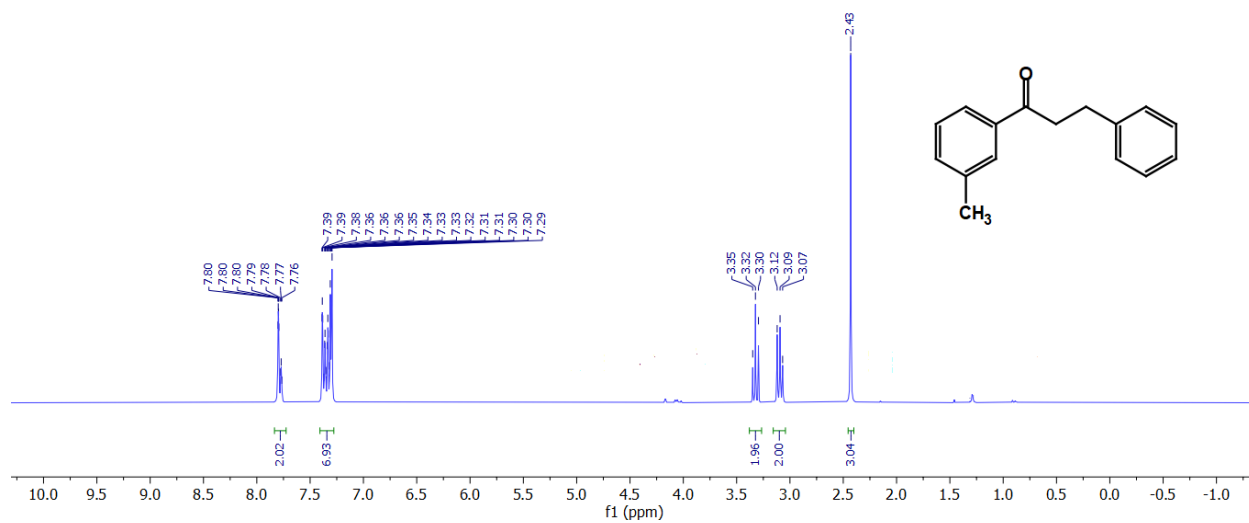
**Fig. S26**  $^{13}\text{C}$  NMR spectrum of compound **5ag** (75 MHz,  $\text{CDCl}_3$ ).



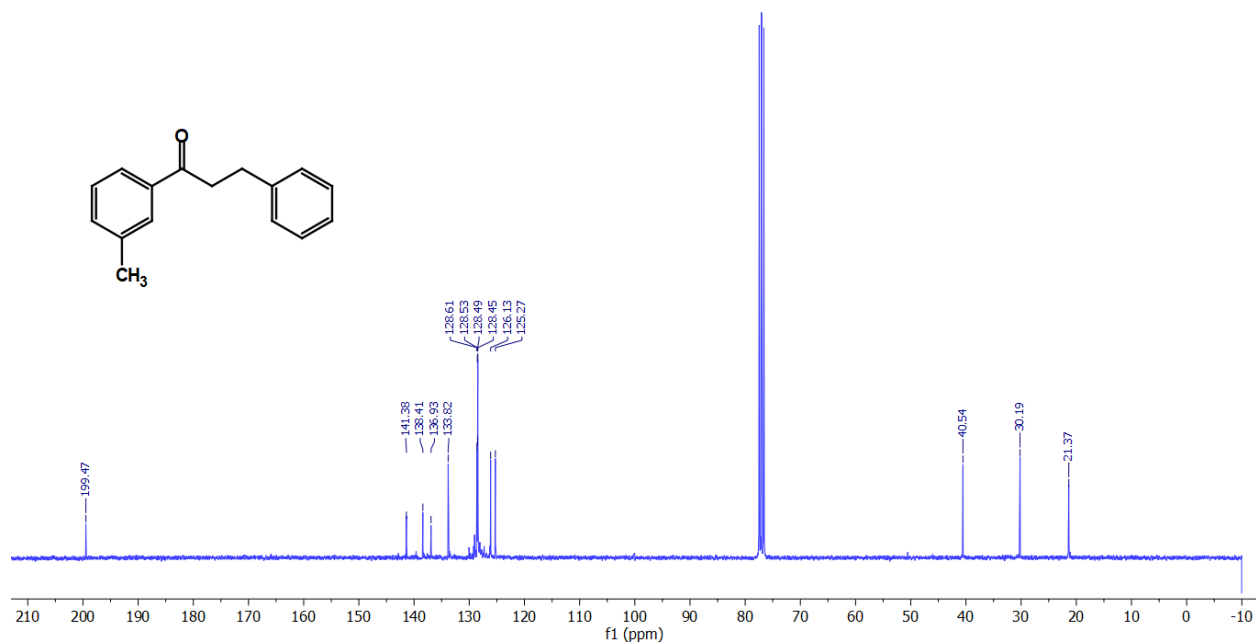
**Fig. S27**  $^1\text{H}$  NMR spectrum of compound **5ah** (300 MHz,  $\text{CDCl}_3$ ).



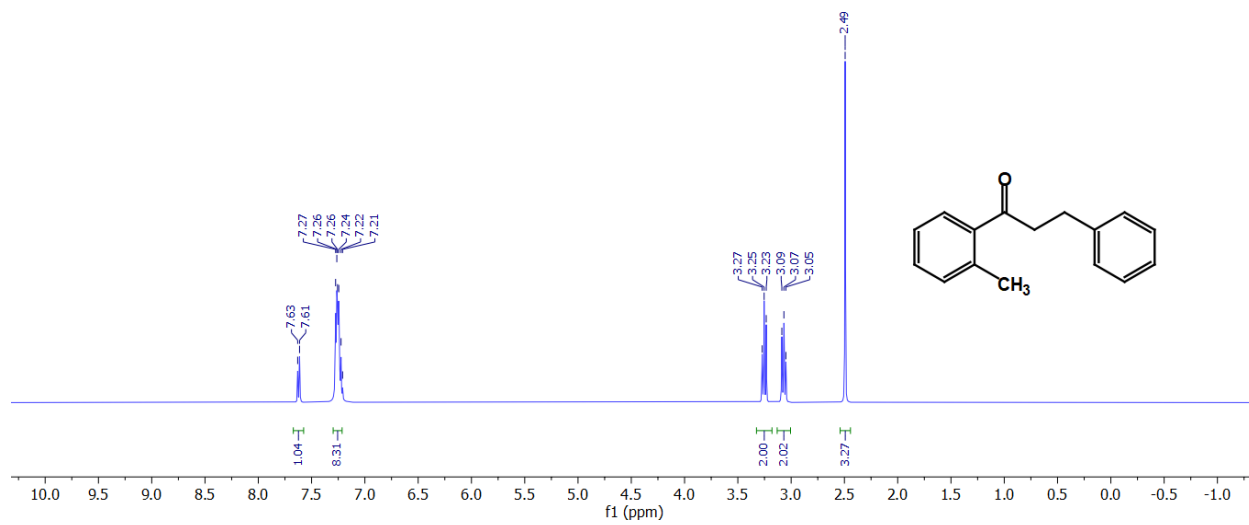
**Fig. S28**  $^{13}\text{C}$  NMR spectrum of compound **5ah** (75 MHz,  $\text{CDCl}_3$ ).



**Fig. S29**  $^1\text{H}$  NMR spectrum of compound **5ai** (300 MHz,  $\text{CDCl}_3$ ).

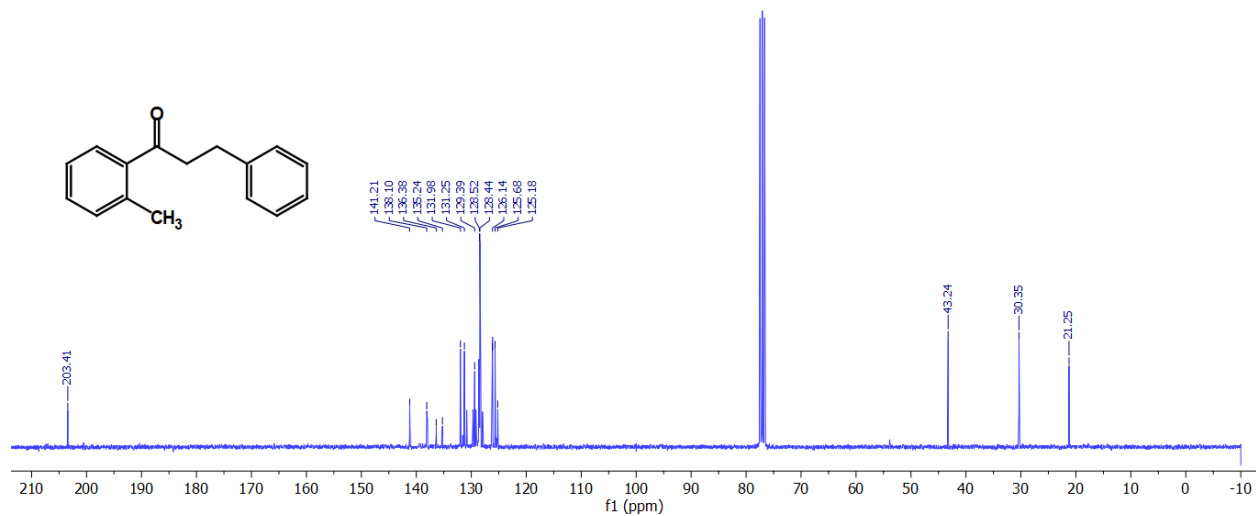


**Fig. S30**  $^{13}\text{C}$  NMR spectrum of compound **5ai** (75 MHz,  $\text{CDCl}_3$ ).

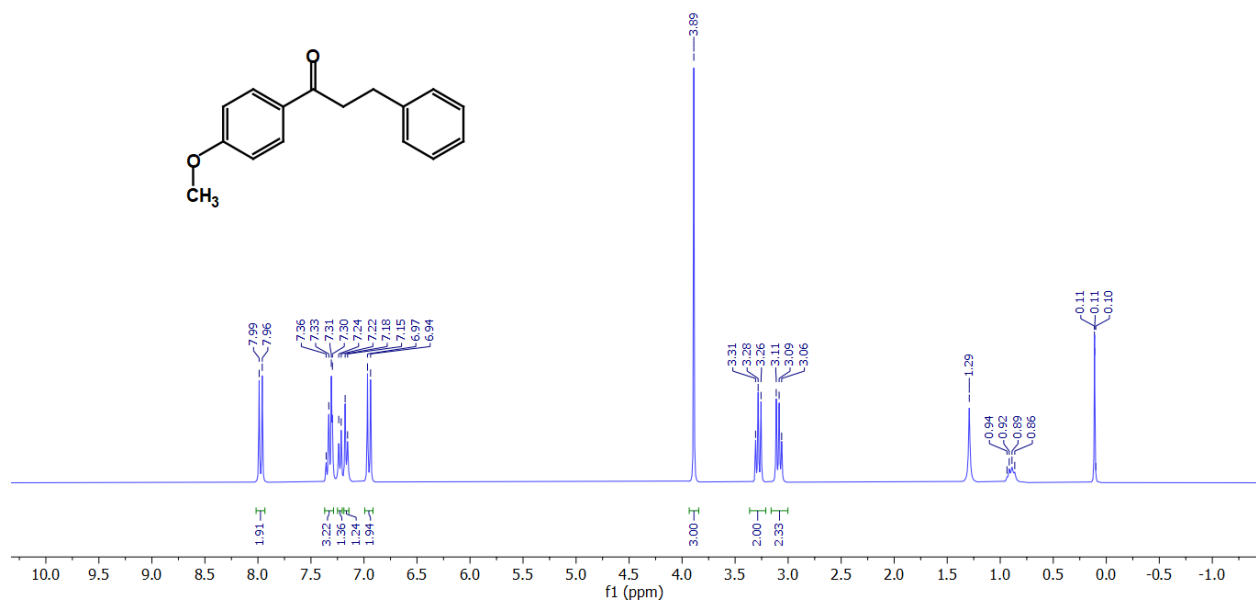


**Fig. S31**  $^1\text{H}$  NMR spectrum of compound **5aj** (300 MHz,  $\text{CDCl}_3$ ).

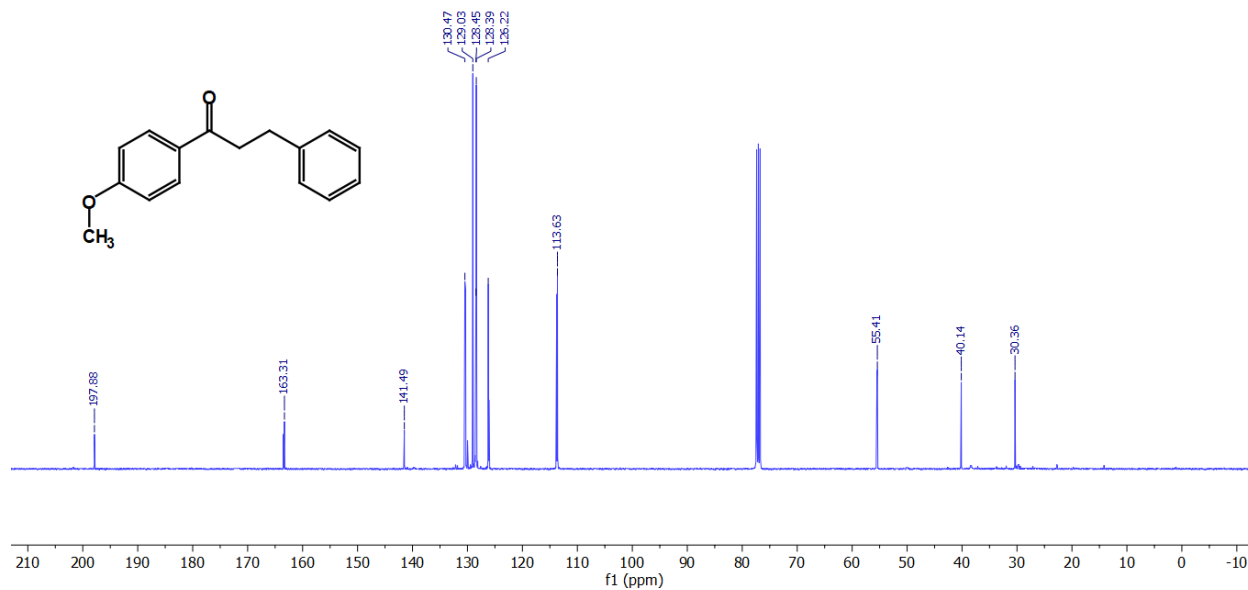




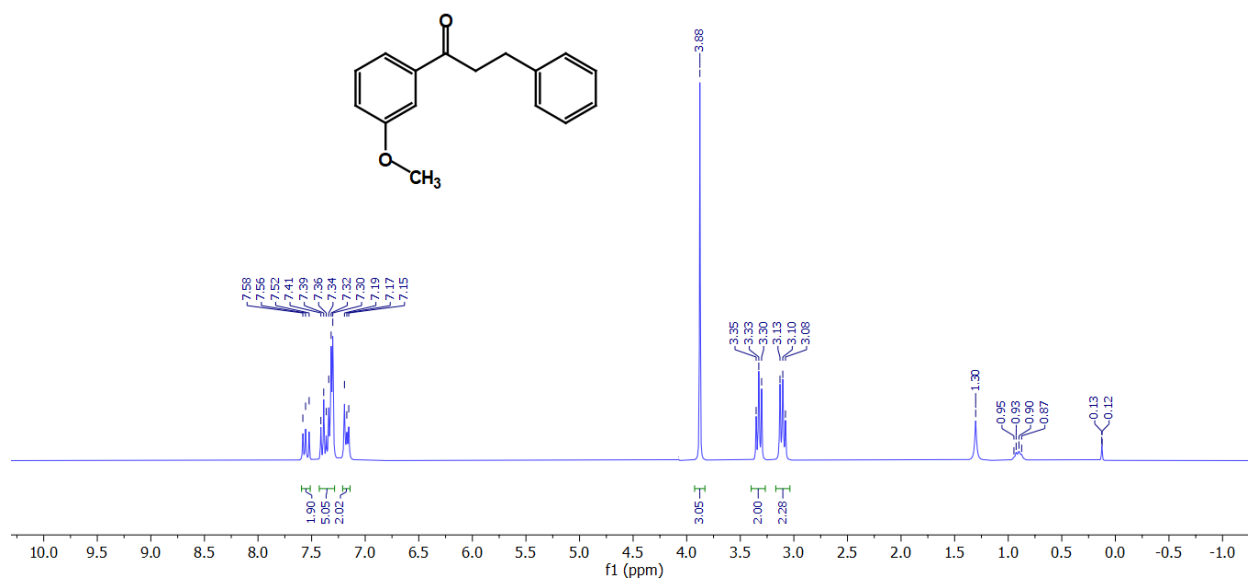
**Fig. S32**  $^{13}\text{C}$  NMR spectrum of compound **5aj** (75 MHz,  $\text{CDCl}_3$ ).



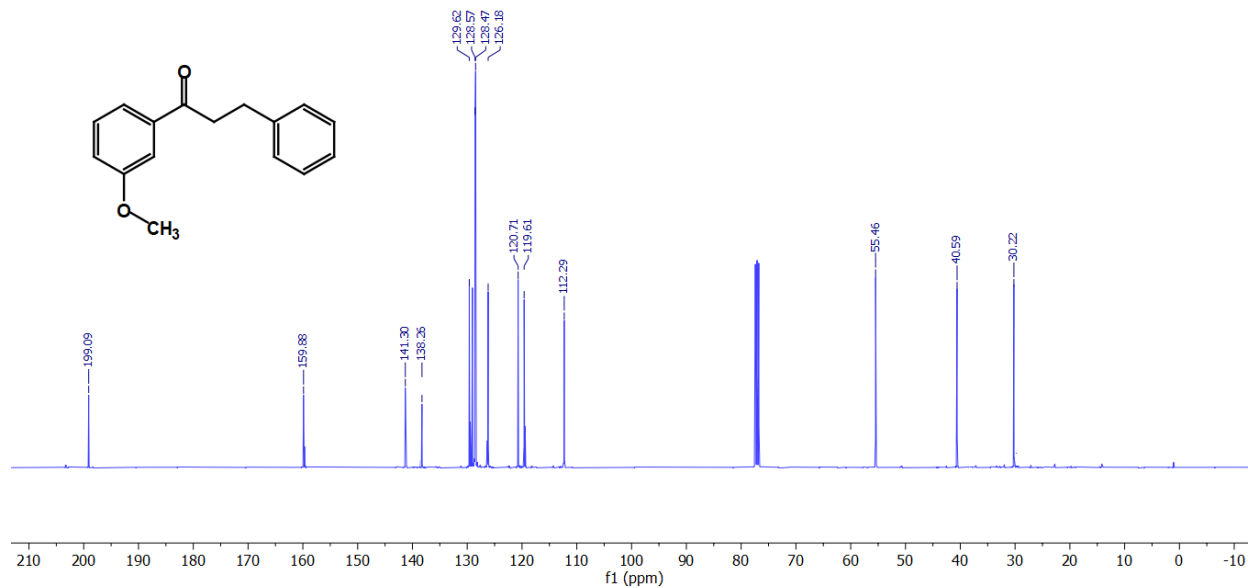
**Fig. S33**  $^1\text{H}$  NMR spectrum of compound **5ak** (300 MHz,  $\text{CDCl}_3$ ).



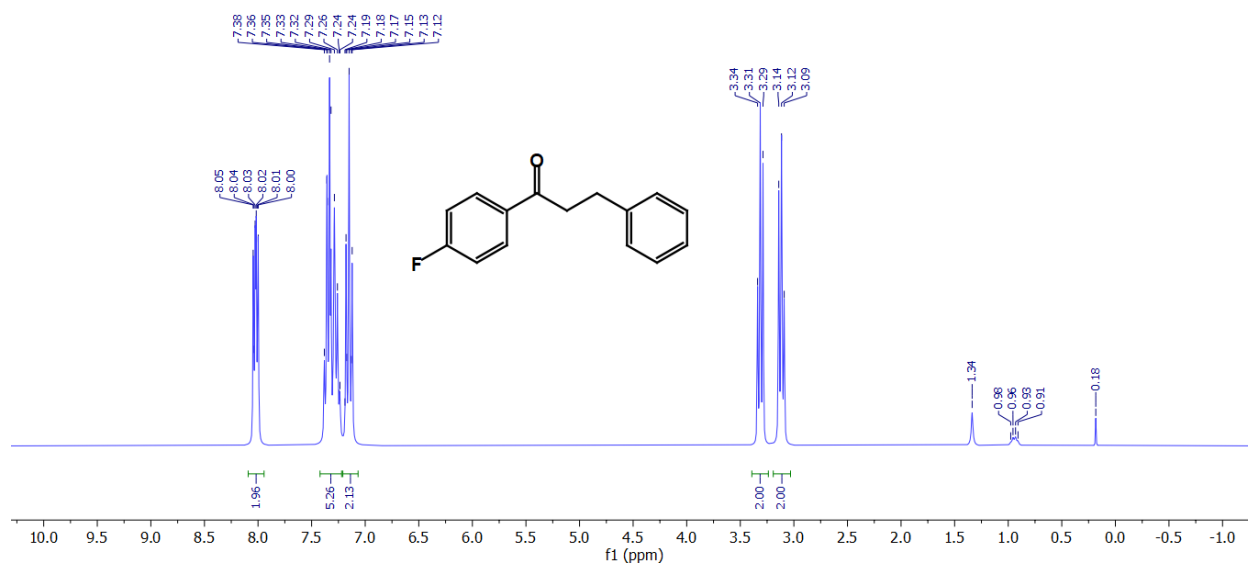
**Fig. S34** <sup>13</sup>C NMR spectrum of compound **5ak** (75 MHz, CDCl<sub>3</sub>).



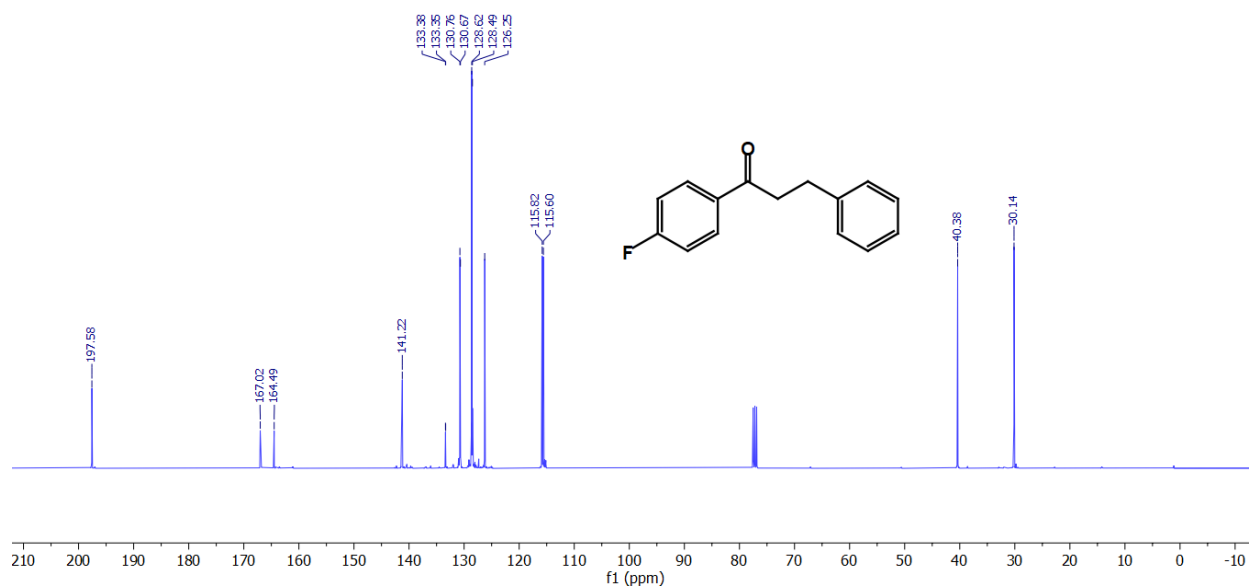
**Fig. S35** <sup>1</sup>H NMR spectrum of compound **5al** (300 MHz, CDCl<sub>3</sub>).



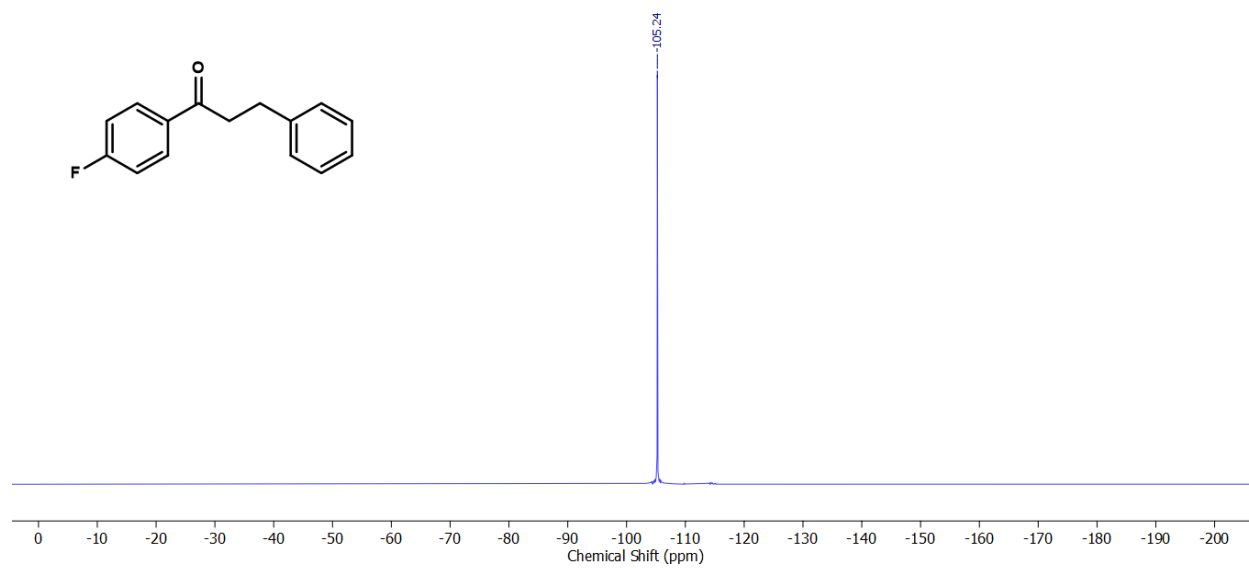
**Fig. S36**  $^{13}\text{C}$  NMR spectrum of compound **5al** (75 MHz,  $\text{CDCl}_3$ ).



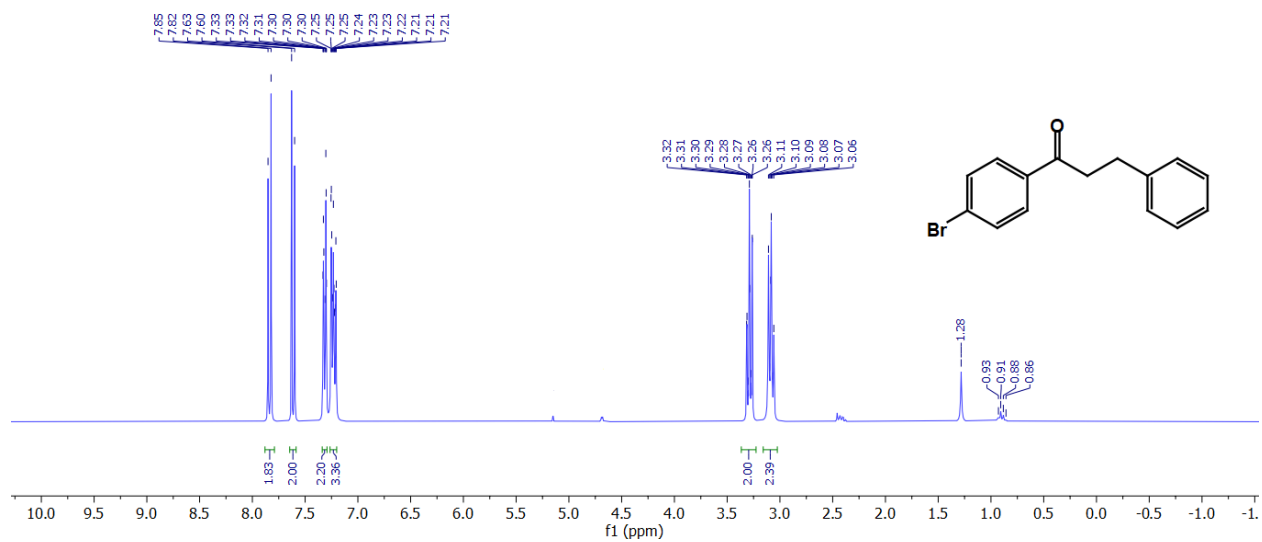
**Fig. S37**  $^1\text{H}$  NMR spectrum of compound **5am** (300 MHz,  $\text{CDCl}_3$ ).



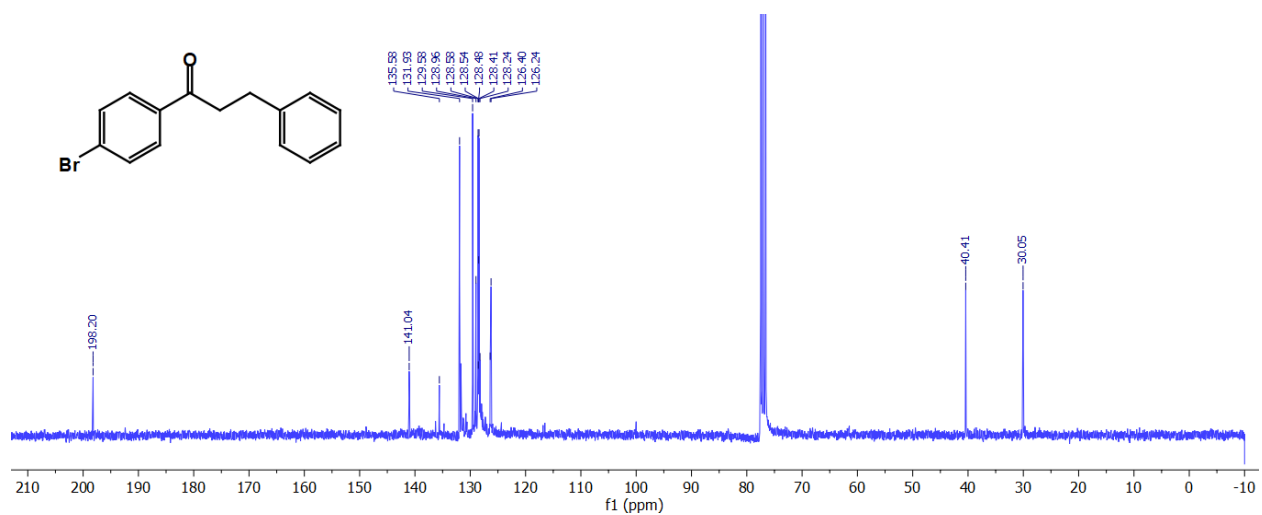
**Fig. S38**  $^{13}\text{C}$  NMR spectrum of compound **5am** (75 MHz,  $\text{CDCl}_3$ ).



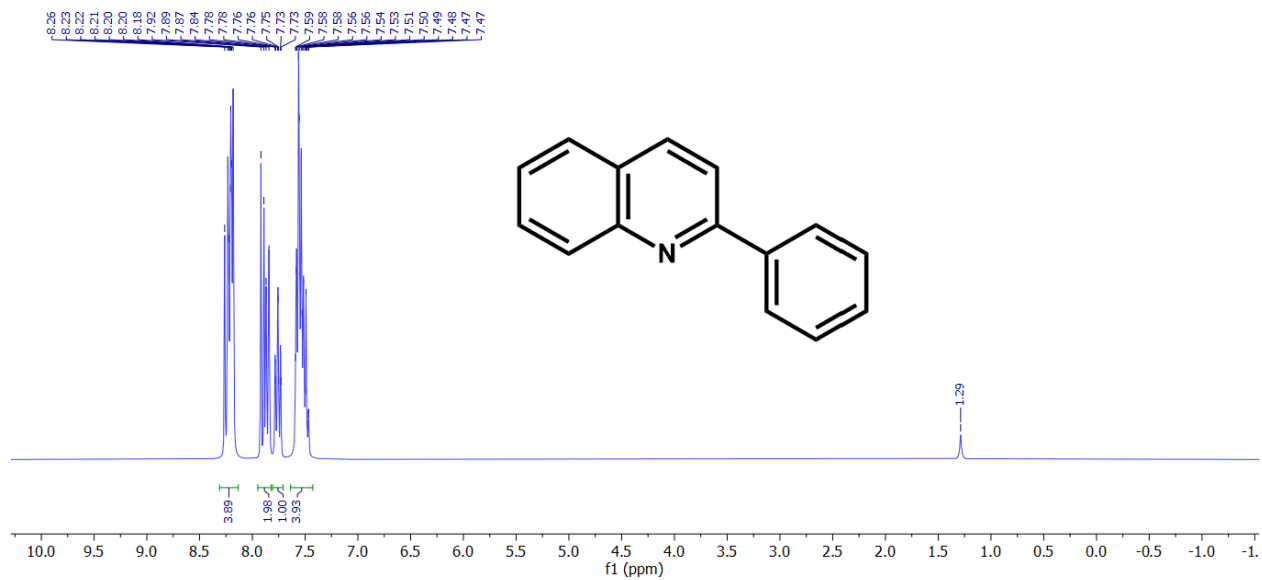
**Fig. S39**  $^{19}\text{F}$  NMR spectrum of compound **5am** (282 MHz,  $\text{CDCl}_3$ ).



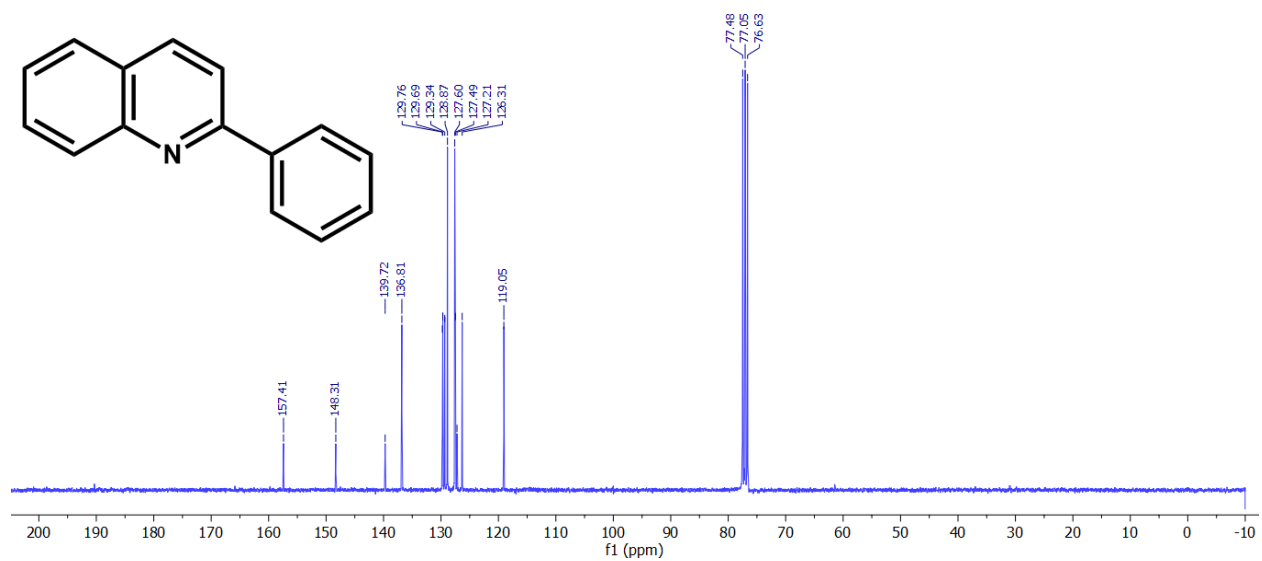
**Fig. S40** <sup>1</sup>H NMR spectrum of compound **5an** (300 MHz, CDCl<sub>3</sub>).



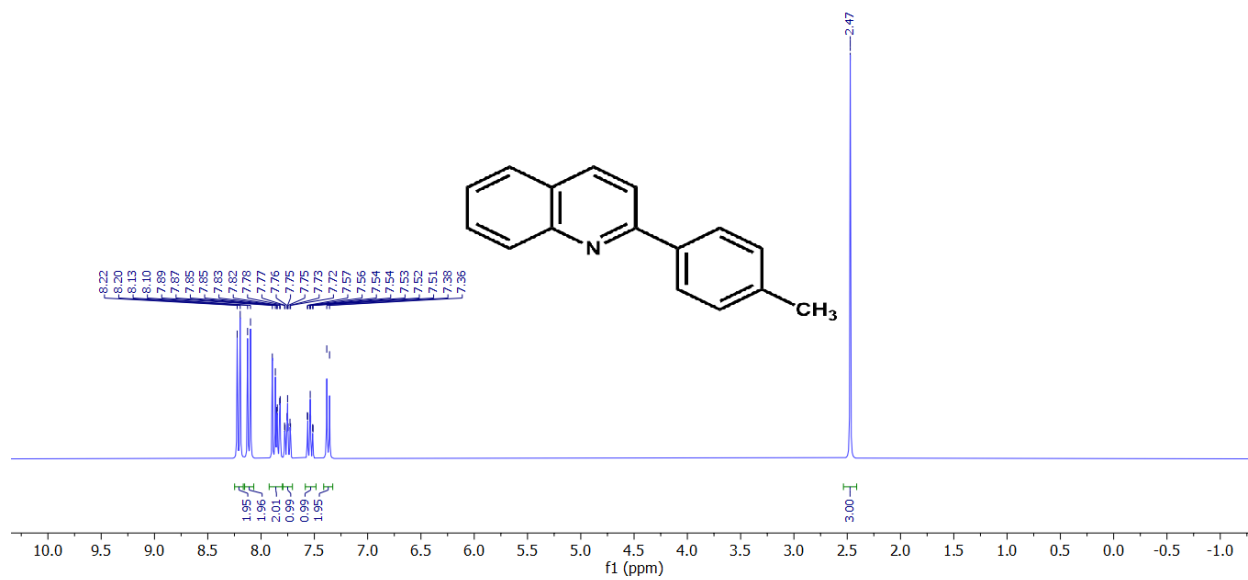
**Fig. S41** <sup>13</sup>C NMR spectrum of compound **5an** (75 MHz, CDCl<sub>3</sub>).



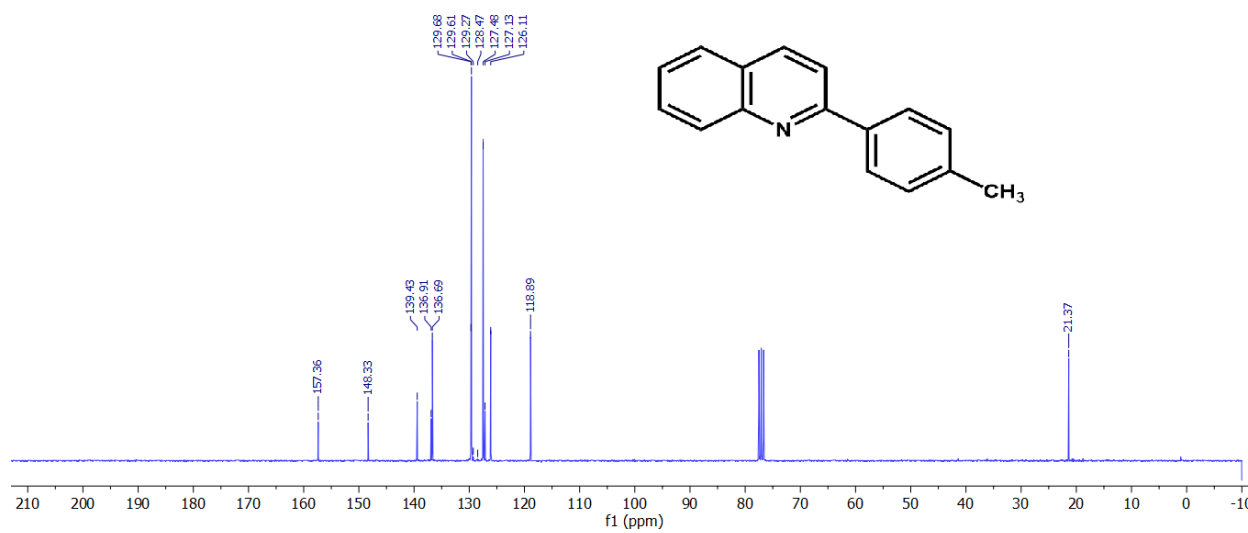
**Fig. S42**  $^1\text{H}$  NMR spectrum of compound **9aa** (300 MHz,  $\text{CDCl}_3$ ).



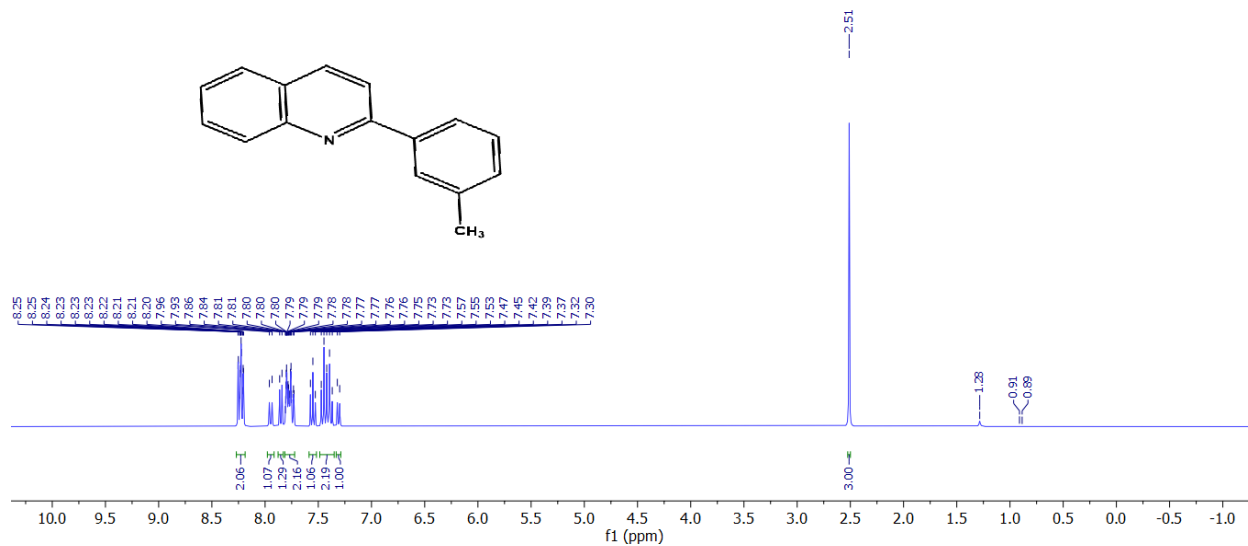
**Fig. S43**  $^{13}\text{C}$  NMR spectrum of compound **9aa** (75 MHz,  $\text{CDCl}_3$ ).



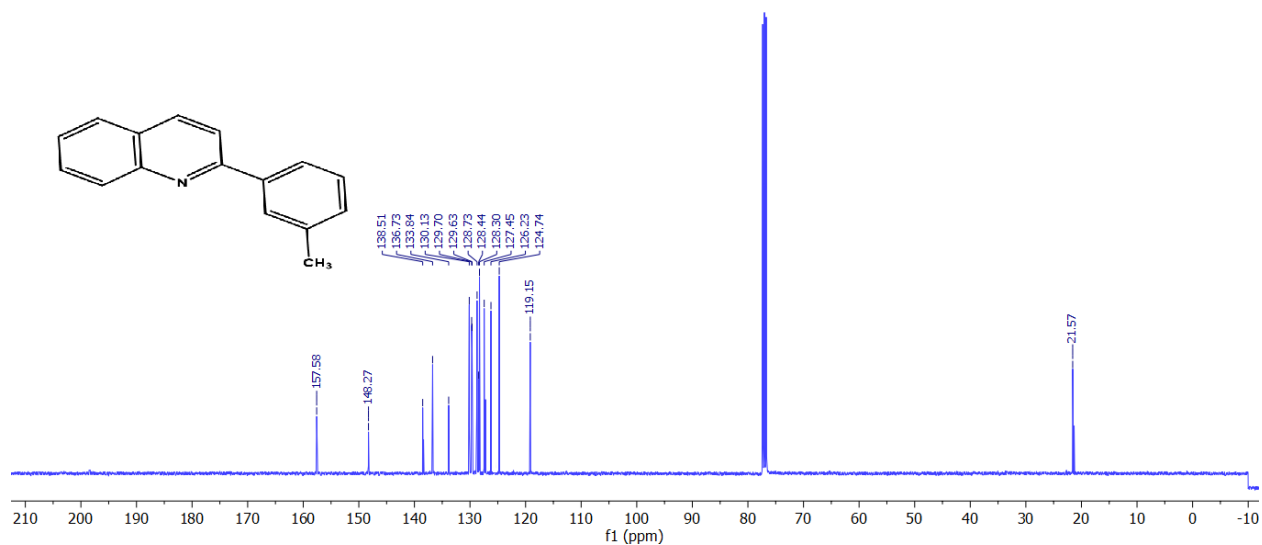
**Fig. S44**  $^1\text{H}$  NMR spectrum of compound **9ab** (300 MHz,  $\text{CDCl}_3$ ).



**Fig. S45**  $^{13}\text{C}$  NMR spectrum of compound **9ab** (75 MHz,  $\text{CDCl}_3$ ).

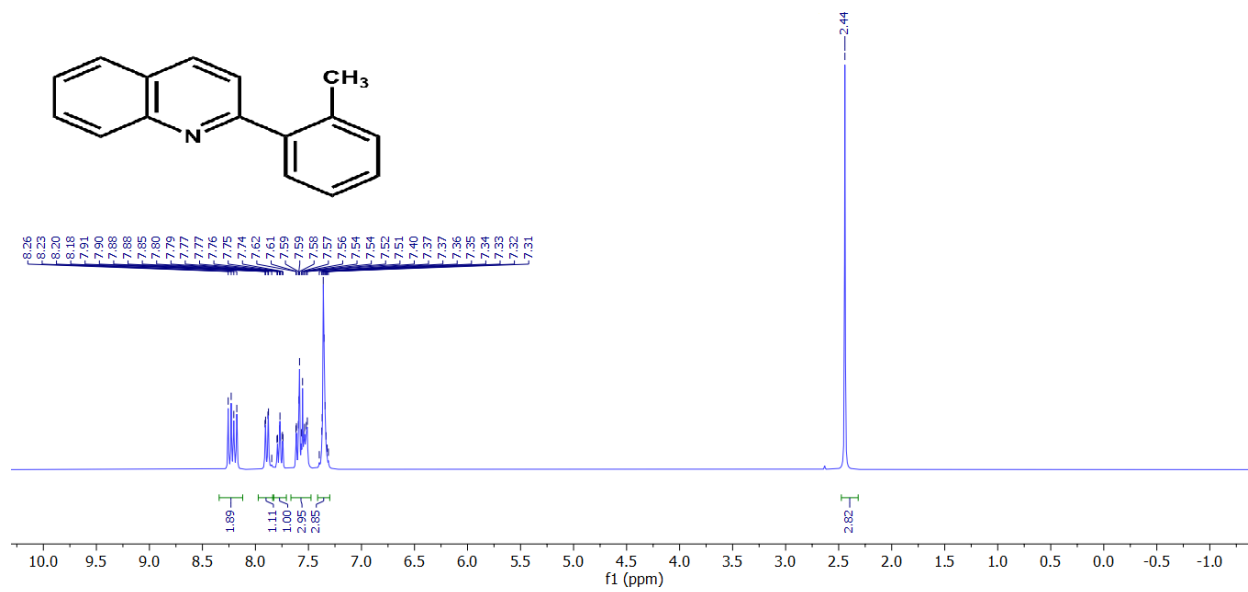


**Fig. S46** <sup>1</sup>H NMR spectrum of compound **9ac** (300 MHz, CDCl<sub>3</sub>).

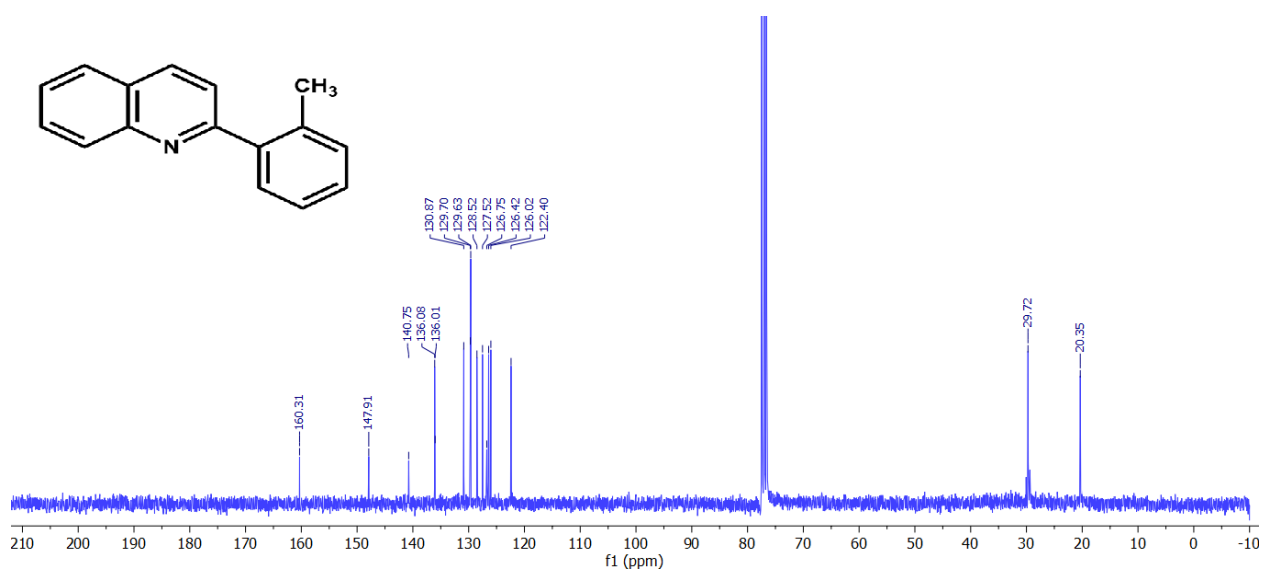


**Fig. S47** <sup>13</sup>C NMR spectrum of compound **9ac** (75 MHz, CDCl<sub>3</sub>).

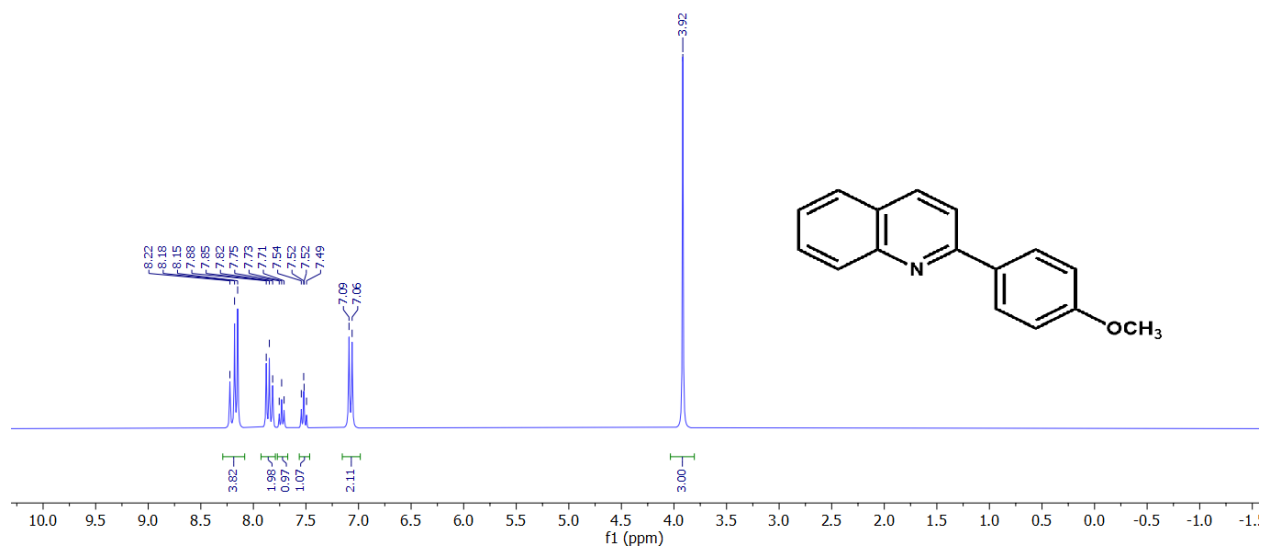




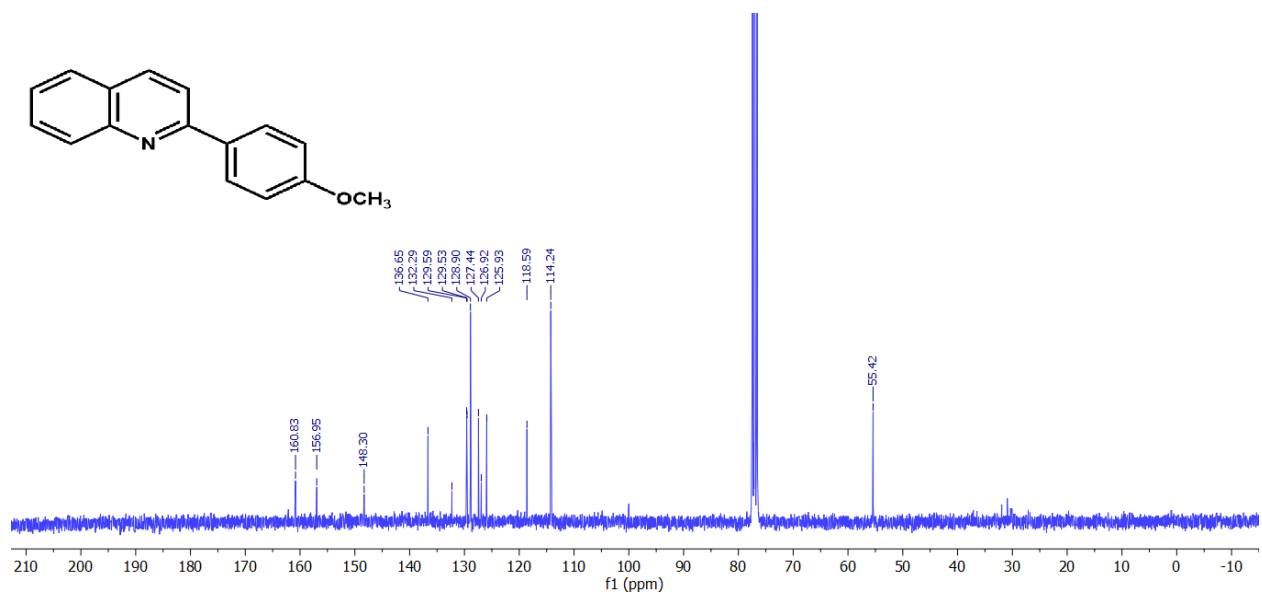
**Fig. S48** <sup>1</sup>H NMR spectrum of compound **9ad** (300 MHz, CDCl<sub>3</sub>).



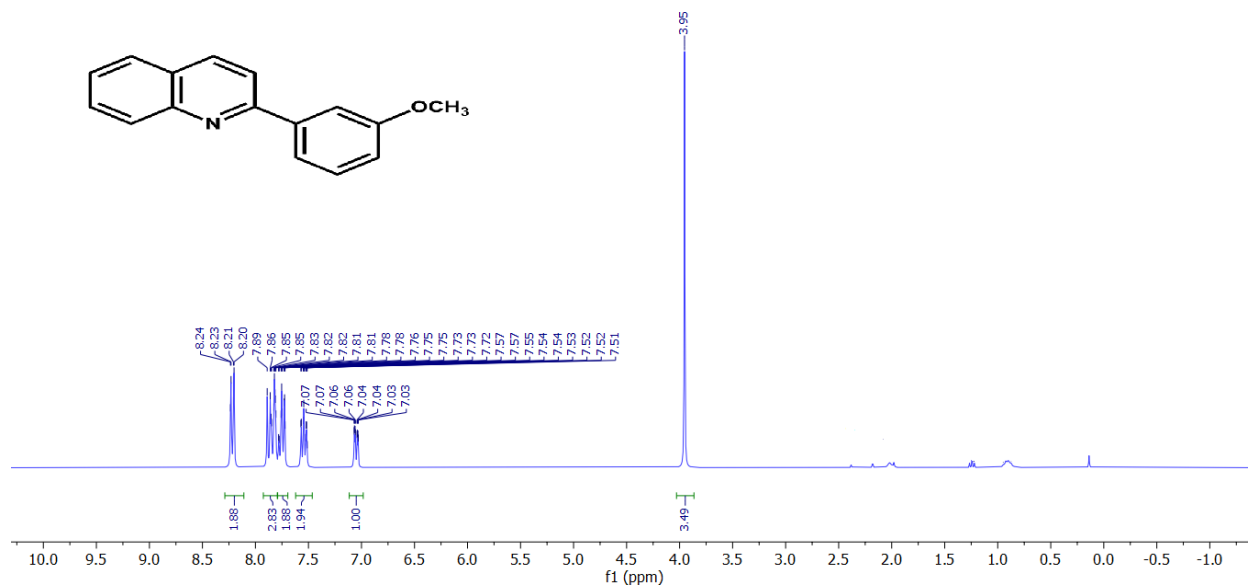
**Fig. S49** <sup>13</sup>C NMR spectrum of compound **9ad** (75 MHz, CDCl<sub>3</sub>).



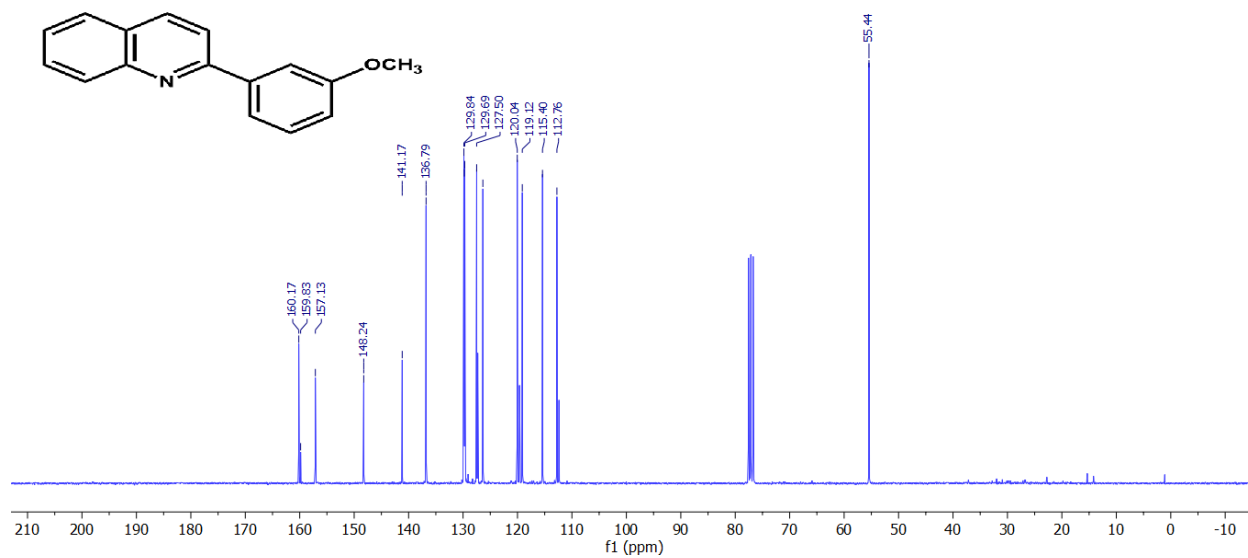
**Fig. S50** <sup>1</sup>H NMR spectrum of compound **9ae** (300 MHz, CDCl<sub>3</sub>).



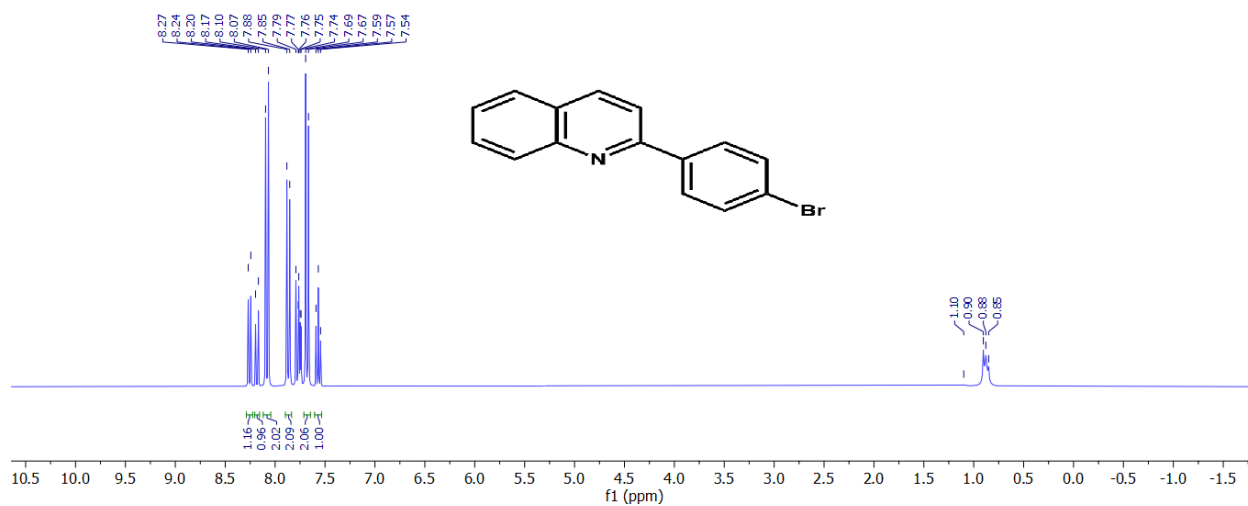
**Fig. S51** <sup>13</sup>C NMR spectrum of compound **9ae** (75 MHz, CDCl<sub>3</sub>).



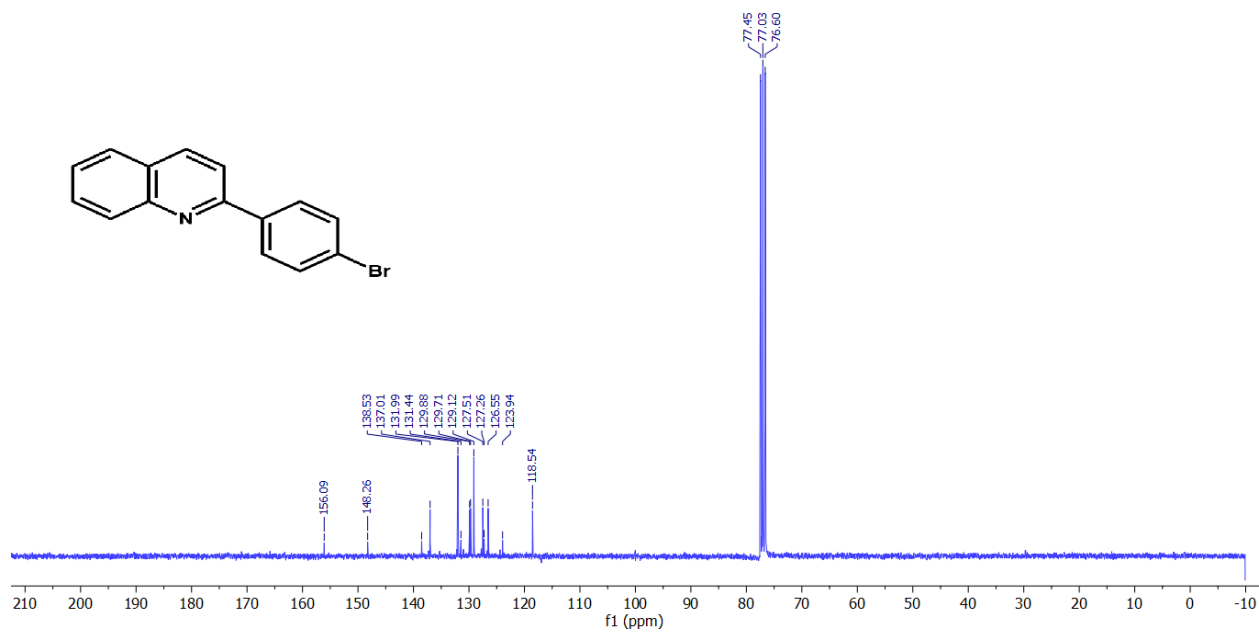
**Fig. S52** <sup>1</sup>H NMR spectrum of compound **9af** (300 MHz, CDCl<sub>3</sub>).



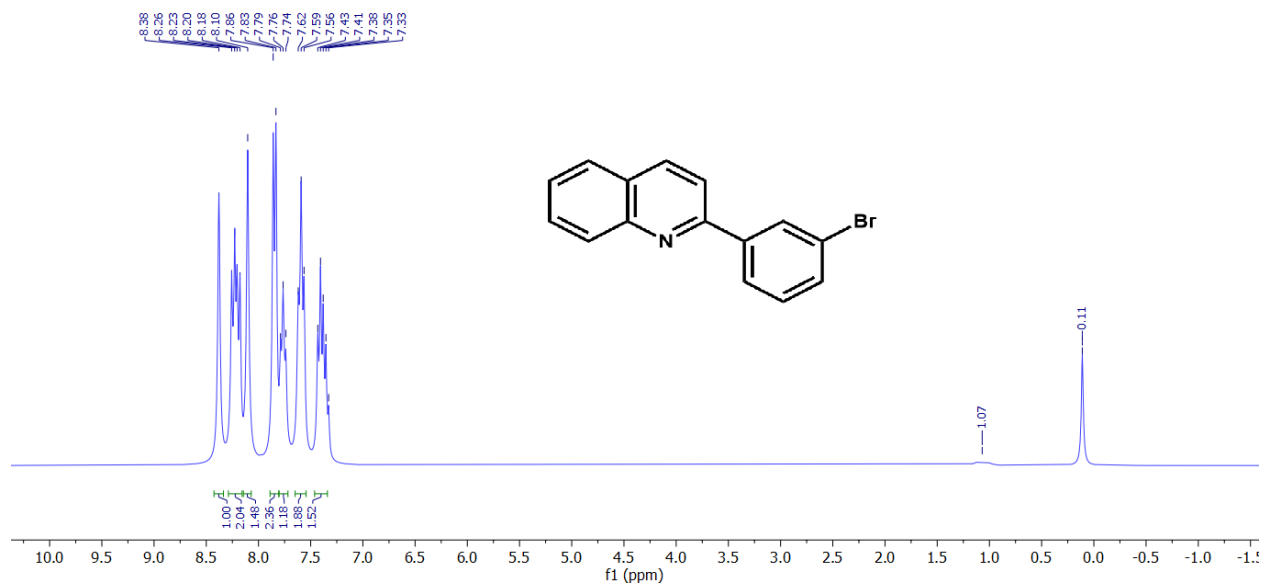
**Fig. S53** <sup>13</sup>C NMR spectrum of compound **9af** (75 MHz, CDCl<sub>3</sub>).



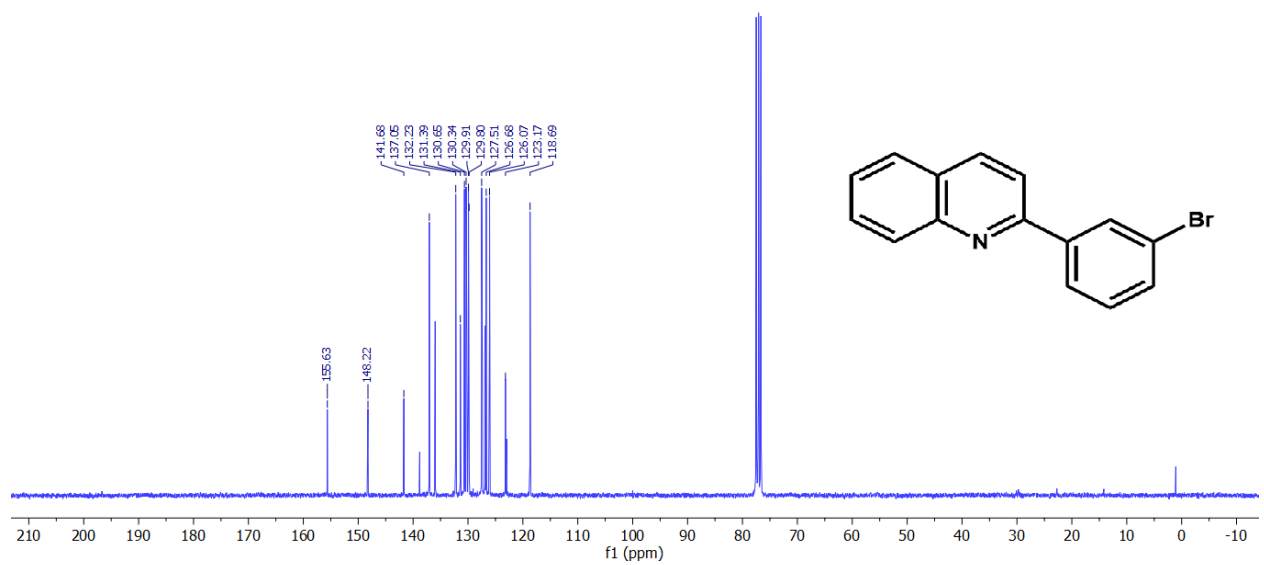
**Fig. S54**  $^1\text{H}$  NMR spectrum of compound **9ag** (300 MHz,  $\text{CDCl}_3$ ).



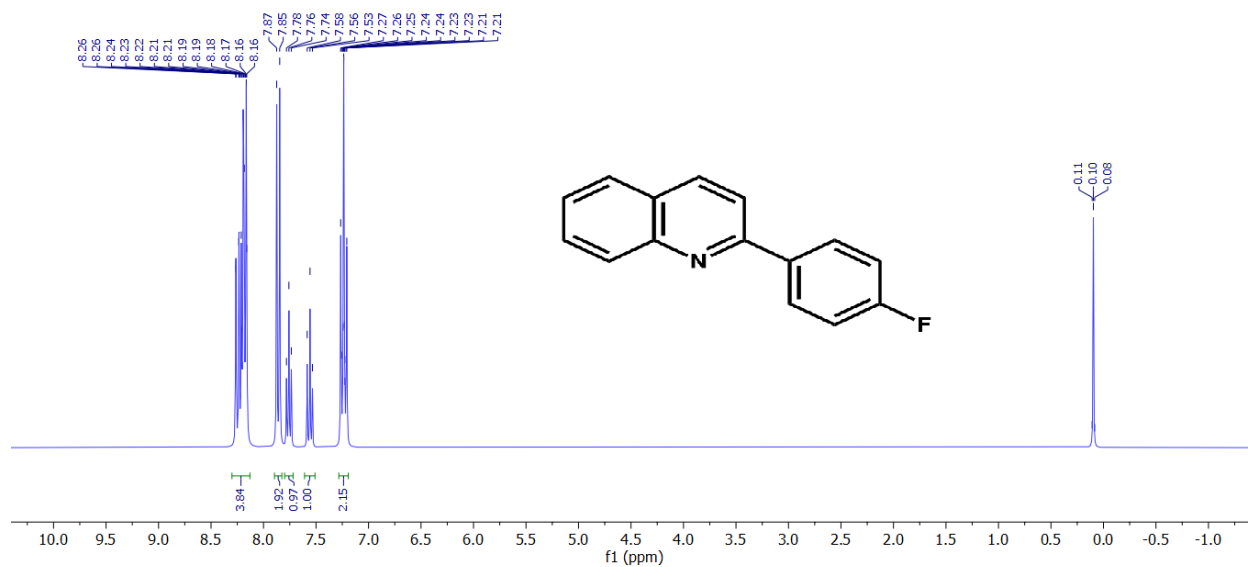
**Fig. S55**  $^{13}\text{C}$  NMR spectrum of compound **9ag** (75 MHz,  $\text{CDCl}_3$ ).



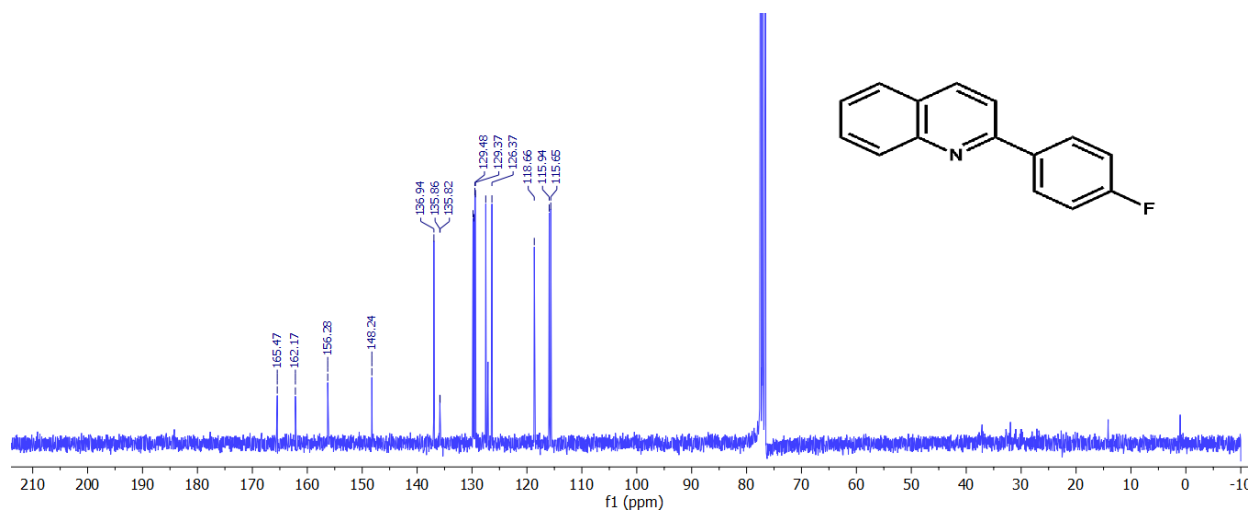
**Fig. S56** <sup>1</sup>H NMR spectrum of compound **9ah** (300 MHz, CDCl<sub>3</sub>).



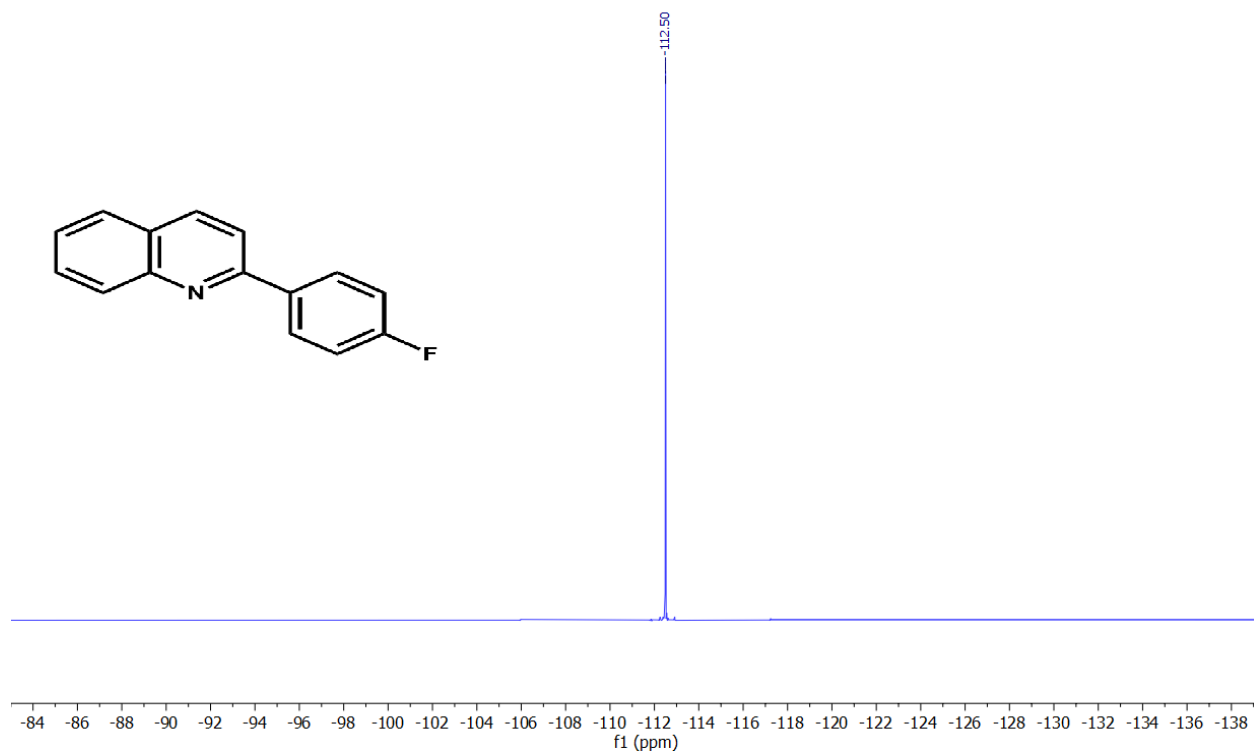
**Fig. S57** <sup>13</sup>C NMR spectrum of compound **9ah** (75 MHz, CDCl<sub>3</sub>).



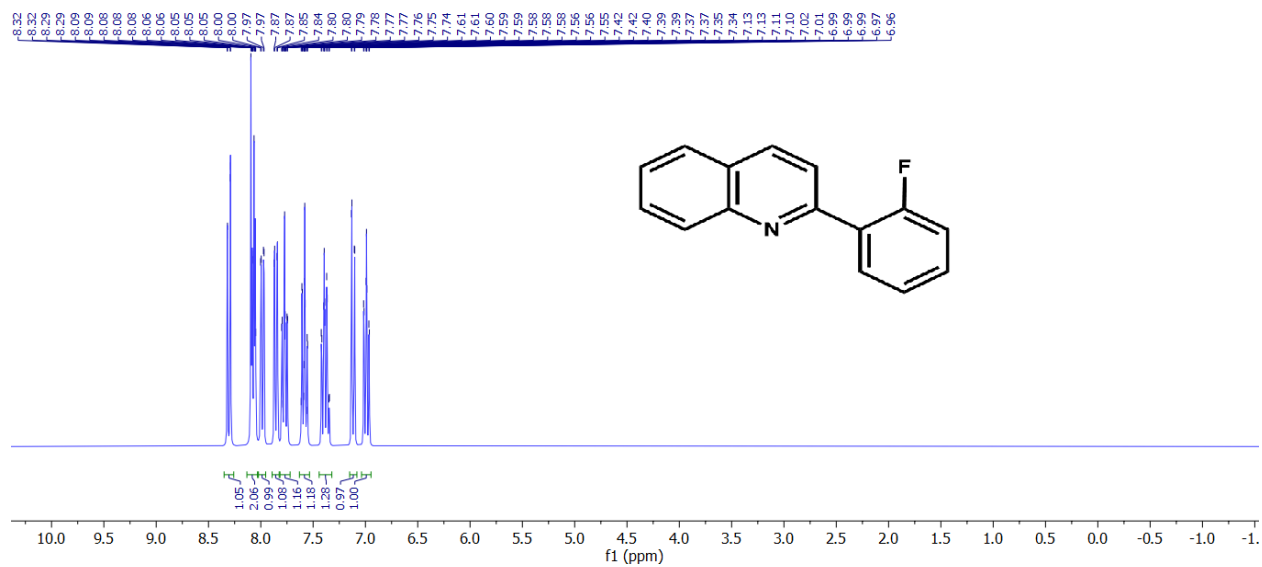
**Fig. S58**  $^1\text{H}$  NMR spectrum of compound **9ai** (300 MHz,  $\text{CDCl}_3$ ).



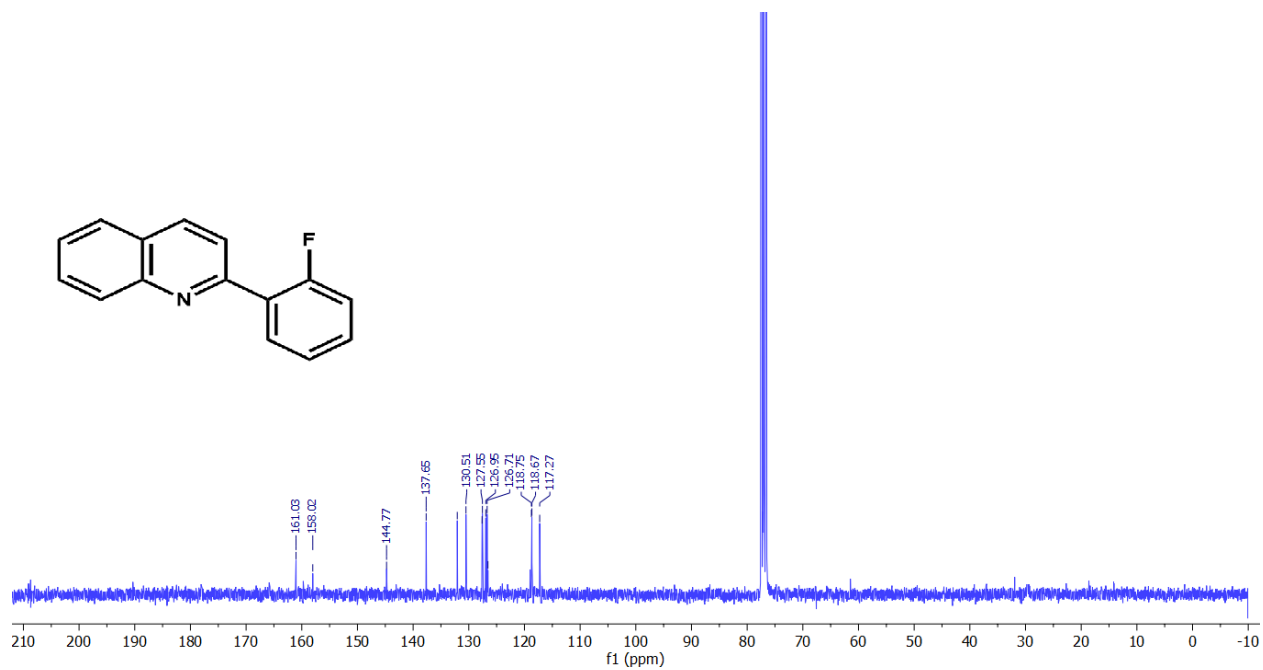
**Fig. S59**  $^{13}\text{C}$  NMR spectrum of compound **9ai** (75 MHz,  $\text{CDCl}_3$ ).



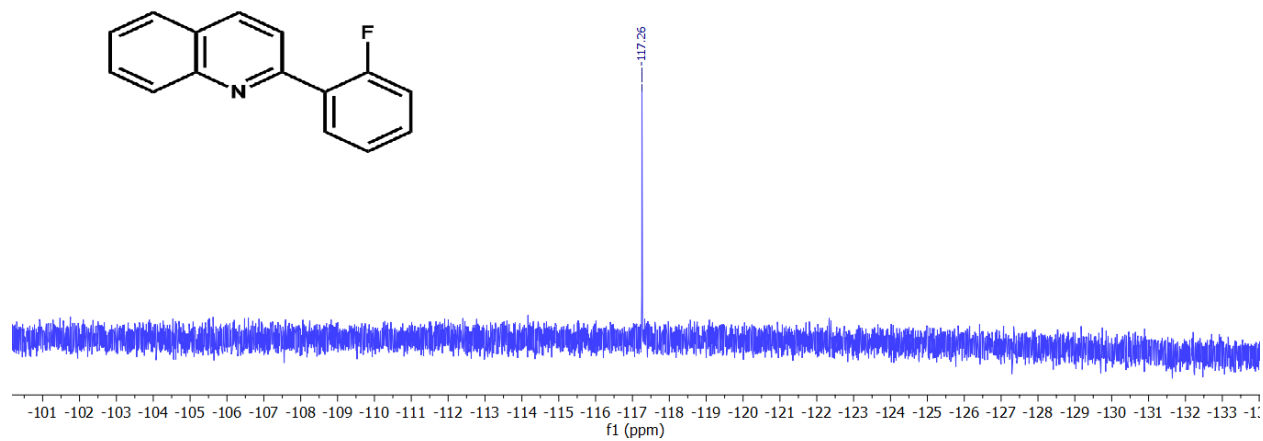
**Fig. S60**  $^{19}\text{F}$  NMR spectrum of compound **9ai** (282 MHz,  $\text{CDCl}_3$ ).



**Fig. S61**  $^1\text{H}$  NMR spectrum of compound **9aj** (300 MHz,  $\text{CDCl}_3$ ).

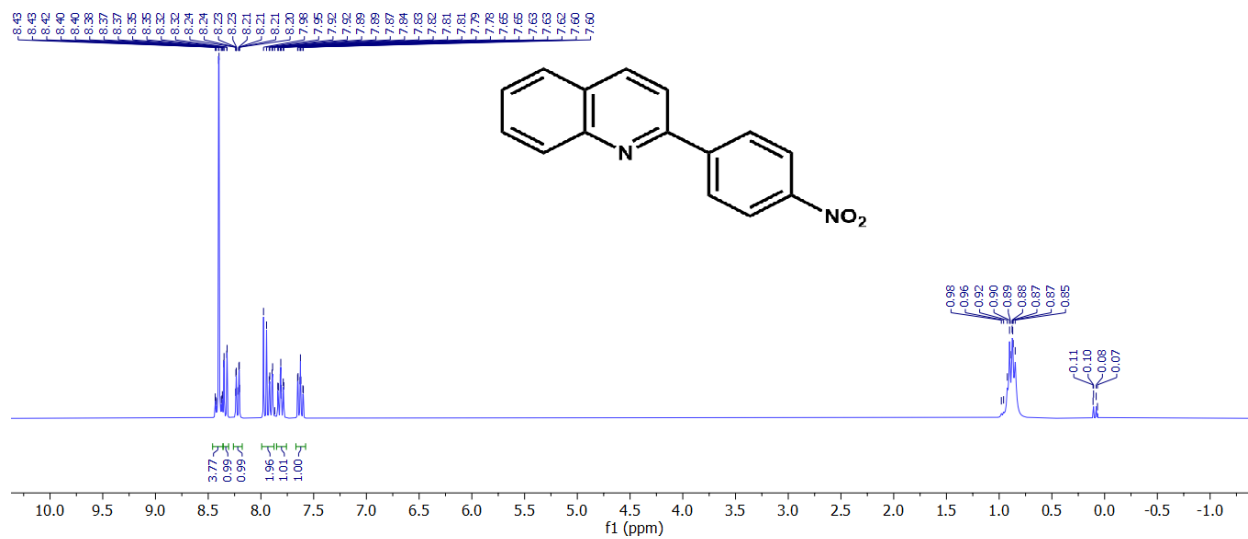


**Fig. S62** <sup>13</sup>C NMR spectrum of compound **9aj** (75 MHz, CDCl<sub>3</sub>).

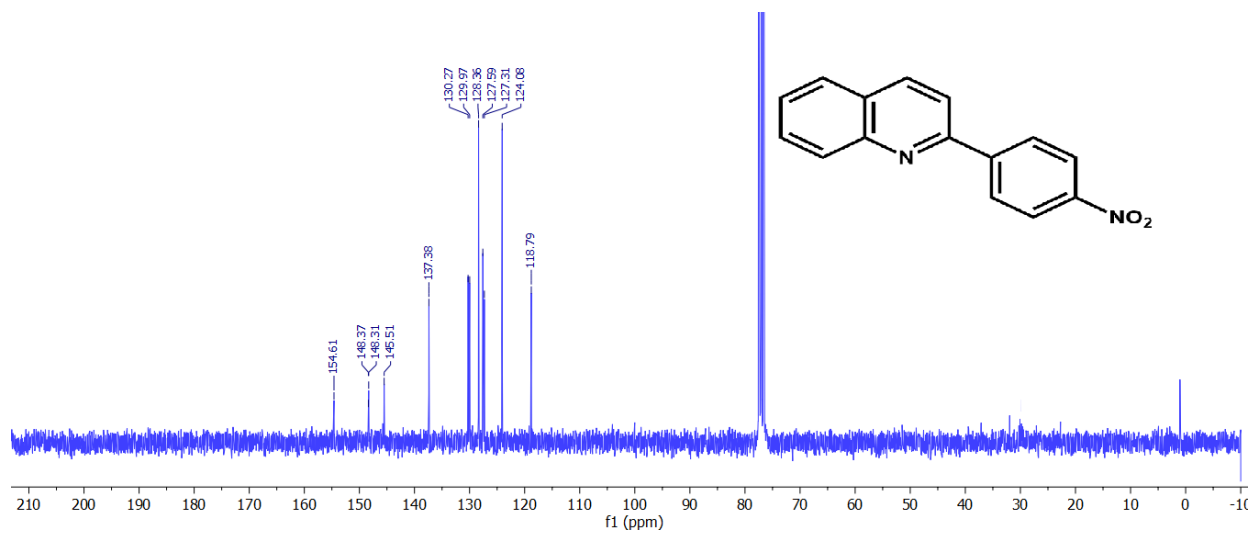


**Fig. S63** <sup>19</sup>F NMR spectrum of compound **9aj** (282 MHz, CDCl<sub>3</sub>).

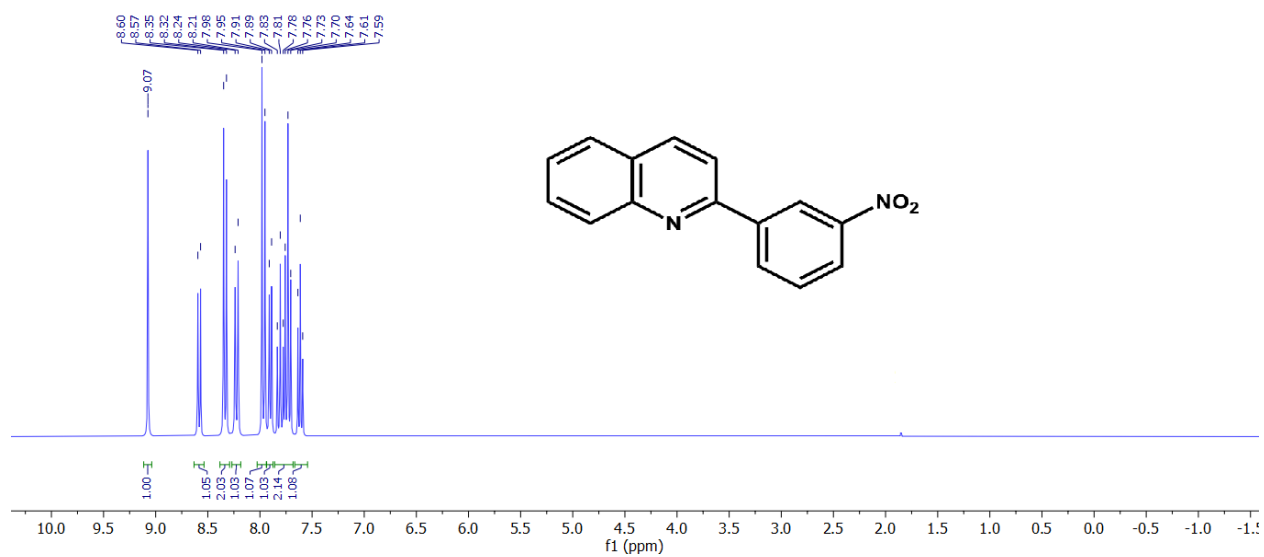




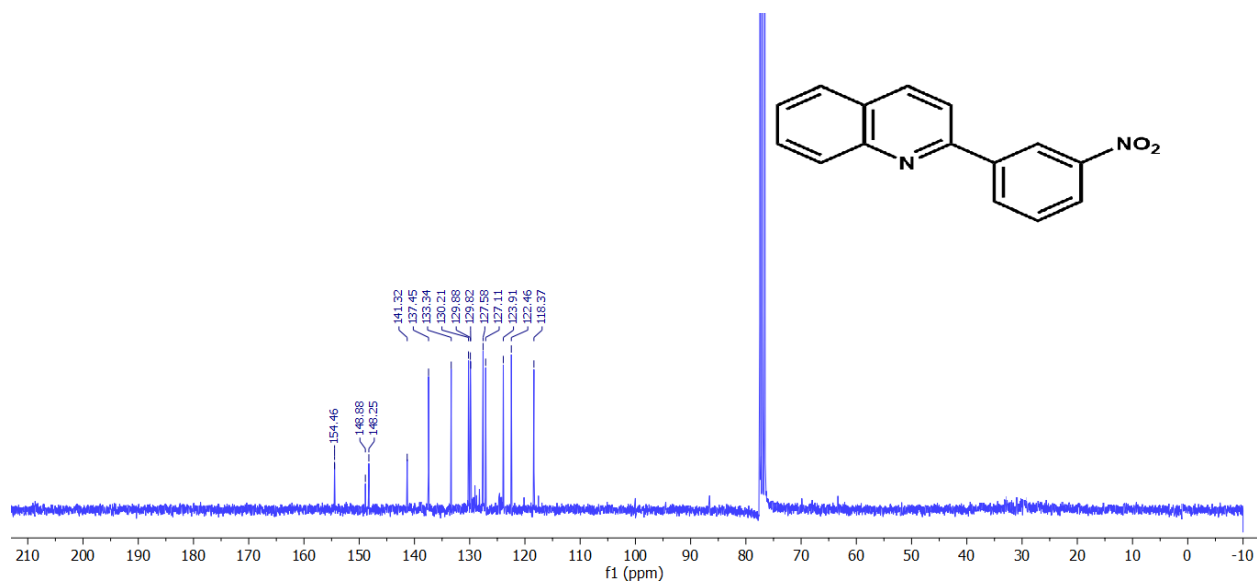
**Fig. S64** <sup>1</sup>H NMR spectrum of compound **9ak** (300 MHz, CDCl<sub>3</sub>).



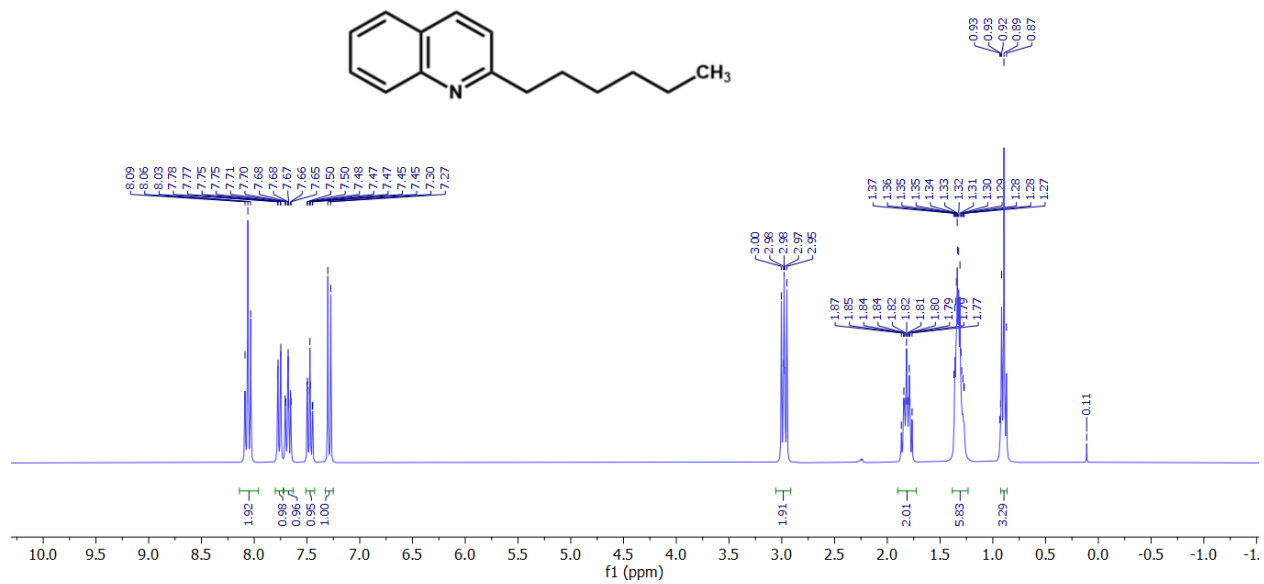
**Fig. S65** <sup>13</sup>C NMR spectrum of compound **9ak** (75 MHz, CDCl<sub>3</sub>).



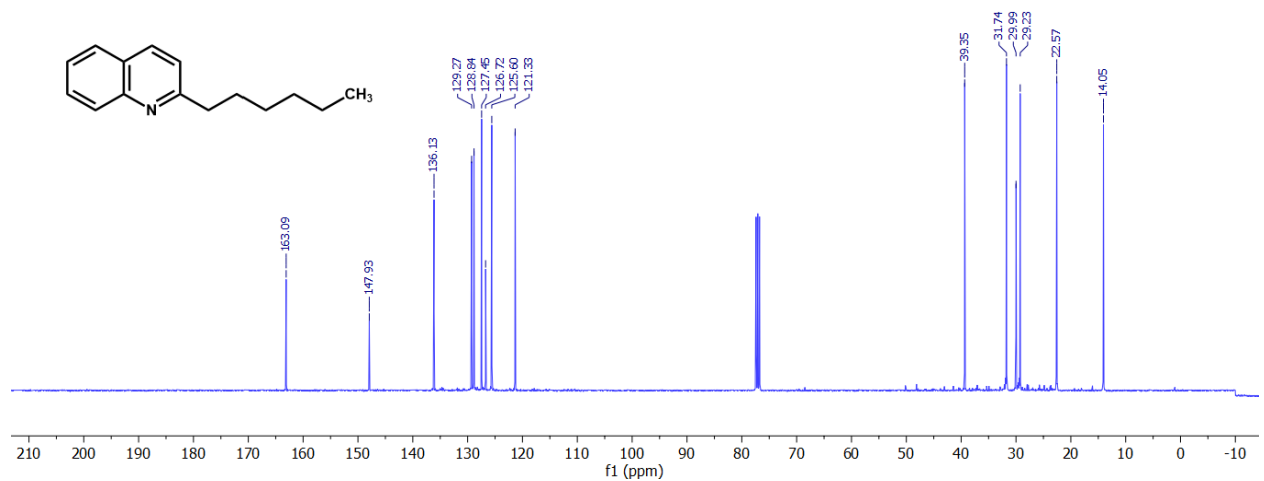
**Fig. S66**  $^1\text{H}$  NMR spectrum of compound **9al** (300 MHz,  $\text{CDCl}_3$ ).



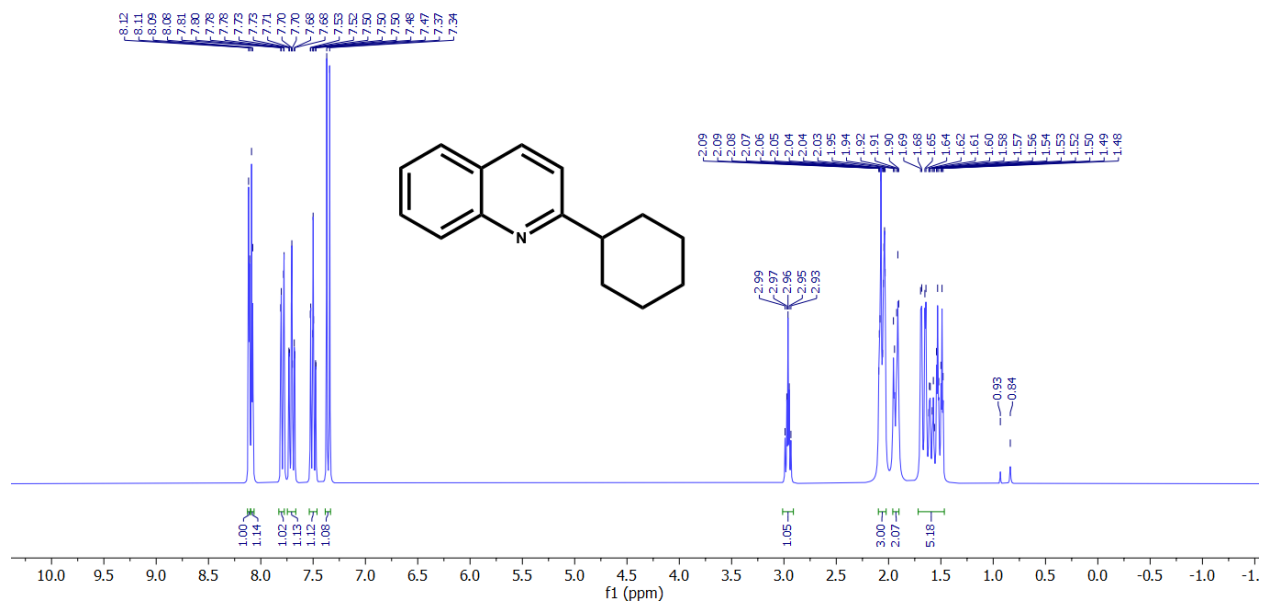
**Fig. S67**  $^{13}\text{C}$  NMR spectrum of compound **9al** (75 MHz,  $\text{CDCl}_3$ ).



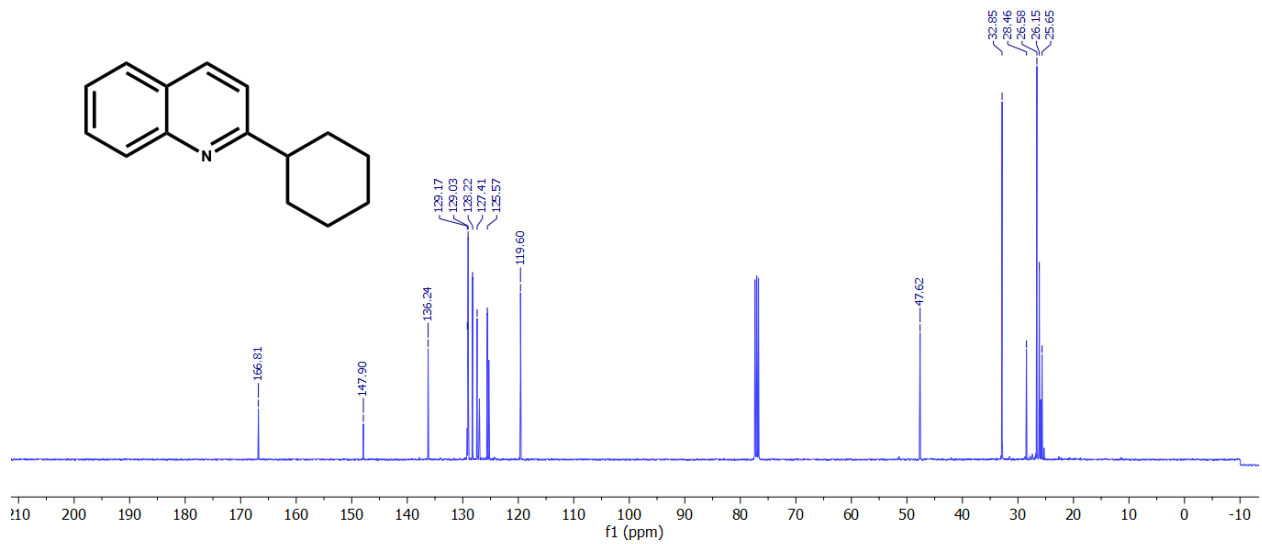
**Fig. S68** <sup>1</sup>H NMR spectrum of compound **9am** (300 MHz, CDCl<sub>3</sub>).



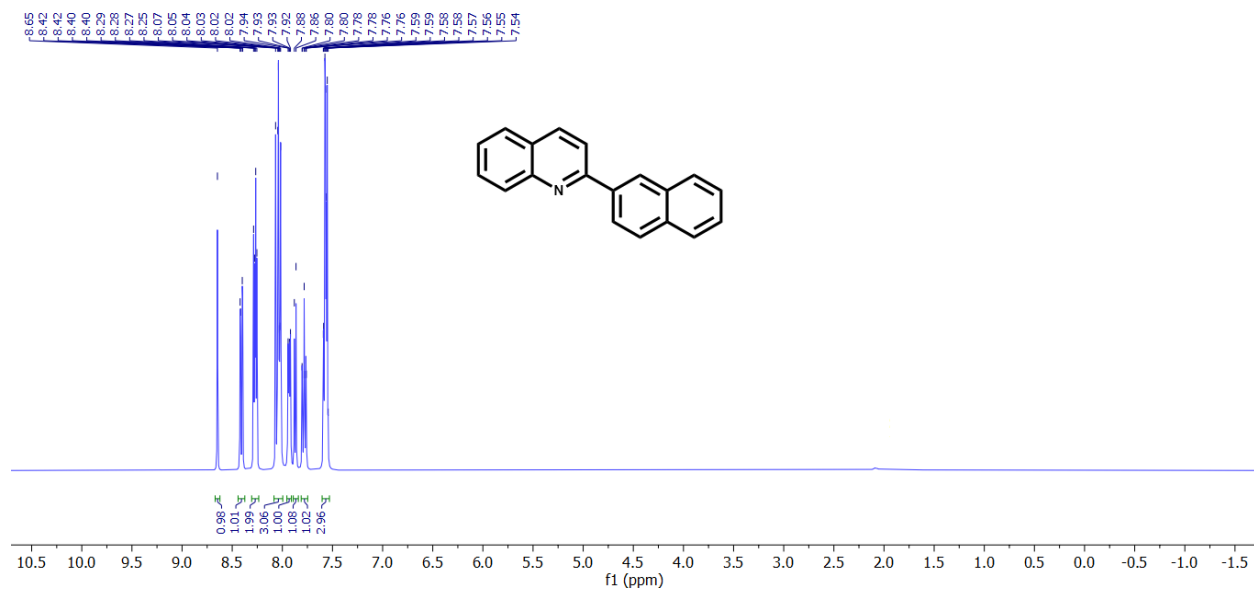
**Fig. S69** <sup>13</sup>C NMR spectrum of compound **9am** (75 MHz, CDCl<sub>3</sub>).



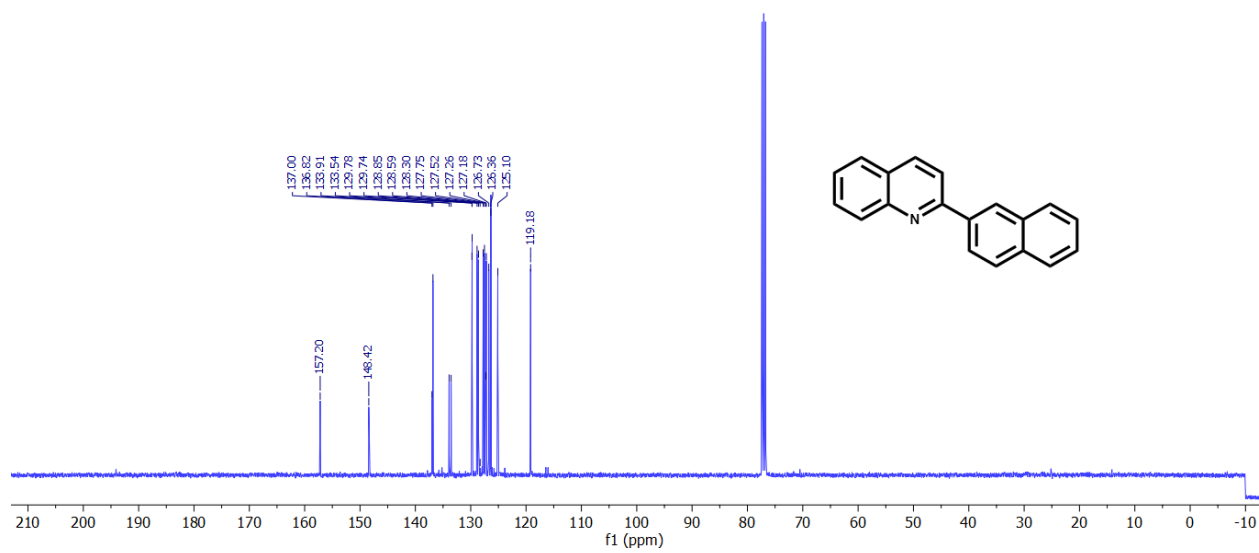
**Fig. S70** <sup>1</sup>H NMR spectrum of compound **9an** (300 MHz, CDCl<sub>3</sub>).



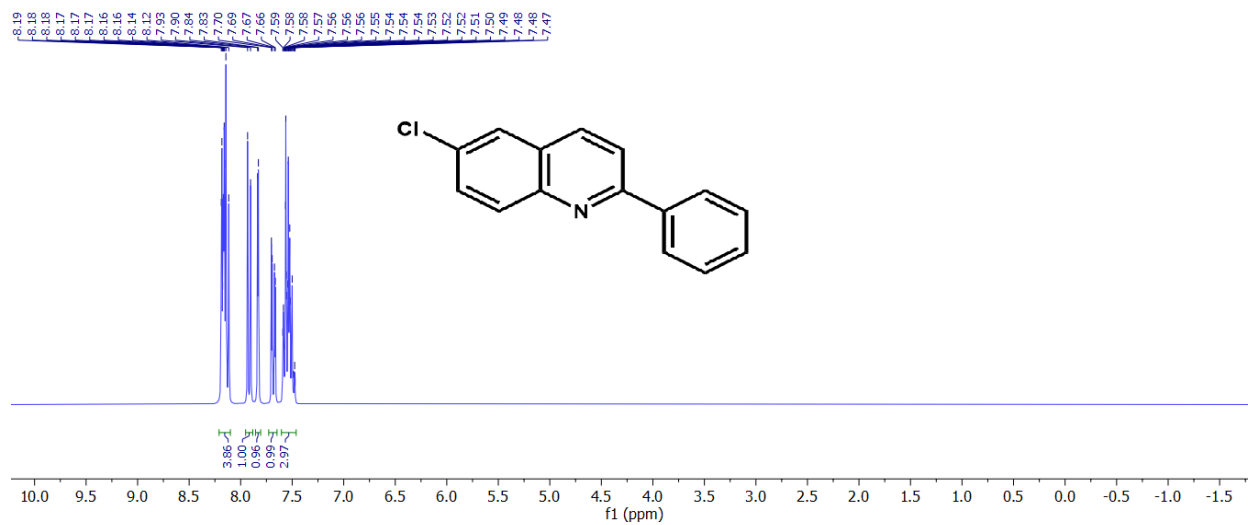
**Fig. S71** <sup>13</sup>C NMR spectrum of compound **9an** (75 MHz, CDCl<sub>3</sub>).



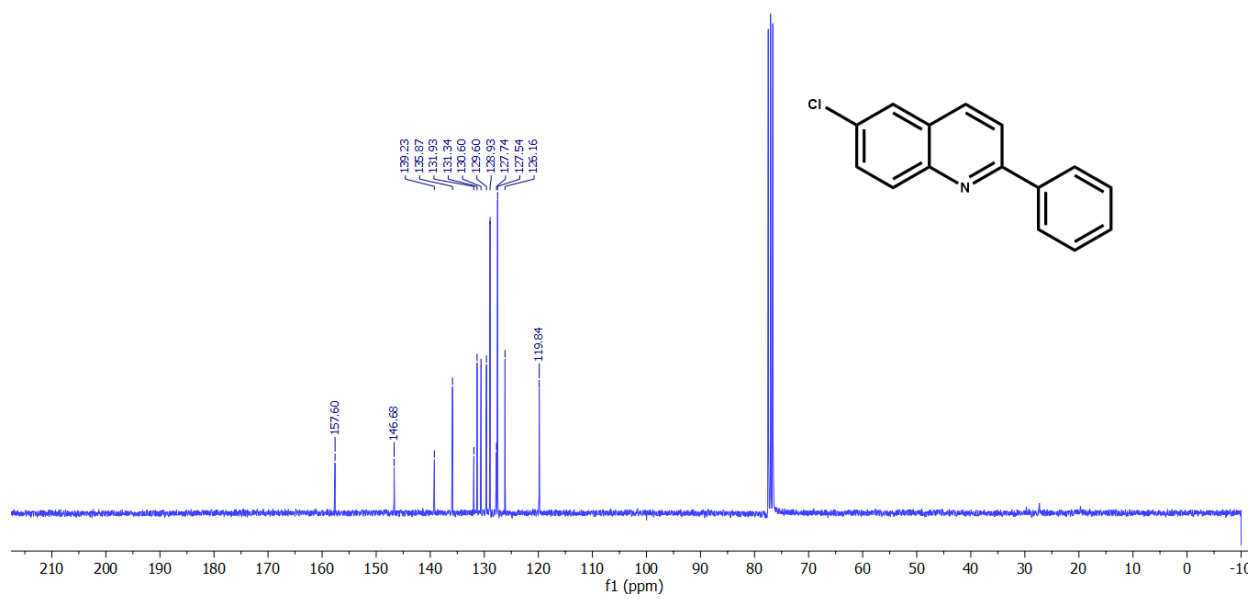
**Fig. S72**  $^1\text{H}$  NMR spectrum of compound **9ao** (300 MHz,  $\text{CDCl}_3$ ).



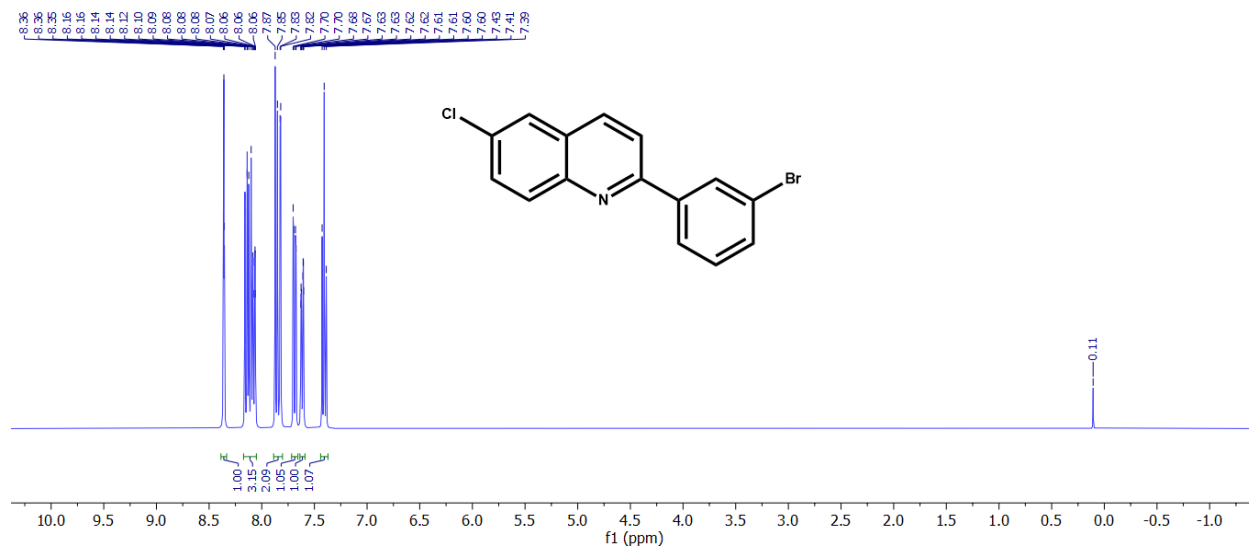
**Fig. S73**  $^{13}\text{C}$  NMR spectrum of compound **9ao** (75 MHz,  $\text{CDCl}_3$ ).



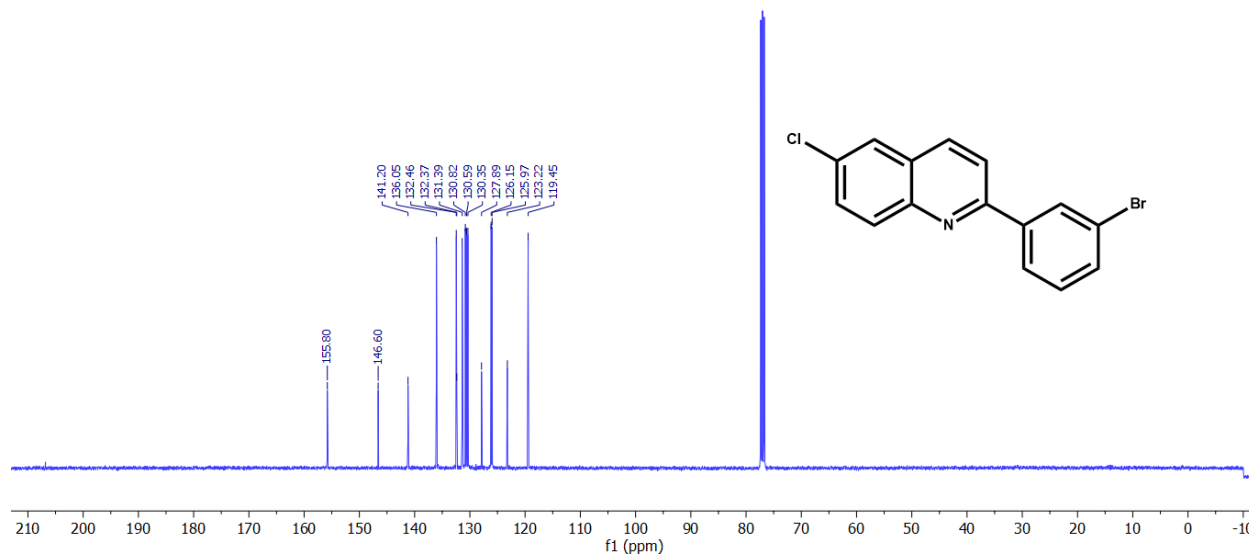
**Fig. S74** <sup>1</sup>H NMR spectrum of compound **10aa** (300 MHz, CDCl<sub>3</sub>).



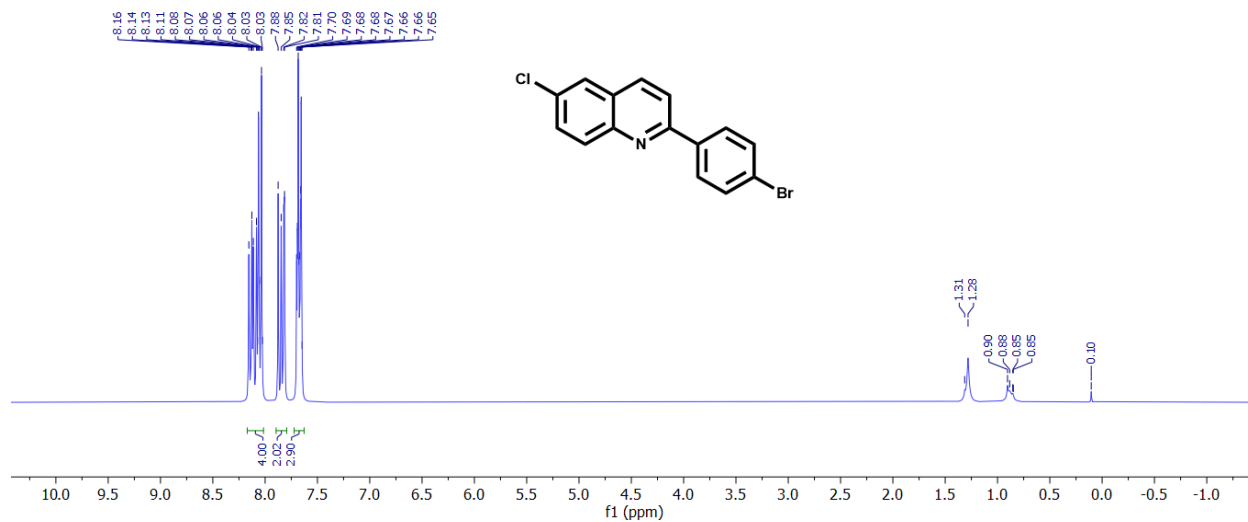
**Fig. S75** <sup>13</sup>C NMR spectrum of compound **10aa** (75 MHz, CDCl<sub>3</sub>).



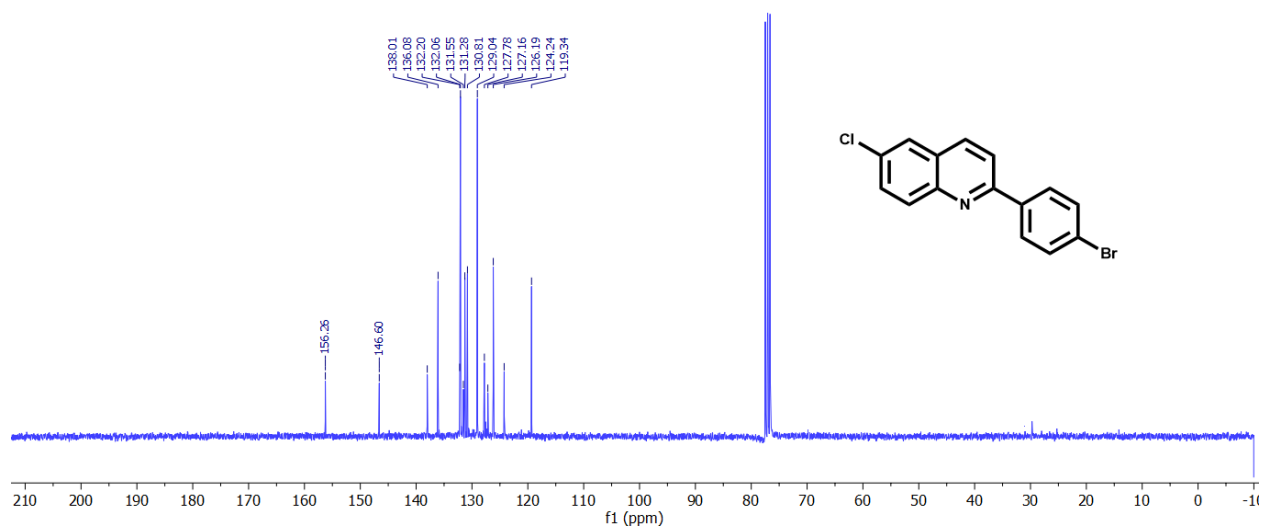
**Fig. S76**  $^1\text{H}$  NMR spectrum of compound **10ab** (300 MHz,  $\text{CDCl}_3$ ).



**Fig. S77**  $^{13}\text{C}$  NMR spectrum of compound **10ab** (75 MHz,  $\text{CDCl}_3$ ).

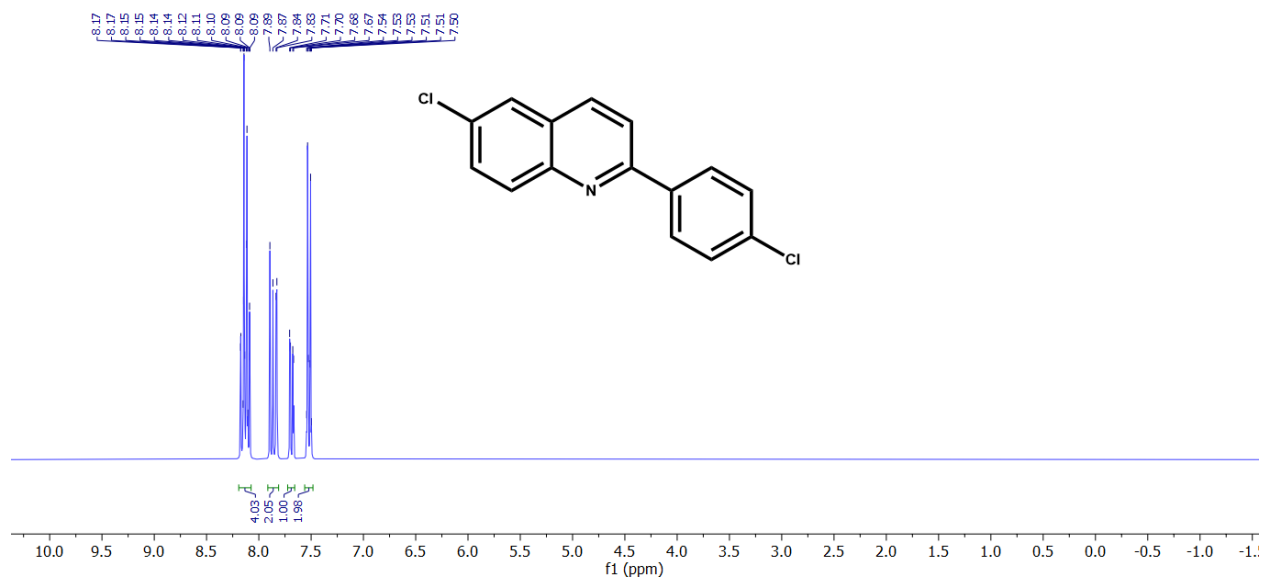


**Fig. S78** <sup>1</sup>H NMR spectrum of compound **10ac** (300 MHz, CDCl<sub>3</sub>).

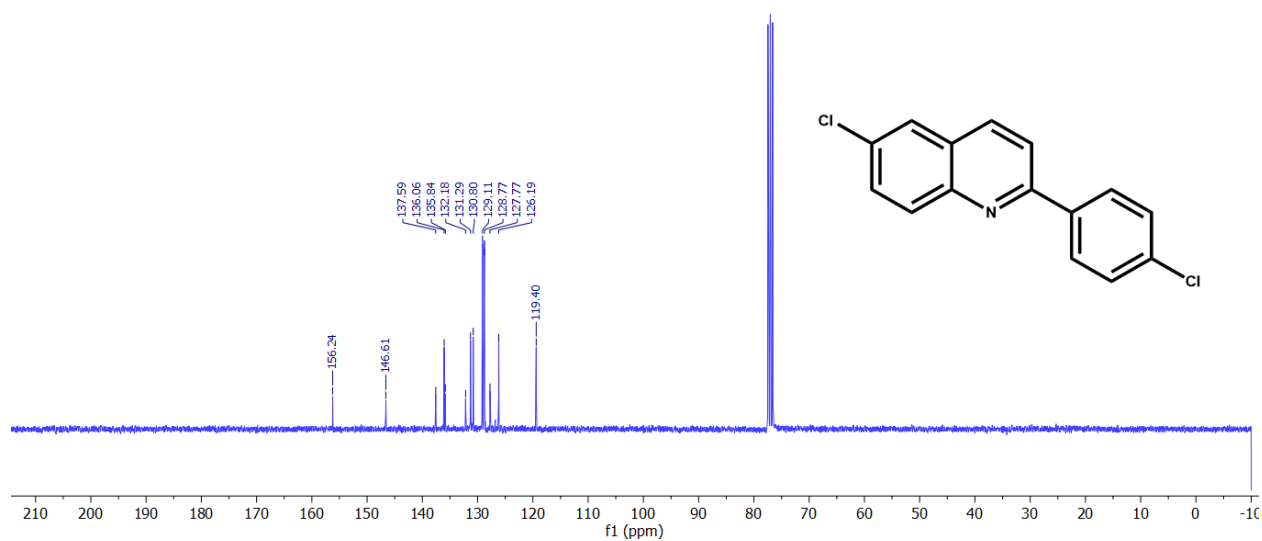


**Fig. S79** <sup>13</sup>C NMR spectrum of compound **10ac** (75 MHz, CDCl<sub>3</sub>).

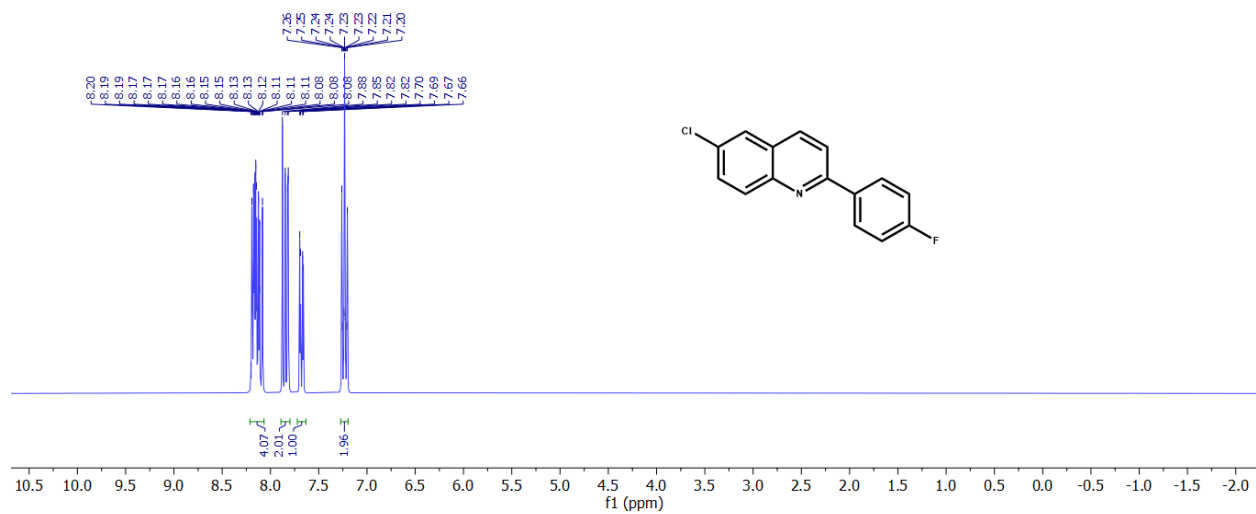




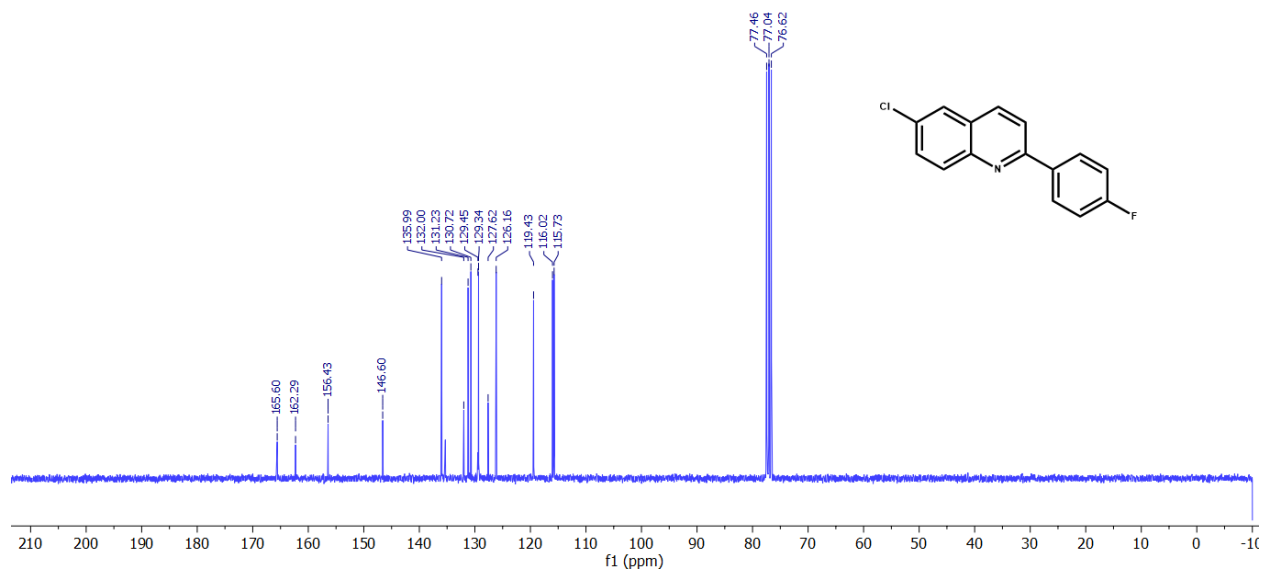
**Fig. S80**  $^1\text{H}$  NMR spectrum of compound **10ad** (300 MHz,  $\text{CDCl}_3$ ).



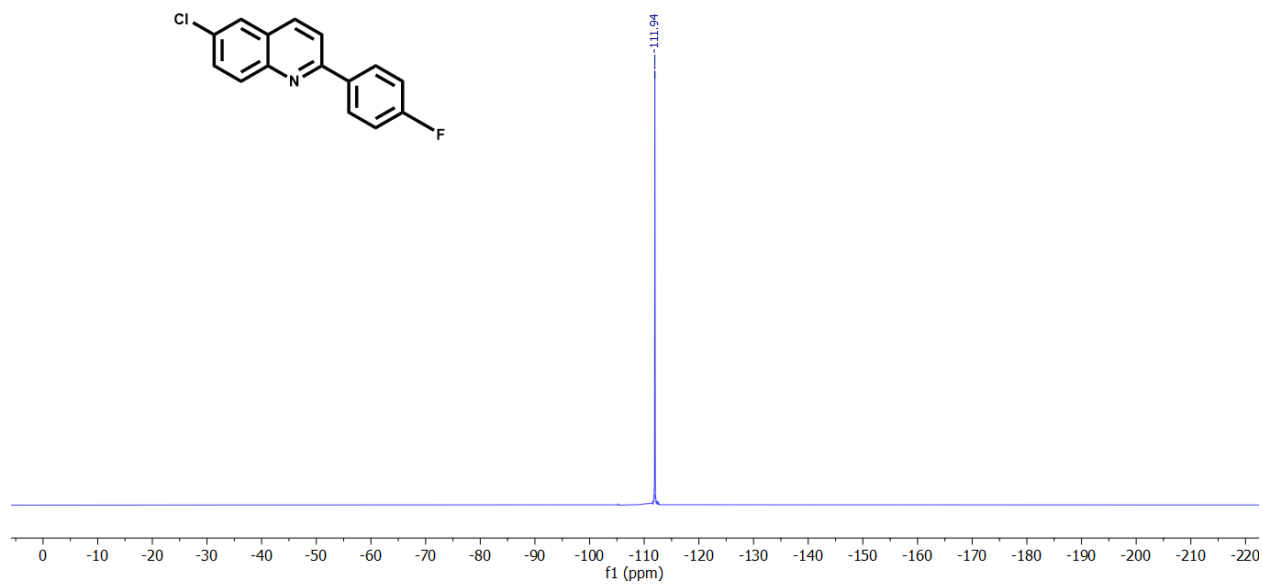
**Fig. S81**  $^{13}\text{C}$  NMR spectrum of compound **10ad** (75 MHz,  $\text{CDCl}_3$ ).



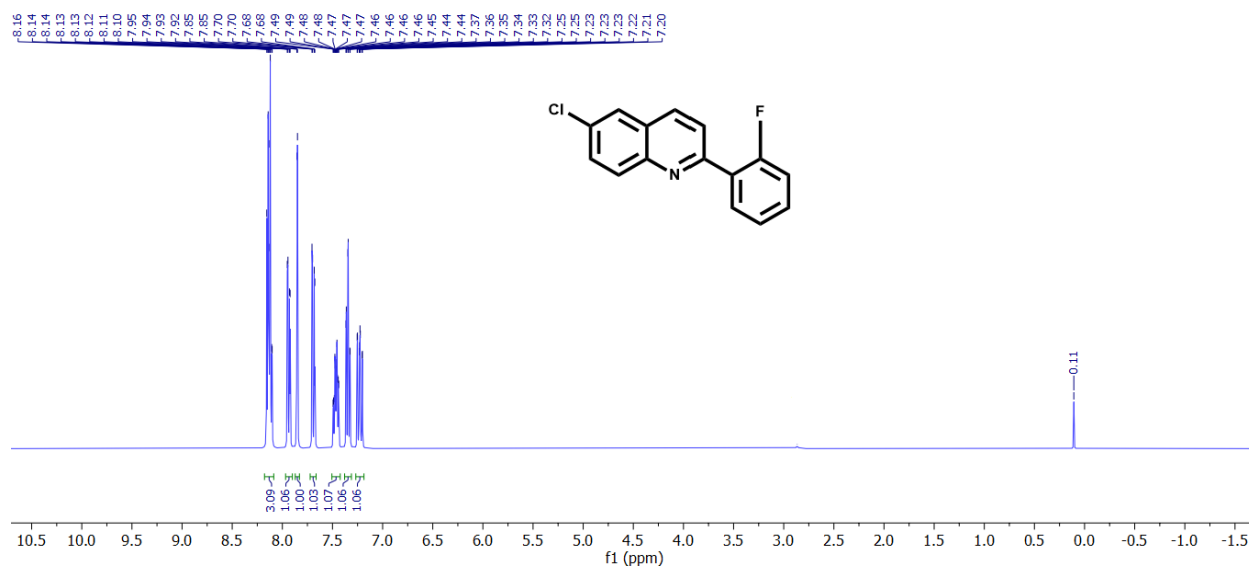
**Fig. S82** <sup>1</sup>H NMR spectrum of compound **10ae** (300 MHz, CDCl<sub>3</sub>).



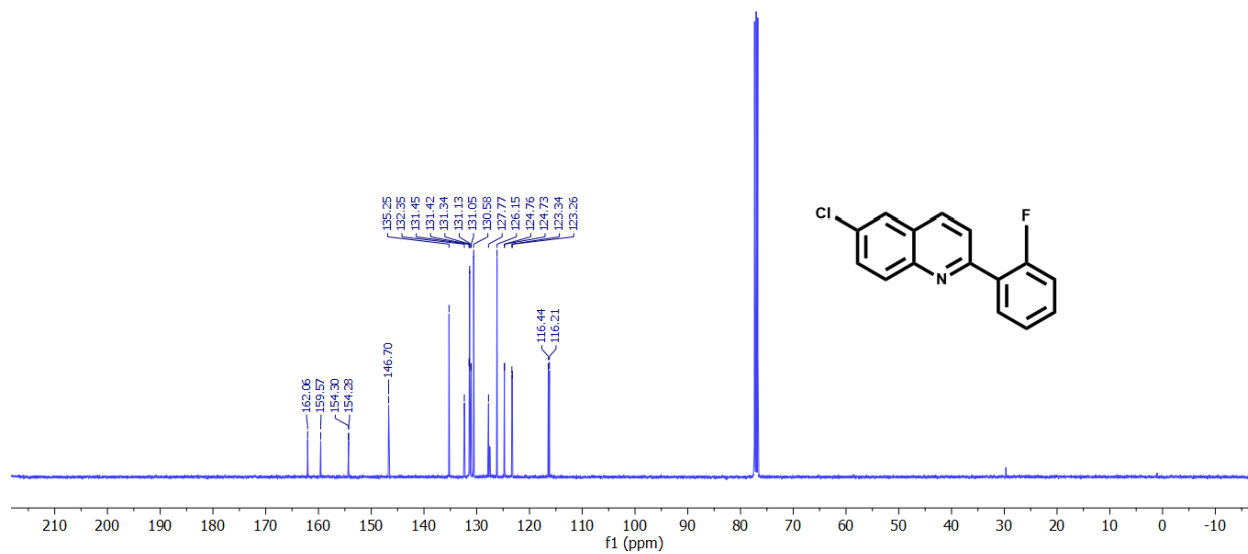
**Fig. S83** <sup>13</sup>C NMR spectrum of compound **10ae** (75 MHz, CDCl<sub>3</sub>).



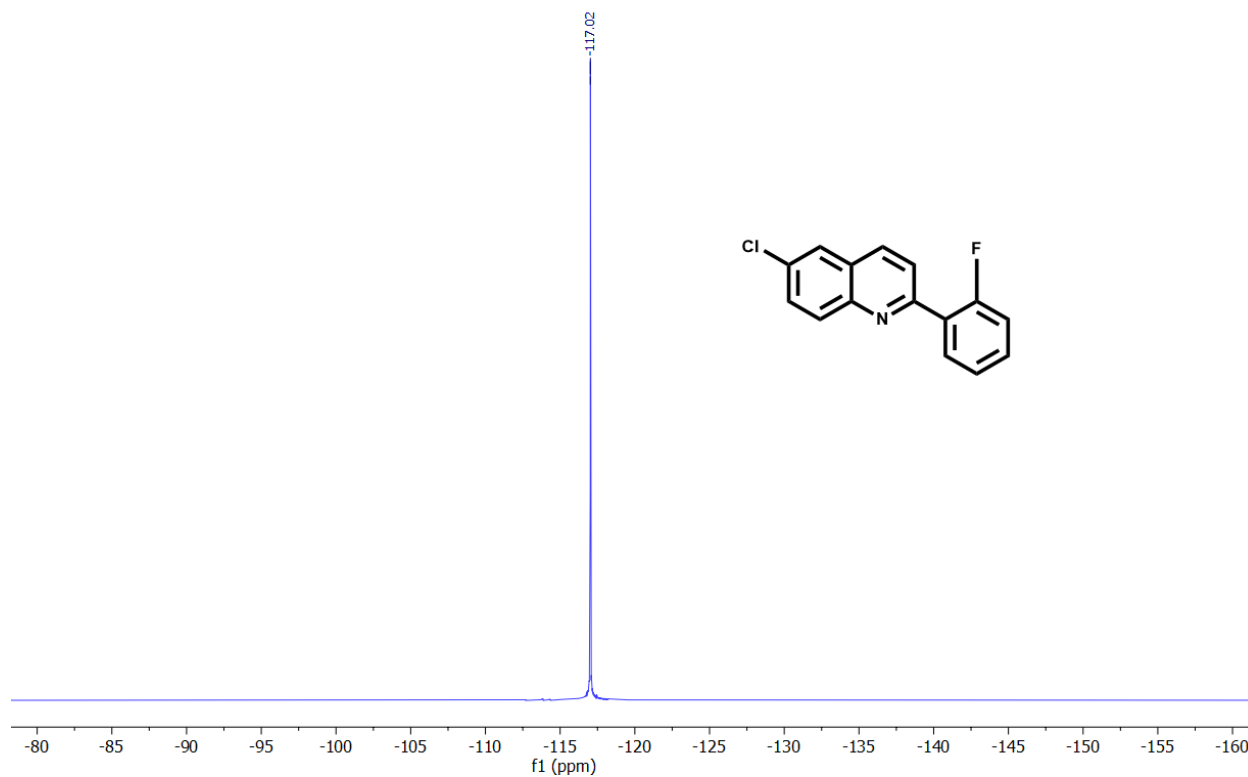
**Fig. S84**  $^{19}\text{F}$  NMR spectrum of compound **10ae** (282 MHz,  $\text{CDCl}_3$ ).



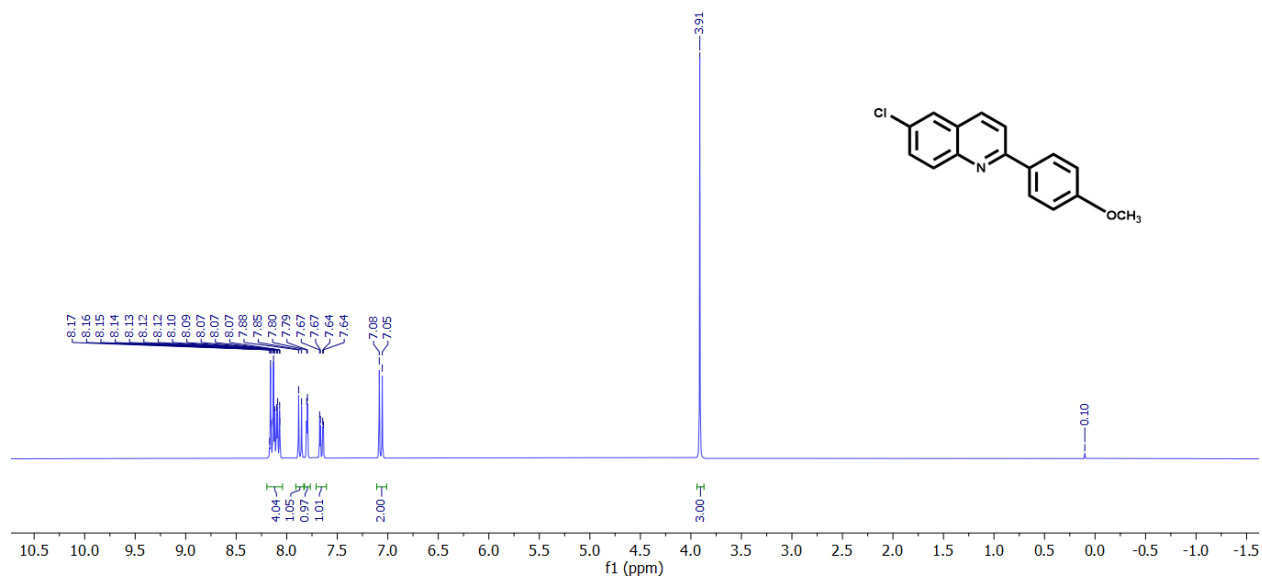
**Fig. S85**  $^1\text{H}$  NMR spectrum of compound **10af** (300 MHz,  $\text{CDCl}_3$ ).



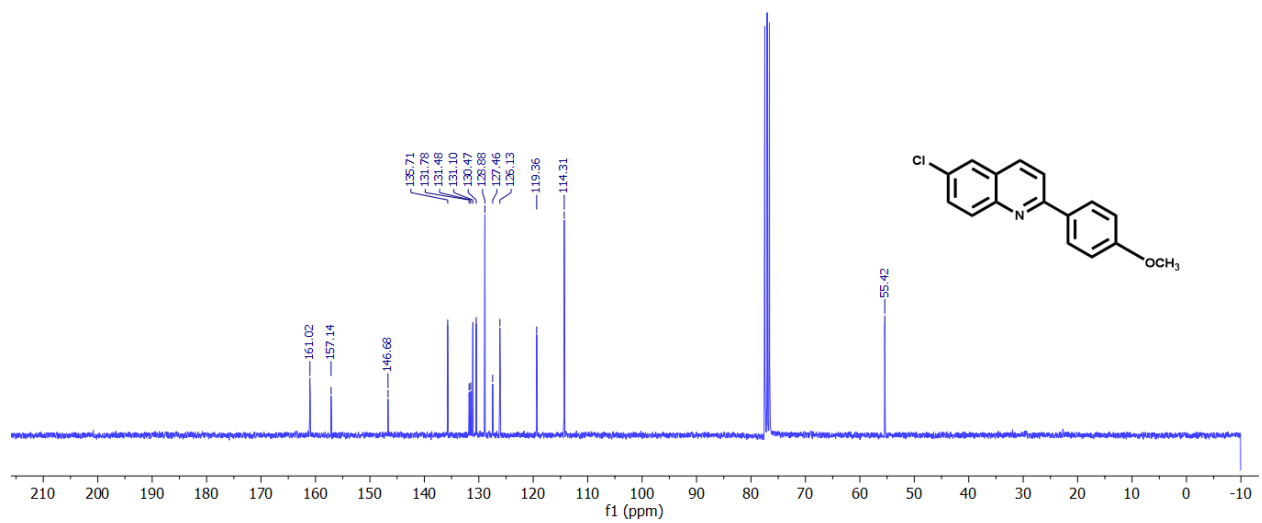
**Fig. S86**  $^{13}\text{C}$  NMR spectrum of compound **10af** (75 MHz,  $\text{CDCl}_3$ ).



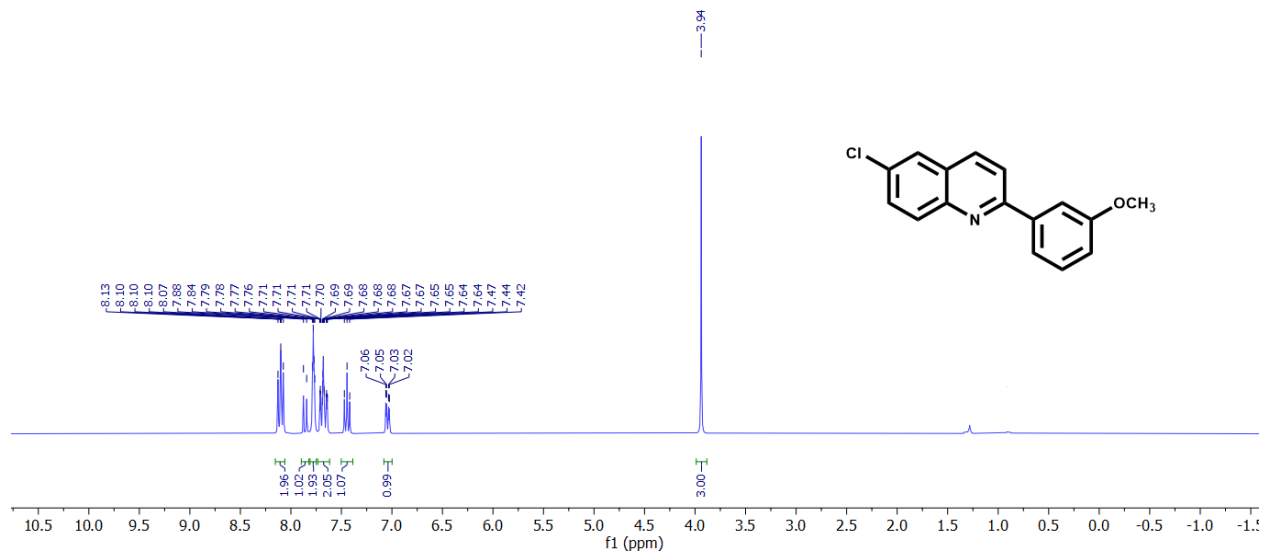
**Fig. S87**  $^{19}\text{F}$  NMR spectrum of compound **10af** (282 MHz,  $\text{CDCl}_3$ ).



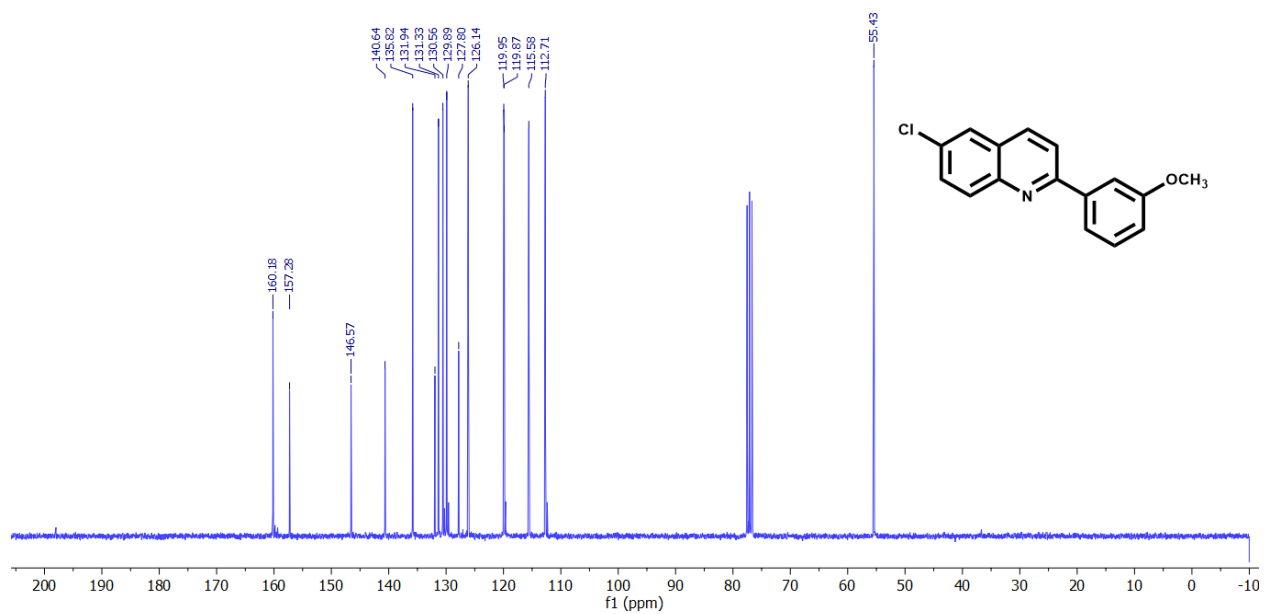
**Fig. S88** <sup>1</sup>H NMR spectrum of compound **10ag** (300 MHz, CDCl<sub>3</sub>).



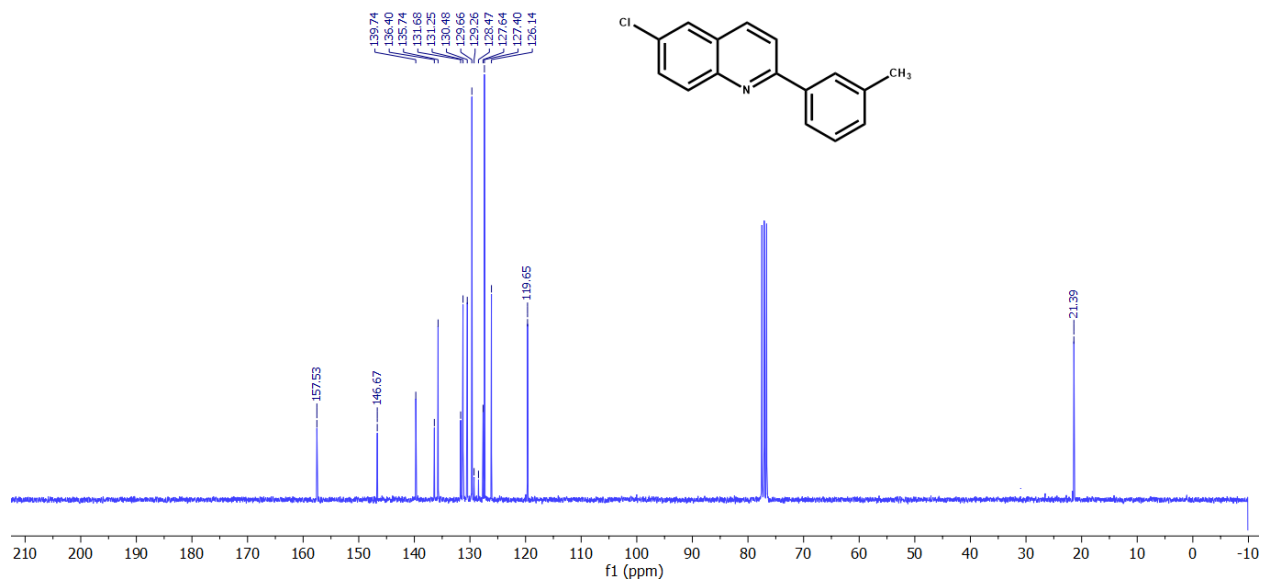
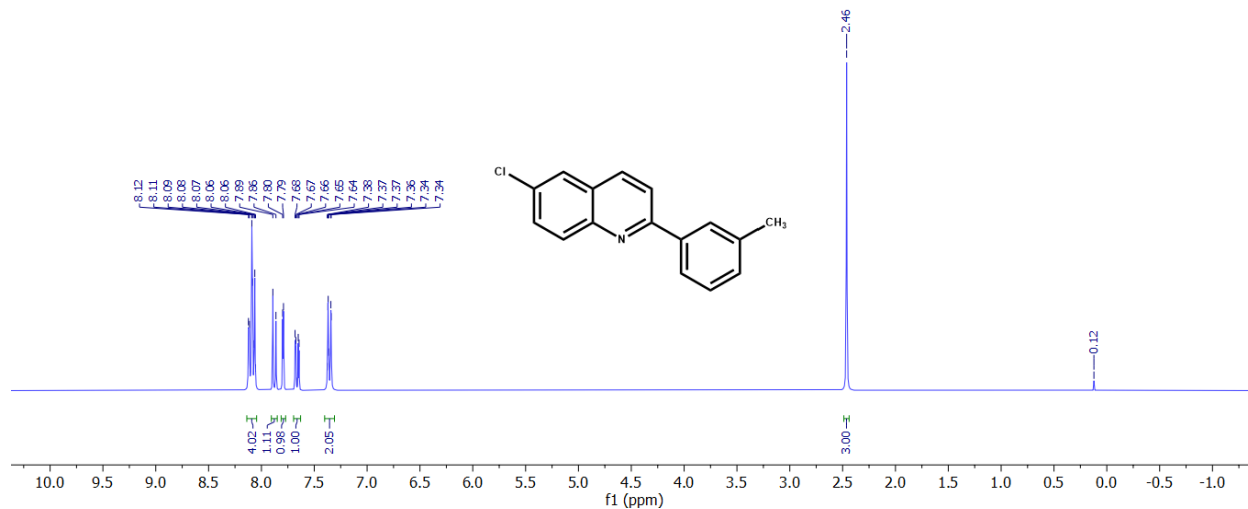
**Fig. S89** <sup>13</sup>C NMR spectrum of compound **10ag** (75 MHz, CDCl<sub>3</sub>).



**Fig. S90** <sup>1</sup>H NMR spectrum of compound **10ah** (300 MHz, CDCl<sub>3</sub>).



**Fig. S91** <sup>13</sup>C NMR spectrum of compound **10ah** (75 MHz, CDCl<sub>3</sub>).



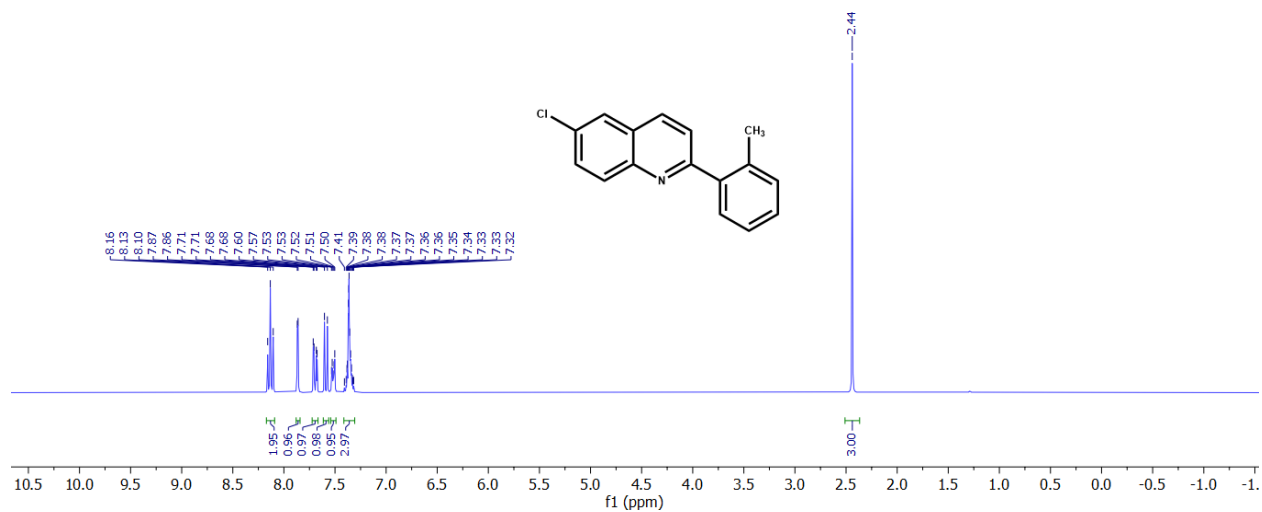


**Fig. S94** <sup>1</sup>H NMR spectrum of compound **10aj** (300 MHz, CDCl<sub>3</sub>).

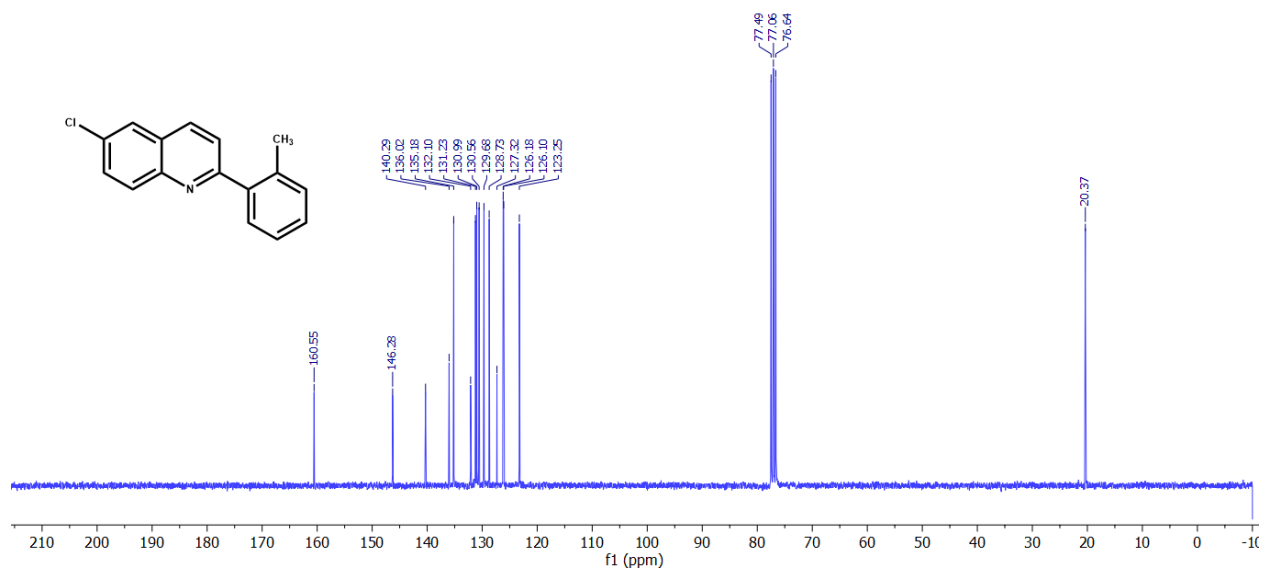


**Fig. S95** <sup>13</sup>C NMR spectrum of compound **10aj** (75 MHz, CDCl<sub>3</sub>).



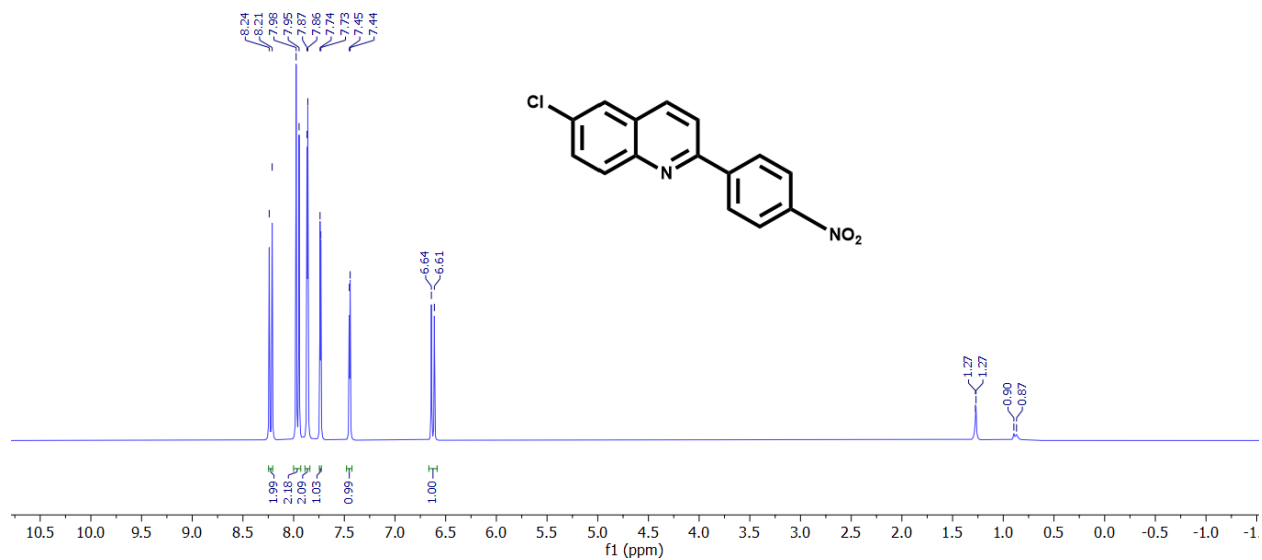


**Fig. S96** <sup>1</sup>H NMR spectrum of compound **10ak** (300 MHz, CDCl<sub>3</sub>).

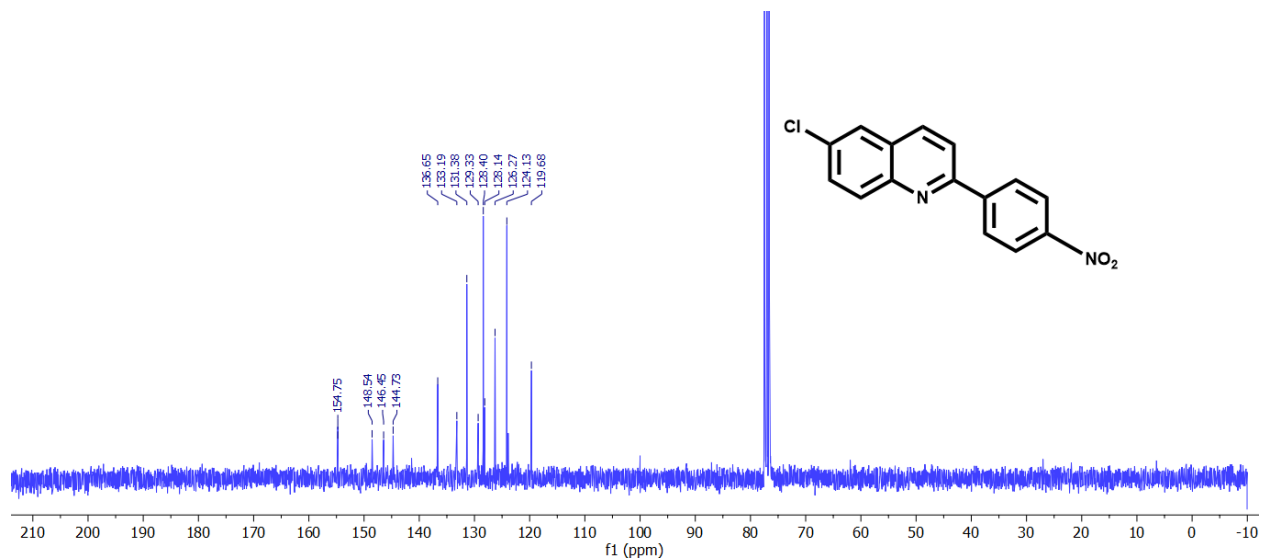


**Fig. S97** <sup>13</sup>C NMR spectrum of compound **10ak** (75 MHz, CDCl<sub>3</sub>).

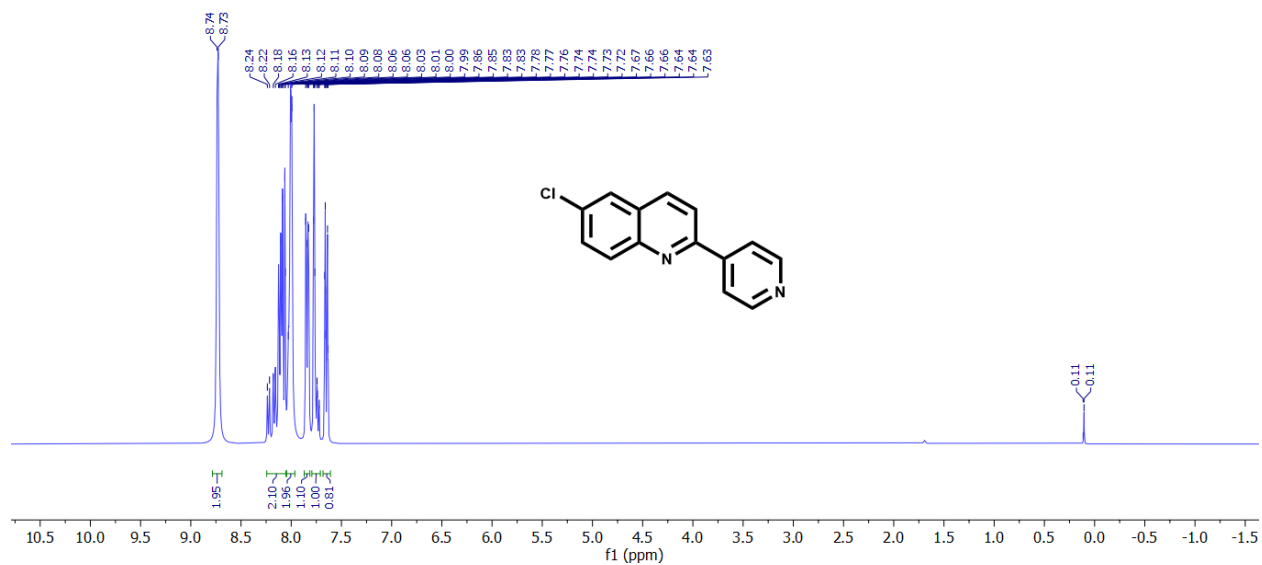


**Fig. S98** <sup>1</sup>H NMR spectrum of compound **10al** (300 MHz, CDCl<sub>3</sub>).

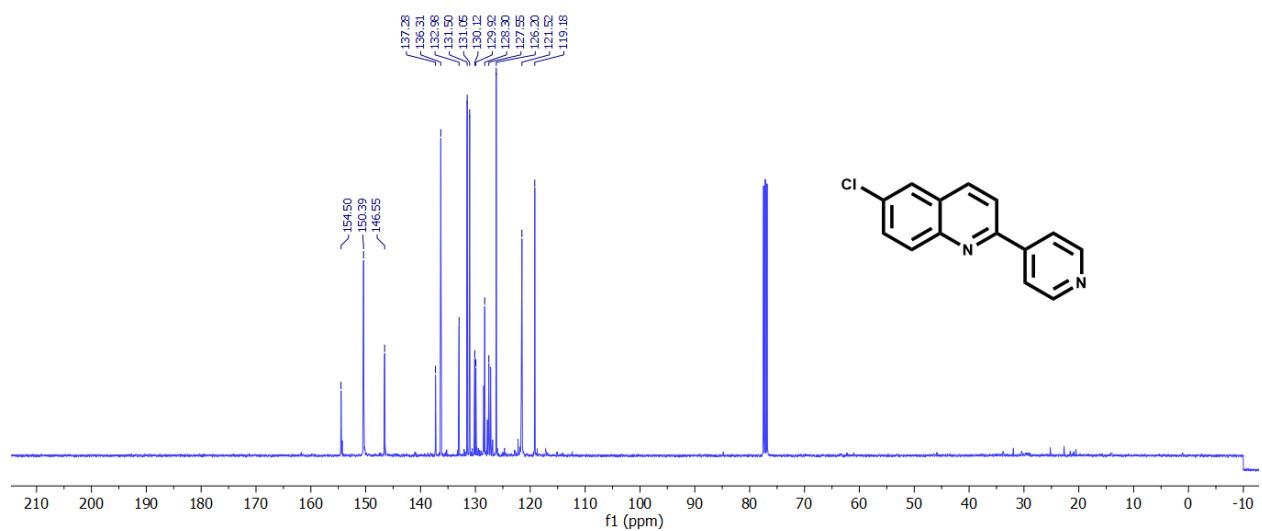


**Fig. S99** <sup>13</sup>C NMR spectrum of compound **10al** (75 MHz, CDCl<sub>3</sub>).

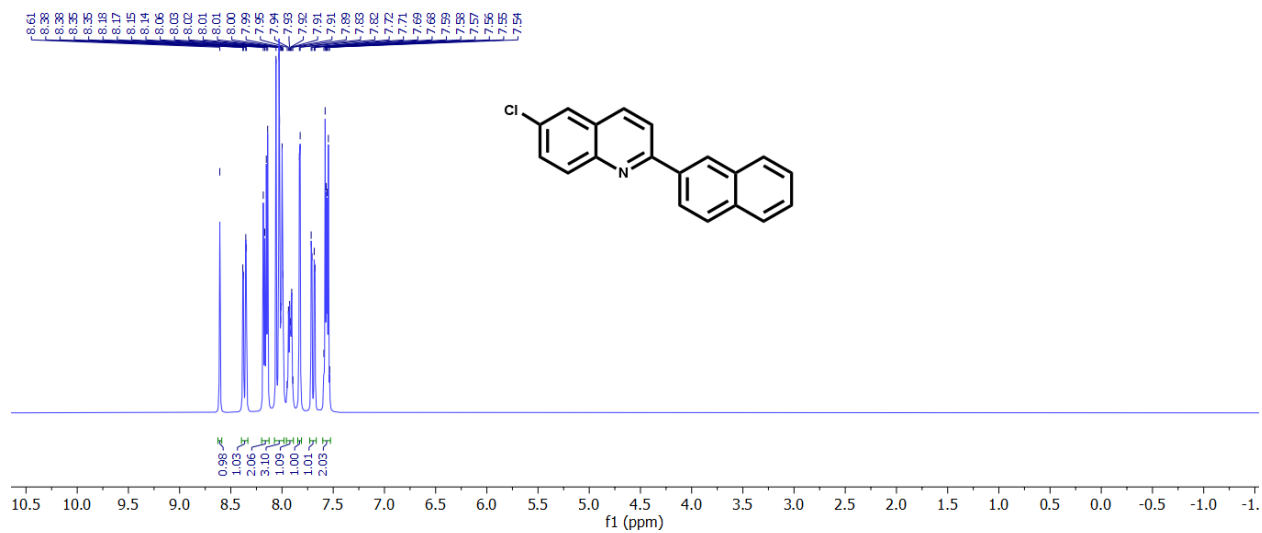


**Fig. S100**  $^1\text{H NMR}$  spectrum of compound **10am** (300 MHz,  $\text{CDCl}_3$ ).

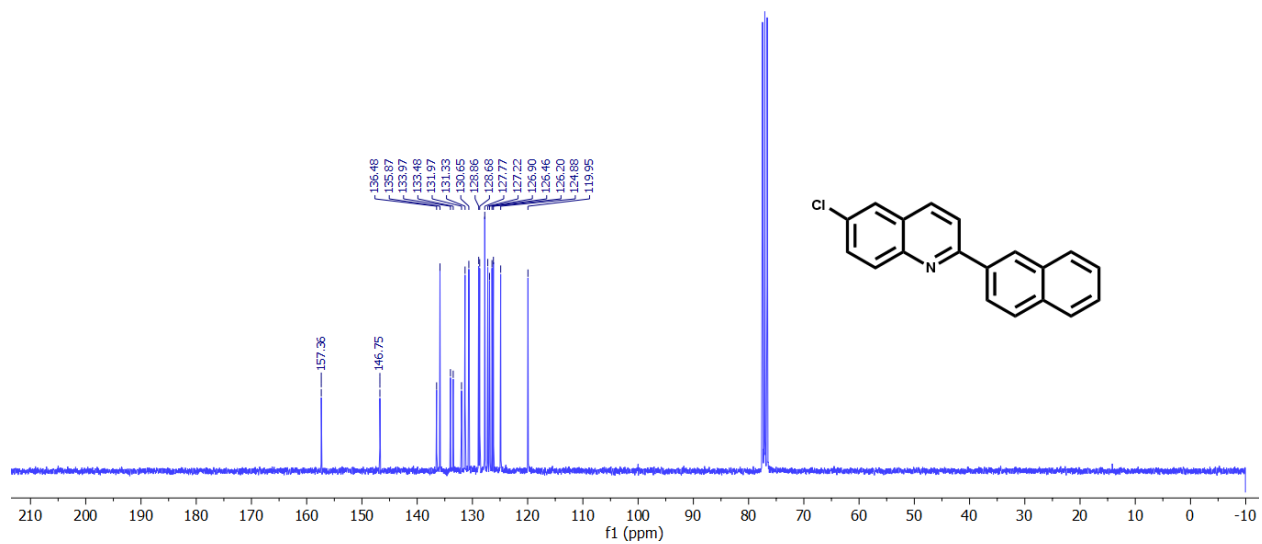


**Fig. S101**  $^{13}\text{C NMR}$  spectrum of compound **10am** (75 MHz,  $\text{CDCl}_3$ ).

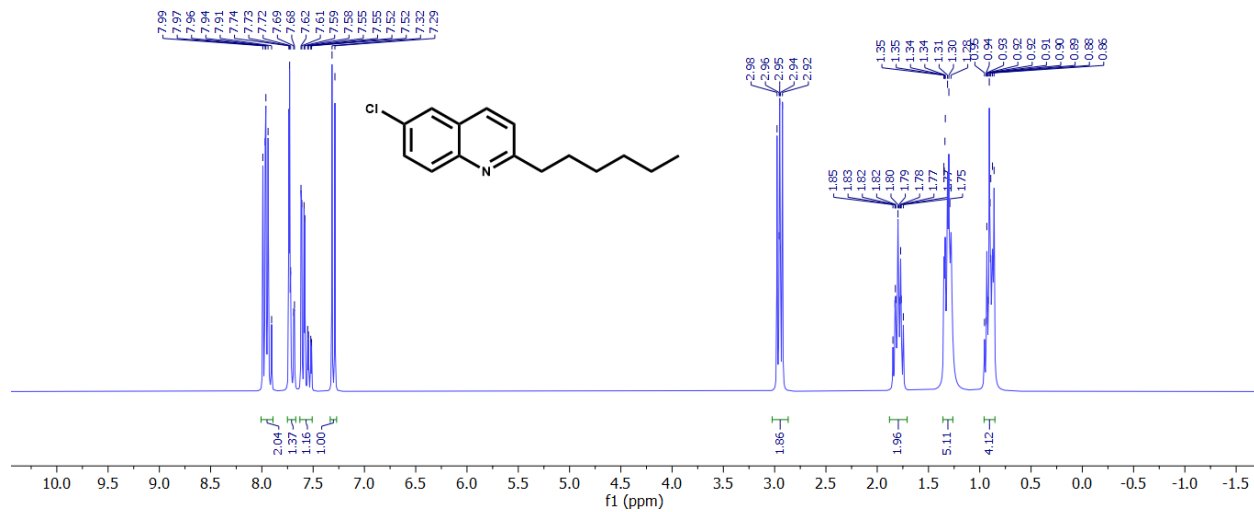


**Fig. S102** <sup>1</sup>H NMR spectrum of compound **10an** (300 MHz, CDCl<sub>3</sub>).

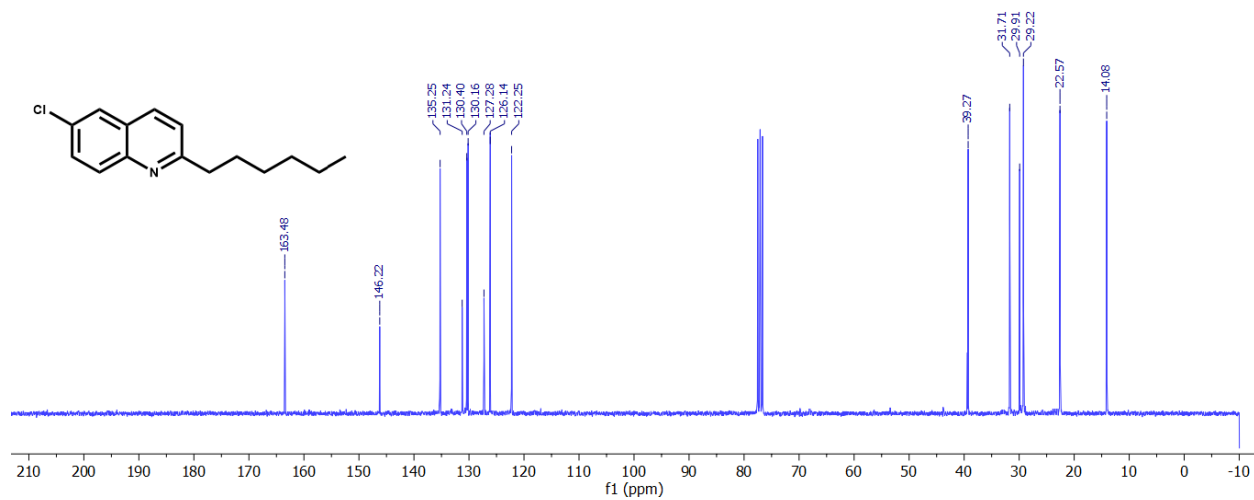


**Fig. S103** <sup>13</sup>C NMR spectrum of compound **10an** (75 MHz, CDCl<sub>3</sub>).

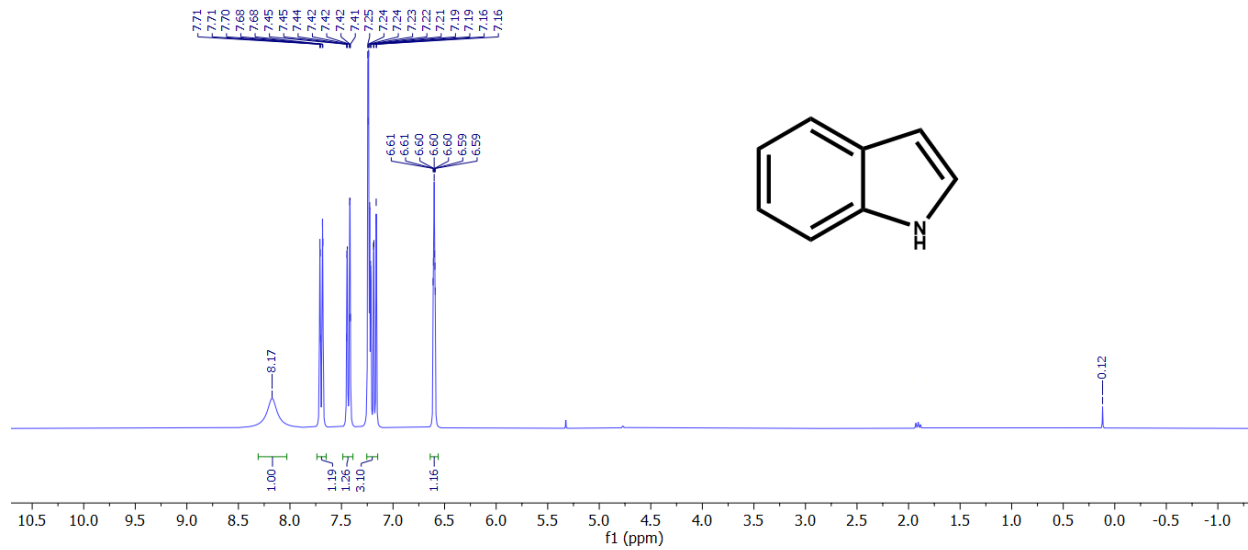


**Fig. S104** <sup>1</sup>H NMR spectrum of compound **11a** (300 MHz, CDCl<sub>3</sub>).

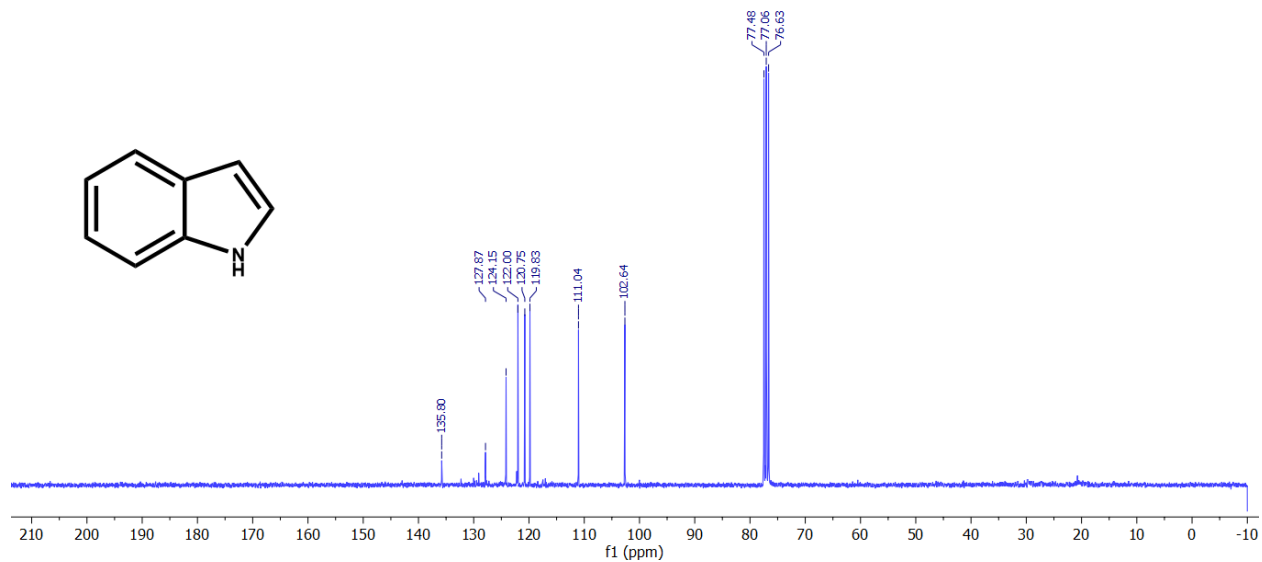


**Fig. S105** <sup>13</sup>C NMR spectrum of compound **11a** (75 MHz, CDCl<sub>3</sub>).

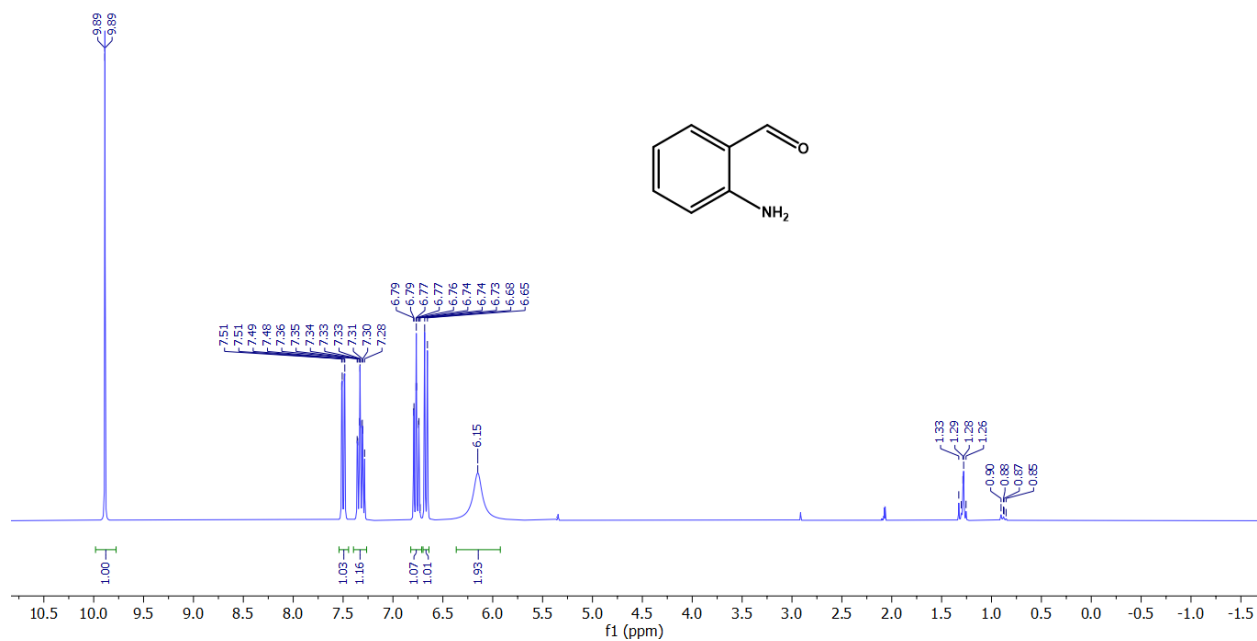


**Fig. S106**  $^1\text{H NMR}$  spectrum of compound **6a'** (300 MHz,  $\text{CDCl}_3$ ).

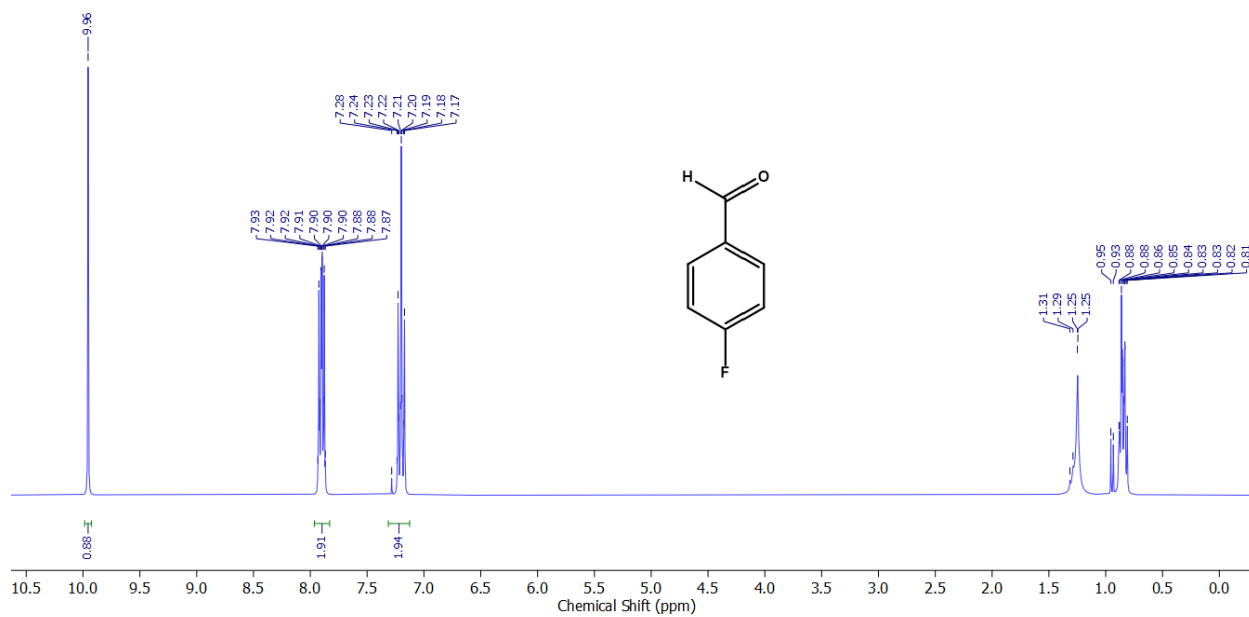


**Fig. S107**  $^1\text{H NMR}$  spectrum of compound **2f'** (300 MHz,  $\text{CDCl}_3$ ).

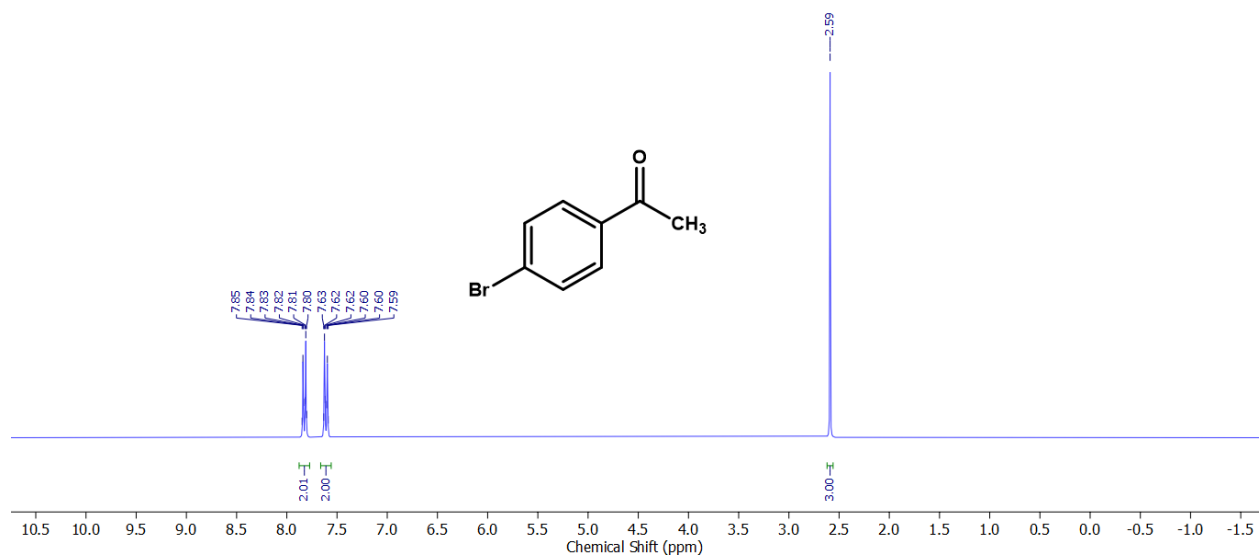


**Fig. S108**  $^1\text{H}$  NMR spectrum of compound **4n''** (300 MHz,  $\text{CDCl}_3$ ).

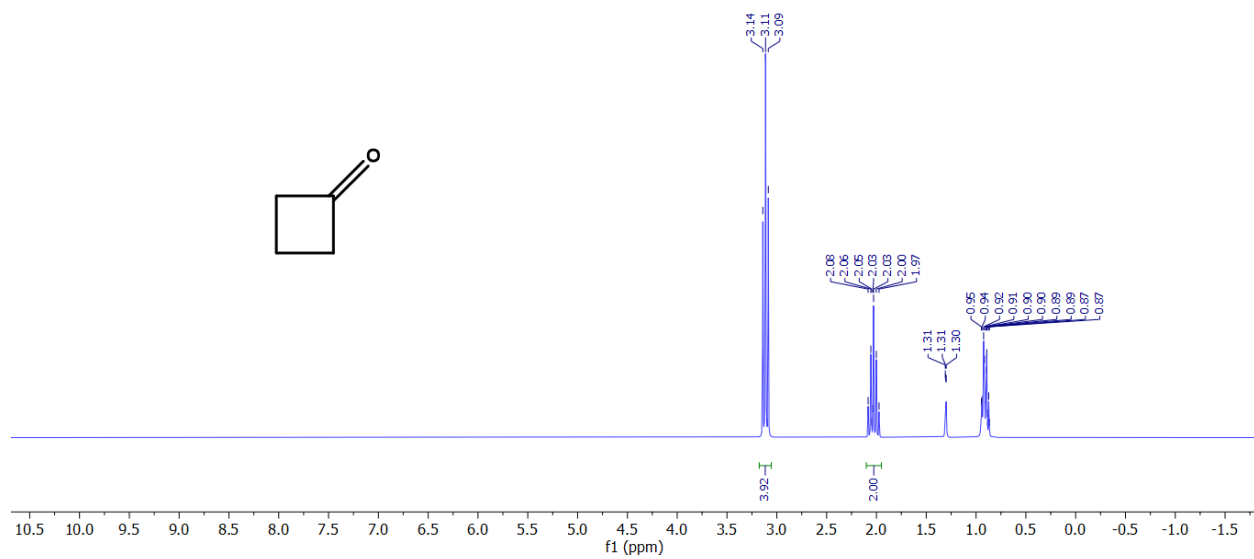


**Fig. S109**  $^1\text{H}$  NMR spectrum of cyclobutanone (300 MHz,  $\text{CDCl}_3$ ).

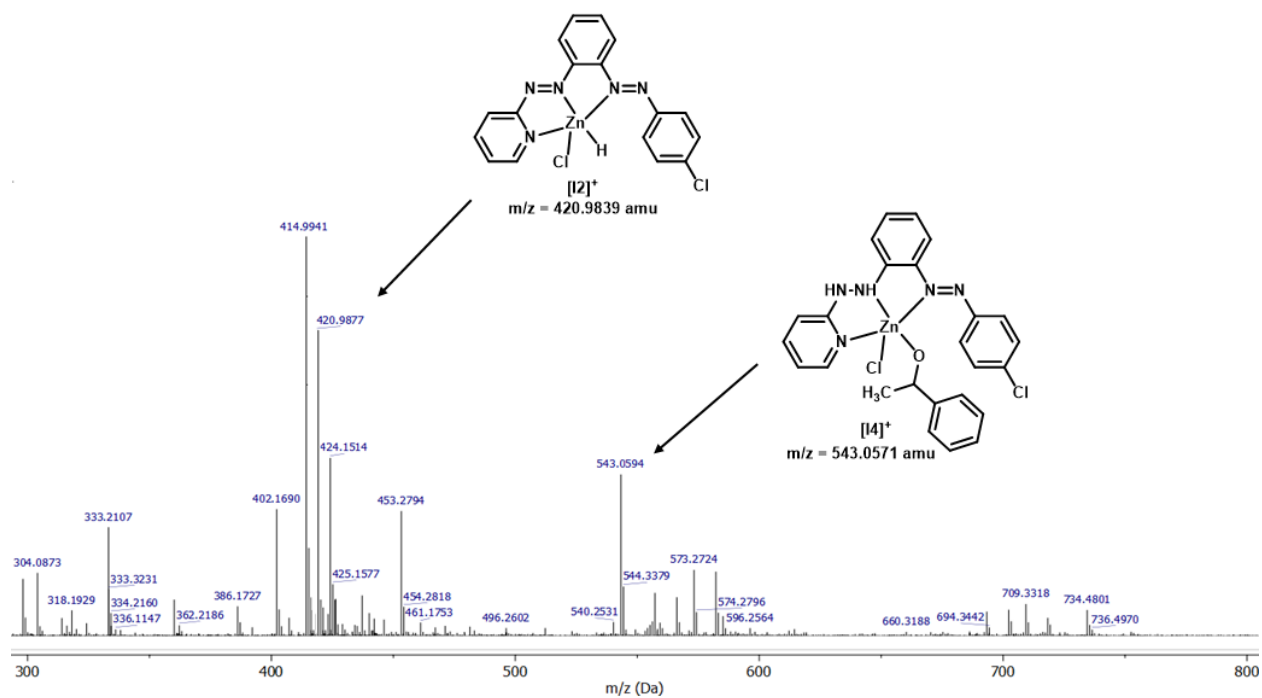
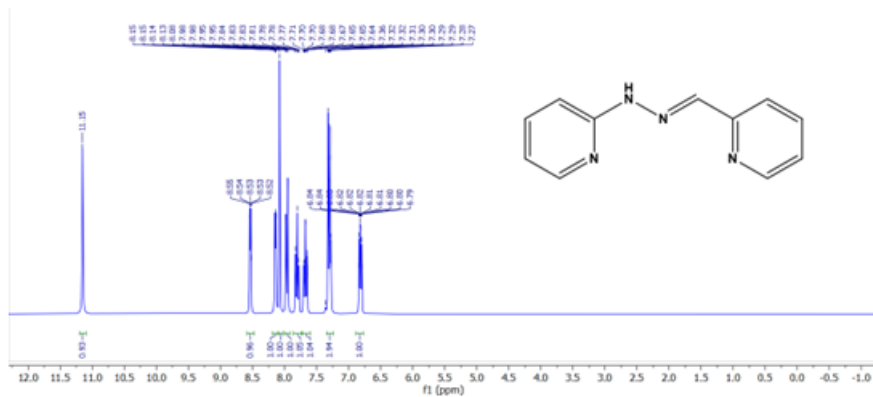
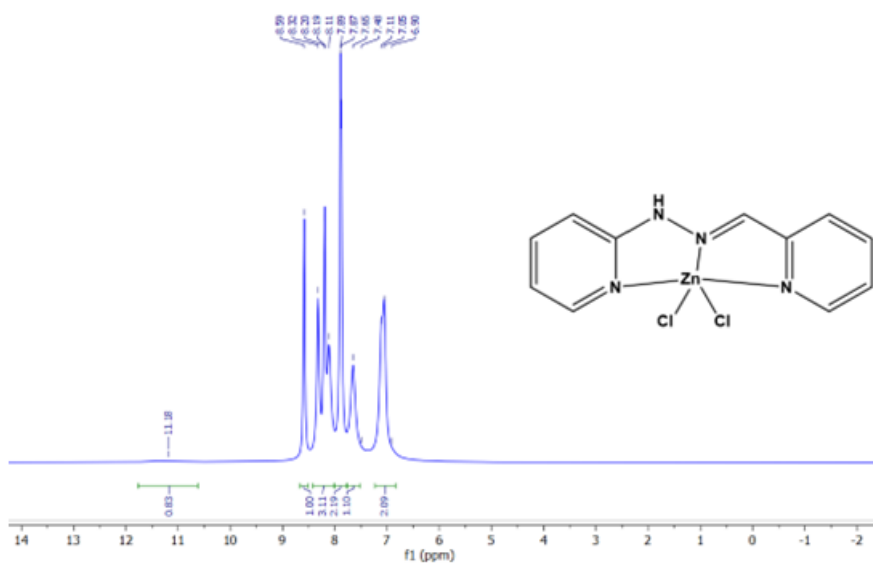


**Fig. S110** HRMS of intermediates  $[I2]^+$ ,  $[I4]^+$ : when the reaction was carried out with 1-phenylethanol and catalyst **1a** in presence of base.





**Pyridyl-Schiff-base ligand**



**ZnCl<sub>2</sub>-pyridyl-Schiff-base ligand**

**Fig. S111** <sup>1</sup>H NMR spectrum of ligand (N<sub>py</sub><sup>^</sup>N<sub>imine</sub><sup>^</sup>N<sub>py</sub> = py-CH=N-NH-py) and [Zn(N<sub>py</sub><sup>^</sup>N<sub>imine</sub><sup>^</sup>N<sub>py</sub>)Cl<sub>2</sub>] **1c** (400 MHz, DMSO-*d*<sub>6</sub>).

## Appendix: supplementary data

CCDC deposition numbers 2348683 (**1a**), 2348684 (**1b**), 2349095 (**5ag**) and 2349099 (**10aj**) contain the supplementary crystallographic data for this paper. These data can be obtained free of charge via [www.ccdc.cam.ac.uk/data\\_request/cif](http://www.ccdc.cam.ac.uk/data_request/cif) or by emailing [data\\_request@ccdc.cam.ac.uk](mailto:data_request@ccdc.cam.ac.uk), or by contacting The Cambridge Crystallographic Data Centre, 12 Union Road, Cambridge CB2 1EZ, U.K.; Fax: + 44 1223 336033.

## References

1. A.D. Becke, *J. Chem. Phys.* 1993, **98**, 5648-5652.
2. C. Lee, W. Yang, R.G. Parr, *Phys. Rev. B: Condens. Matter* 1988, **37**, 785-789.
3. M. J. Frisch, G. W. Trucks, H. B. Schlegel, G. E. Scuseria, M. A. Robb, J. R. Cheeseman, G. Scalmani, V. Barone, B. Mennucci, G. A. Petersson, H. Nakatsuji, M. Caricato, X. Li, H. P. Hratchian, A. F. Izmaylov, J. Bloino, G. Zheng, J. L. Sonnenberg, M. Hada, M. Ehara, K. Toyota, R. Fukuda, J. Hasegawa, M. Ishida, T. Nakajima, Y. Honda, O. Kitao, H. Nakai, T. Vreven, J. A. Montgomery Jr., J. E. Peralta, F. Ogliaro, M. Bearpark, J. J. Heyd, E. Brothers, K. N. Kudin, V. N. Staroverov, R. Kobayashi, J. Normand, K. Raghavachari, A. Rendell, J. C. Burant, S. S. Iyengar, J. Tomasi, M. Cossi, N. Rega, J. M. Millam, M. Klene, J. E. Knox, J. B. Cross, V. Bakken, C. Adamo, J. Jaramillo, R. Gomperts, R. E. Stratmann, O. Yazyev, A. J. Austin, R. Cammi, C. Pomelli, J. W. Ochterski, R. L. Martin, K. Morokuma, V. G. Zakrzewski, G. A. Voth, P. Salvador, J. J. Dannenberg, S. Dapprich, A. D. Daniels, O. Farkas, J. B. Foresman, J. V. Ortiz, J. Cioslowski, D. J. Fox, GAUSSIAN 09 (Revision A.01), Gaussian, Inc., Wallingford, CT, (2009).
4. J. Autschbach, T. Ziegler, S.J.A. Gisbergen, E.J. Baerends, *J. Chem. Phys.* 2002, **116**, 6930-6940.
5. K.L. Bak, P. Jørgensen, T. Helgaker, K. Rund, H.J.A. Jensen, *J. Chem. Phys.* 1993, **98**, 8873-8887.
6. T. Helgaker, P. Jørgensen, *J. Chem. Phys.* 1991, **95**, 2595-2601.
7. E.K.U. Gross, W. Kohn, *Adv. Quantum Chem.* 1990, **21**, 255-291.
8. M. Cossi, N. Rega, G. Scalmani, V. Barone, *J. Comput. Chem.* 2003, **24**, 669-681.

9. M. Cossi, V. Barone, *J. Chem. Phys.* 2001, **115**, 4708-4717.
10. V. Barone, M. Cossi, *J. Phys. Chem.* 1998, **102**, 1995-2001.
11. T. Liu, H.X. Zhang, B.H. Xia, *J. Phys. Chem.* 2007, **111**, 8724-8730.
12. A. Albertino, C. Garino, S. Ghiani, *J. Organomet. Chem.* 2007, **692**, 1377-1391.
13. X. Zhou, H.X. Zhang, Q.J. Pan, B.H. Xia, *J. Phys. Chem.* 2005, **109**, 8809-8818.
14. X. Zhou, A.M. Ren, J.K. Feng, *J. Organomet. Chem.* 2005, **690**, 338-347.
15. P.J. Hay, W.R. Wadt, *J. Chem. Phys.* 1985, **82**, 299-310.
16. P.J. Hay, W.R. Wadt, *J. Chem. Phys.* **82** (1985) 270–283.
17. M.S. Gordon, J.S. Binkley, J.A. Pople, W.J. Pietro, W.J. Hehre, *J. Am. Chem. Soc.* 1982, **104**, 2797-2803.
18. J.S. Binkley, J.A. Pople, W.J. Hehre, *J. Am. Chem. Soc.* 1980, **102**, 939-947.
19. N.M. O’Boyle, A.L. Tenderholt, K.M. Langner, *J. Comput. Chem.* 2008, **29**, 839-845.
20. S. Roy, S. Pramanik, S. C. Patra, B. Adhikari, A. Mondal, S. Ganguly and K. Pramanik, *Inorg. Chem.*, 2017, **56**, 12764–12774.
21. SAINT, Data Reduction and Frame Integration Program for the CCD Area-Detector System. Bruker Analytical X-ray Systems, Madison, Wisconsin, USA, 1997–2006.
22. G.M. Sheldrick, SADABS, Program for Area Detector Absorption Correction, Institute for Inorganic Chemistry, University of Göttingen, Germany (1996).
23. G.M. Sheldrick, *Acta Crystallogr. Sect. C: Struct. Chem.* 2015, **71**, 3-8.
24. O.V. Dolomanov, L.J. Bourhis, R.J. Gildea, J.A.K. Howard, H. Puschmann, *J. Appl. Cryst.* 2009, **42**, 339-341.
25. A. Charvieux, J. B. Giorgi, N. Duguet, E. Métay, *Green Chem.* 2018, **20**, 4210-4216.
26. G. Zhang, J. Wu, H. Zeng, S. Zhang, Z. Yin, S. Zheng, *Org. Lett.* 2017, **19**, 1080–1083.
27. C. Chaudhari, K. Sato, Y. Ogura, S.-I. Miyahara, K. Nagaoka, *ChemCatChem* 2020, **12**, 2198–22.
28. B. Guo, T.-Q. Yu, H.-X. Li, S.-Q. Zhang, P. Braunstein, D. J. Young, H.-Y. Li, J.-P. Lang, *ChemCatChem* 2019, **11**, 2500–2510.
29. S. Das, S. Sinha, D. Samanta, R. Mondal, Gargi Chakraborty, P. Brandaõ, N. D. Paul, *J. Org. Chem.* 2019, **84**, 10160–10171.
30. A. Maji, A. Singh, N. Singh, K. Ghosh, *ChemCatChem* 2020, **12**, 3108–3125.

31. S. Chakraborty, R. Mondal, S. Pal, A. K. Guin, L. Roy, N. D. Paul, *J. Org. Chem.* 2023, **88**, 771–787.
32. K. Das, A. Mondala, D. Srimani, *Chem. Commun.* 2018, **54**, 10582-10585.
33. J. Zhou, Y. Zou, P. Zhou, Z. Chen and J. Li, *Org. Chem. Front.*, 2019, **6**, 1594-1598.